

**COMPLEX MACROMOLECULAR AND ELECTRO-/PHOTO-ACTIVE  
STRUCTURES BY “CLICK CHEMISTRY”**

**Ph.D. Thesis by  
Burçin GACAL**

**Department : Polymer Science and Technology**

**Programme : Polymer Science and Technology**

**JUNE 2011**







**COMPLEX MACROMOLECULAR AND ELECTRO-/PHOTO-ACTIVE  
STRUCTURES BY “CLICK CHEMISTRY”**

**Ph. D. Thesis by  
Burçin GACAL  
(515042010)**

**Date of submission : 27 April 2011  
Date of defence examination: 07 June 2011**

**Supervisor (Chairman) : Prof. Dr. Yusuf YAĞCI (ITU)  
Members of the Examining Committee : Prof. Dr. Ümit TUNCA (ITU)  
Assoc. Dr. A. Ersin ACAR (BU)  
Prof. Dr. Oğuz OKAY (ITU)  
Prof. Dr. Nergis ARSU (YTU)**

**JUNE 2011**



**İSTANBUL TEKNİK ÜNİVERSİTESİ ★ FEN BİLİMLERİ ENSTİTÜSÜ**

**KOMPLEKS MAKROMOLEKÜLER VE ELEKTRO-/FOTO- AKTİF  
YAPILARDA “KLİK KİMYASI”**

**DOKTORA TEZİ  
Burçin GACAL  
(515042010)**

**Tezin Enstitüye Verildiği Tarih : 27 Nisan 2011  
Tezin Savunulduğu Tarih : 07 Haziran 2011**

**Tez Danışmanı : Prof. Dr. Yusuf YAĞCI (İTÜ)  
Diğer Jüri Üyeleri : Prof. Dr. Ümit TUNCA (İTÜ)  
Doç. Dr. A. Ersin ACAR (BÜ)  
Prof. Dr. Oğuz OKAY (İTÜ)  
Prof. Dr. Nergis ARSU (YTÜ)**

**NİSAN 2011**





## FOREWORD

First of all, I would like to thank my thesis supervisor, Prof. Yusuf Yağcı, for giving me the opportunity to work in his group. He made me realize the wonderful world of polymer chemistry through his wide knowledge. I am deeply indebted to him for his kind guidance, valuable criticism, support, understanding and help in all possible ways throughout this research. I gratefully acknowledge the effort, the time and valuable suggestions of the members of my thesis committee: Prof. Ümit Tunca and Assoc. Dr. A. Ersin Acar.

I wish to thank all the past and present members of “Yağcı Group” for their help, friendship and the nice environment they created not only inside, but also outside the lab. In particular, Assist. Prof. Mehmet Atilla Taşdelen, Dr. Yasemin Yüksel Durmaz, Muhammet Ü. Kahveci, Dr. Ioan Cianga, Res. Asst. Ali Görkem Yılmaz, Dr. Barış Kışkan, Selim Beyazıt, Kübra Demir, Manolya Kukul, Elif Şahkulubey, Alev Tüzün, Zeynep Beyazkılıç, Hande Çelebi, Bahadır Gacal, Mustafa Uygun, Serdar Okçu, Halime Cengiz, Gökhan Açık, Dilek Sureka, Banu Köz, Ayfer Fırat and Mihrace Ergin for being helpful co-workers.

I also would like to thank Res. Asst. Ufuk Saim Günay, Res. Asst. Ilgın Nar Res. Asst. Özlem Aldaş, Res. Asst. Tuba Çakır, Res. Asst. Tuba Başkan, Dr. Bünyamin Karagöz, Dr. Abdullah Aydoğan, Dr. Volkan Kumbaracı, Dr. Şebnem İnceoğlu, Dr. Cüneyt H. Ünlü, Dr. Hakan Durmaz and Dr. Füsün Ş. Güngör.

I wish to express my warm thanks to my best friends Demet Göen Çolak, Gökçe Merey, Müfide Karahasanoğlu, Deniz Tunç, Mirnur A. Barın, Engin I. Abanoz, Şennur Ö. Özçelik, Çağatay Altınkök, Ali Ekber Özen and Feti Şahin.

I am deeply grateful to my mother Gürsel Gacal, my father Adnan Gacal and the deepest color of my life, my brother, the deepest colour of my life, Bahadır N. Gacal for their endless love, care, faith, support and understanding throughout my life.

Saving the most important for last, I would like to express my loving thanks to Orkan Özcan for his unconditional love and care, confidence, patience, support and encouragement.

Finally, I would like to dedicate this thesis to my brother, Bahadır Gacal, my mother Gürsel Gacal and my father Adnan Gacal.

This work is supported by ITU Graduate School of Science, Engineering and Technology.

June 2011

Burçin GACAL

Chemist, M.Sc.



## TABLE OF CONTENTS

	<u>Page</u>
<b>FOREWORD</b> .....	<b>v</b>
<b>TABLE OF CONTENTS</b> .....	<b>vii</b>
<b>ABBREVIATIONS</b> .....	<b>xi</b>
<b>LIST OF TABLES</b> .....	<b>xiii</b>
<b>LIST OF FIGURES</b> .....	<b>xv</b>
<b>SUMMARY</b> .....	<b>xix</b>
<b>ÖZET</b> .....	<b>xxiii</b>
<b>1. INTRODUCTION</b> .....	<b>1</b>
<b>2. THEORETICAL PART</b> .....	<b>3</b>
2.1 Click Chemistry .....	3
2.1.1 Copper(I)-catalyzed azide-alkyne cycloaddition (CuAAC).....	3
2.1.1.1 Mechanistic considerations on the Cu(I) catalysis .....	5
2.1.1.2 The Cu(I) source .....	7
2.1.1.3 The influence of ligands on Cu(I) catalysis .....	9
2.1.1.4 Reactivity of the alkyne and azide substrates.....	11
2.1.1.5 Proximity effects in the efficiency and rate of the triazole formation .....	12
2.1.2 Diels-Alder Reaction.....	14
2.1.2.1 Diene and dienophile.....	15
2.1.2.2 Stereochemistry of Diels-Alder reaction.....	17
2.1.2.3 Catalysis of Diels-Alder reactions by Lewis acids.....	20
2.1.2.4 Retro Diels-Alder reaction .....	21
2.1.3 Thiol-ene reaction .....	22
2.2 Photopolymerization.....	24
2.2.1 Photoinitiated free radical polymerization .....	26
2.2.1.1 <i>Type I</i> photoinitiators (unimolecular photoinitiator system).....	27
2.2.1.2 <i>Type II</i> photoinitiators (bimolecular photoinitiator systems) .....	30
2.2.1.3 Monomers.....	33
2.3 Conducting Polymers (CP).....	34
2.3.1 Band Theory .....	35
2.3.2 Synthesis of conjugated polymers.....	39
2.3.3 Electrochemical polymerization.....	39
2.3.4 Oxidative chemical polymerization .....	40
2.3.5 Electrochemical techniques .....	41
2.3.5.1 Constant-current electrolysis (Galvanostatic).....	42
2.3.5.2 Constant-potential electrolysis .....	42
2.3.5.3 Cyclic voltammetry (CV).....	42

<b>3. EXPERIMENTAL WORK .....</b>	<b>45</b>
3.1 Materials and Chemicals .....	45
3.1.1 Monomers.....	45
3.1.2 Solvents .....	45
3.1.3 Other chemicals .....	45
3.2 Equipment.....	47
3.2.1 Photoreactor .....	47
3.2.2 Nuclear magnetic resonance spectroscopy (NMR) .....	47
3.2.3 Infrared spectrophotometer (FT-IR).....	47
3.2.4 UV-Visible spectrophotometer .....	47
3.2.5 Gel permeation chromatography (GPC) .....	47
3.2.6 Differential scanning calorimetry (DSC) .....	48
3.2.7 Thermal gravimetric analyzer (TGA) .....	48
3.2.8 Fluorescence spectrophotometer .....	48
3.2.9 Electrochemical measurements .....	48
3.3 Preparation Methods.....	48
3.3.1 Synthesis of 4-(2-{{(3-acetyl-7-oxabicyclo[2.2.1]hept-5-en-2-yl) carbonyl}amino}ethoxy)-4-oxobutanoic acid (3).....	49
3.3.2 Preparation of PEG-maleimide (PEG-MI).....	49
3.3.3 Preparation of PMMA-maleimide (PMMA-MI).....	49
3.3.4 General procedure for etherification of chloromethyl moieties (8, 30 and 50%) of poly(styrene-co-chloromethyl styrene) P(S-co-CMS) .....	50
3.3.5 General procedure for preparation of graft copolymer via DA reaction of PMMA-MI and PS with anthryl pendant groups (PS-Anth) .....	50
3.3.6 General procedure for preparation of graft copolymer via DA reaction of PEG-MI and PS-Anth .....	51
3.3.7 Preparation of samples for AFM .....	51
3.3.8 Synthesis of octa(nitrophenyl)silsesquioxane (ONO <sub>2</sub> PS).....	51
3.3.9 Synthesis of octa(aminophenyl)silsesquioxane (ONH <sub>2</sub> PS).....	51
3.3.10 Synthesis of octa(azidophenyl)silsesquioxane (ON <sub>3</sub> PS).....	52
3.3.11 Synthesis of prop-2-ynyl thiophene-3-carboxylate ( <i>Propargyl</i> thiophene).....	53
3.3.12 General procedure for synthesis of octa( <i>Thiophenephenyl</i> ) silsesquioxane via click Chemistry ( <i>OThiophenePS</i> ) .....	53
3.3.13 Synthesis of PPy and OPS-PPy.....	54
<b>4. RESULTS AND DISCUSSION .....</b>	<b>55</b>
4.1 Anthracene-maleimide-based Diels-Alder “Click Chemistry” as a novel route to graft copolymers.....	55
4.2 Synthesis and characterization of polymeric thioxanthone photoinitiators via double Click reactions .....	67
4.3 Poly(ethylene glycol)-thioxanthone prepared by Diels-Alder "Click Chemistry" as one-component polymeric photo initiator for aqueous free radical polymerization .....	75
4.4 Enhancing electrochromic properties of polypyrrole by silsesquioxane nanocages .....	82
4.5 Cyclic voltammetry .....	89
4.6 Electrochromic properties of OPS-PPy.....	90
4.6.1 Spectroelectrochemistry .....	90
4.6.2 Optical contrast .....	92
4.6.3 Switching time.....	93

4.6.4 Colorimetry .....	95
<b>5. CONCLUSION .....</b>	<b>97</b>
<b>REFERENCES .....</b>	<b>101</b>
<b>CURRICULUM VITAE .....</b>	<b>117</b>



## ABBREVIATIONS

<b><sup>1</sup>H NMR</b>	: Hydrogen Nuclear Magnetic Resonance Spectroscopy
<b>FT-IR</b>	: Fourier Transform Infrared Spectrophotometer
<b>UV</b>	: Ultra Violet
<b>GPC</b>	: Gel Permeation Chromatography
<b>DSC</b>	: Differential Scanning Calorimetry
<b>GC</b>	: Gas Chromatography
<b>AFM</b>	: Atomic Force Microscopy
<b>TEMPO</b>	: 2,2,6,6-Tetramethylpiperidine- <i>N</i> -oxyl
<b>PMDETA</b>	: <i>N, N, N', N'', N'''</i> -Pentamethyldiethylenetriamine
<b>ATRP</b>	: Atom Transfer Radical Polymerization
<b>RAFT</b>	: Reversible Addition Fragmentation Chain Transfer
<b>NMP</b>	: Nitroxide Mediated Polymerization
<b>CH<sub>2</sub>Cl<sub>2</sub></b>	: Dichloromethane
<b>CDCl<sub>3</sub></b>	: Deuterated Chloroform
<b>THF</b>	: Tetrahydrofuran
<b>MMA</b>	: Methyl Methacrylate
<b>PMMA</b>	: Poly(methyl methacrylate)
<b>St</b>	: Styrene
<b>PS</b>	: Poly(styrene)
<b>CuAAC</b>	: Copper Catalyzed Azide-Alkyne Cycloaddition
<b>DA</b>	: Diels-Alder
<b>r-DA</b>	: Retro-Diels-Alder
<b>PEG</b>	: Poly(ethylene glycol)
<b>TEA</b>	: Triethylamine
<b>EtOAc</b>	: Ethyl Acetate
<b>MWD</b>	: Molecular Weight Distribution
<b>DMF</b>	: <i>N,N</i> -dimethylformamide
<b>PDI</b>	: Polydispersity Index
<b>DVB</b>	: Divinyl Benzene





## LIST OF TABLES

	<u>Page</u>
<b>Table 2.1</b> Representative dienes [90] .....	15
<b>Table 2.2</b> Representative dienophiles [90]. .....	17
<b>Table 2.3:</b> Structures of typical <i>Type I</i> radical photoinitiators. ....	29
<b>Table 2.4:</b> Structures of typical <i>Type II</i> photoinitiators. ....	31
<b>Table 4.1:</b> Molecular weights and functionalities of the polymers at various stages. ....	57
<b>Table 4.2:</b> The glass transition temperatures ( $T_g$ ) of the polymers at various stages. ....	66
<b>Table 4.3:</b> Photoinitiated polymerization of methyl methacrylate (MMA) with macrophotoinitiator in $\text{CH}_2\text{Cl}_2$ . ....	73
<b>Table 4.4:</b> Effect of solvent on the photoinitiated polymerization of methyl methacrylate (MMA) with PS-TX at room temperature. ....	74
<b>Table 4.5:</b> Photoinitiated polymerization of hydrophilic vinyl monomers. ....	80
<b>Table 4.6:</b> Electrochromic properties of OPS-PPy and PPy .....	95



## LIST OF FIGURES

### Page

<b>Figure 1:</b> General presentation of grafting process by Diels-Alder “Click Chemistry”	xx
<b>Figure 2:</b> Side-chain functionalization of PS-N <sub>3</sub> with anthracene-thioxanthone (TX-A) in the presence of <i>N</i> -propargyl-7-oxynorbornene (PON) as click linker via double click chemistry	xxi
<b>Figure 3:</b> Synthesis of one-component polymeric photoinitiator by Diels-Alder click chemistry	xxii
<b>Figure 4:</b> Synthesis of O thiophene PS by click chemistry	xxii
<b>Figure 2.1 :</b> General representation of thermal and copper catalyzed cycloaddition	4
<b>Figure 2.2 :</b> Proposed catalytic cycle for CuAAC. The density functional theory (DFT) investigation described [22,41,42]	6
<b>Figure 2.3 :</b> Effective ligands used to promote the Cu(I) catalyzed triazole formation	10
<b>Figure 2.4 :</b> Proximity effects in the efficiency and rate of the triazole formation on calixarenes	13
<b>Figure 2.5 :</b> Bis-azide compounds	14
<b>Figure 2.6 :</b> General mechanism of Diels-Alder/retro Diels-Alder reactions of dienophile and diene	15
<b>Figure 2.7 :</b> Examples of activated substrates susceptible to hydrothiolation via a base/nucleophile-mediated process [21]	24
<b>Figure 2.8 :</b> Structures of typical conductive polymers	35
<b>Figure 2.9 :</b> The $\pi$ -system model	36
<b>Figure 2.10 :</b> Molecular orbital (MO) diagram	36
<b>Figure 2.11 :</b> Band structures of insulator, semiconductor and conductor [9]	37
<b>Figure 2.12 :</b> Neutral and doped forms of polyacetylene	38
<b>Figure 2.13 :</b> Band structures of a) neutral polymer b) lightly doped polymer c) heavily doped polymer	39
<b>Figure 2.14 :</b> Triangular wave function	43
<b>Figure 2.15 :</b> Cyclic voltammogram of reversible process	43
<b>Figure 4.1:</b> General presentation of grafting process by Diels-Alder click chemistry	55
<b>Figure 4.2:</b> Incorporation of anthryl moieties by etherification process	56
<b>Figure 4.3:</b> <sup>1</sup> H NMR spectrum of PS-Anth (30%) in CDCl <sub>3</sub>	58
<b>Figure 4.4:</b> Intermediates used for maleimide functionalization	59
<b>Figure 4.5:</b> Grafting by <i>in situ</i> retro DA and DA processes	60
<b>Figure 4.6:</b> <sup>1</sup> H NMR spectrum of PS- <i>g</i> -PEG (30%) in CDCl <sub>3</sub>	61
<b>Figure 4.7:</b> <sup>1</sup> H NMR spectrum of PS- <i>g</i> -PMMA (30%) in CDCl <sub>3</sub>	62
<b>Figure 4.8:</b> Evolution of GPC traces: PEG-MI PS-Anth (50%), and PS- <i>g</i> -PEG (50%) (a), and PMMA-MI, PS-Anth (30%), and PS- <i>g</i> -PMMA (30%) (b)	63

<b>Figure 4.9:</b> Absorption spectra of PS-Anth (8%), PS- <i>g</i> -PEG (8%), and PS- <i>g</i> -PMMA (8%); $c = 2 \times 10^{-5}$ M in $\text{CCl}_4$ .....	64
<b>Figure 4.10:</b> Emission spectra of PS-Anth (8%), PS- <i>g</i> -PEG (8%), and PS- <i>g</i> -PMMA (8%); $\lambda_{\text{exc.}} = 390$ nm; $c = 2 \times 10^{-5}$ M in $\text{CCl}_4$ .....	65
<b>Figure 4.11:</b> Atomic force microscopy pictures: height (a) and phase (b) picture of PS- <i>g</i> -PMMA (8%); height (c) and phase (d) picture of PS- <i>g</i> -PEG (8%). All pictures correspond to an area of $2 \mu\text{m} \times 2 \mu\text{m}$ .....	67
<b>Figure 4.12:</b> Side-chain functionalization of PS-N <sub>3</sub> with anthracene-thioxanthone (TX-A) in the presence of N-propargyl-7-oxynorbornene (PON) as click linker via double click chemistry. ....	68
<b>Figure 4.13:</b> <sup>1</sup> H NMR spectrum of TX-A, PS-N <sub>3</sub> and PS-TX (27%) in $\text{CDCl}_3$ .....	69
<b>Figure 4.14:</b> Absorption spectra of PS-TX (27%), TX-A and TX in $\text{CH}_2\text{Cl}_2$ . The concentrations are $1 \times 10^{-5}$ M in terms of thioxanthone moieties. ....	71
<b>Figure 4.15:</b> Emission spectra of TX-A and PS-TX (27%) in DMF; $\lambda_{\text{exc}}=360$ nm. The concentrations are $2 \times 10^{-5}$ M in terms of thioxanthone moieties. ....	72
<b>Figure 4.16:</b> Photoinitiated free radical polymerization of methyl methacrylate (MMA) by using PS-TX macrophotoinitiator.....	72
<b>Figure 4.17:</b> Photo-DSC profile for polymerization of TPTA in the presence of TEA and PS-TX (27%) macrophotoinitiator, cured at 30°C by UV light with an intensity of $180 \text{ mw/cm}^2$ . ....	75
<b>Figure 4.18:</b> Conversion vs. time, for polymerization of TPTA in the presence of TEA and PS-TX (27%) macrophotoinitiator, cured at 30°C by UV light with an intensity of $180 \text{ mw/cm}^2$ . ....	75
<b>Figure 4.19:</b> Synthesis of one-component polymeric photoinitiator by Diels-Alder click chemistry. ....	76
<b>Figure 4.20:</b> <sup>1</sup> H NMR spectra of TX-A, PEG-MI and PEG-TX in $\text{CDCl}_3$ . ....	77
<b>Figure 4.21:</b> Absorbtion spectra of TX-A and PEG-TX in $\text{CH}_2\text{Cl}_2$ . The concentrations are $1 \times 10^{-5}$ M.....	78
<b>Figure 4.22:</b> Absorbtion spectra of PEG-TX in $\text{CH}_2\text{Cl}_2$ and water. The concentrations are $1 \times 10^{-5}$ M.....	78
<b>Figure 4.23:</b> Emission spectra of TX-A and PEG-TX in $\text{CH}_2\text{Cl}_2$ ; $\lambda_{\text{exc}}= 360$ nm. The concentrations are $2 \times 10^{-5}$ M.....	79
<b>Figure 4.24:</b> Photoinitiated free radical polymerization of HEMA by using PEG-TX.....	80
<b>Figure 4.24:</b> Photo-DSC profile for photoinitiated polymerization of AM, HEMA, AA and VP in the presence of PEG-TX macrophotoinitiator at 30 <sup>0</sup> C. The light intensity: $180 \text{ mV/cm}^2$ .....	81
<b>Figure 4.25:</b> Conversion versus time for the photoinitiated polymerization of AM, HEMA, AA and VP in the presence of PEG-TX macrophotoinitiator at 30 <sup>0</sup> C. The light intensity: $180 \text{ mV/cm}^2$ . ....	81
<b>Figure 4.26:</b> Synthesis of octa(aminophenyl) silsesquioxane (ON <sub>3</sub> PS).....	83
<b>Figure 4.27:</b> Synthesis of octa(azidophenyl) silsesquioxane (ON <sub>3</sub> PS).....	83
<b>Figure 4.28:</b> Synthesis of Prop-2-ynyl Thiophene-3-carboxylate (Propargylthiophene).....	84
<b>Figure 4.29:</b> Synthesis of OThiophenePS by Click Chemistry. ....	84
<b>Figure 4.30:</b> <sup>1</sup> H NMR spectra of ONO <sub>2</sub> PS, ONH <sub>2</sub> PS and ON <sub>3</sub> PS (R: Aromatic Protons). ....	85
<b>Figure 4.31:</b> FT-IR spectra of ONO <sub>2</sub> PS, ONH <sub>2</sub> PS and ON <sub>3</sub> PS.....	86
<b>Figure 4.32:</b> <sup>1</sup> H NMR Spectra of propargylthiophene , ON <sub>3</sub> PS and OThiophenePS.....	87

<b>Figure 4.33:</b> FT-IR spectra of <i>propargylthiophene</i> , <i>OThiophenePS</i> and <i>ON<sub>3</sub>PS</i> . ....	88
<b>Figure 4.34:</b> FT-IR Spectra of a) OPS-PPy b) <i>OThiophenePS</i> .....	89
<b>Figure 4.35:</b> Cyclic Voltammograms of a) OPS-PPy b) Py and c) <i>O(thiophene)PS</i> .....	90
<b>Figure 4.36:</b> Spectroelectrochemical properties of the PPy in (0.1M) DCM/ TBAFB .....	91
<b>Figure 4.37:</b> Spectroelectrochemical properties of the OPS-PPy in (0.1M) DCM/TBAFB .....	92
<b>Figure 4.38:</b> Transmittance spectra of PPy and OPS-PPy in two extreme (oxidized and neutral) states. ....	93
<b>Figure 4.39:</b> Electrochromic switching, transmittance change monitored at 730 nm for a) PPy b) OPS-PPy c) OPS-PPy and PPy (Consecutive two cycles) .....	94



## COMPLEX MACROMOLECULAR AND ELECTRO-/PHOTO-ACTIVE STRUCTURES BY “CLICK CHEMISTRY”

### SUMMARY

The modification of polymers after the successful achievement of a polymerization process represents an important task in macromolecular science. The “click”-type reactions, among them the metal catalyzed azide/alkyne ‘click’ reaction (a variation of the Huisgen 1,3-dipolar cycloaddition reaction between terminal acetylenes and azides) or the Diels-Alder reaction (DA), [4 + 2] system, generally consists of a coupling of a diene and a dienophile by intra- or intermolecular reaction represent an important contribution towards this endeavor.

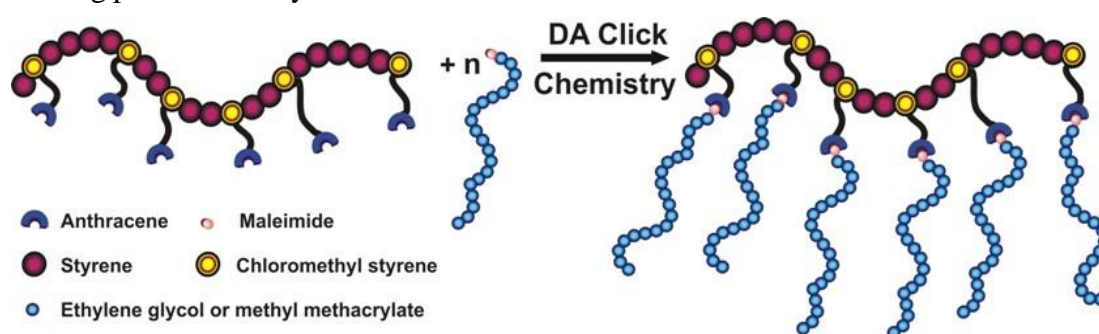
This approach brings an enormous potential in material science. The key features in “click” chemistry is represented by quantitative yields, high tolerans of functional groups, simple product isolations, lack of by-product, superior regioselectivity, and mild and simple reaction conditions. Since their fast growth, click chemistry strategies have been rapidly integrated into the field of macromolecular engineering and extensively been used in the synthesis of polymers ranging from linear to complex structures.

The photoinitiated free radical polymerization reactions are widely used on a commercial scale for a number of different applications such as curing of coatings on various materials, adhesives, printing inks and photorezists. The growth of radiation curing industry is dependent on continued innovation to support this technology. A wide range of free radical photoinitiating systems, fullfilling requirements for industrial application, e.g. wavelength selectivity, solubility etc. is now available. A large portion of today’s relevant research concerns photoinitiators, i.e. introduction of new initiators or improving the solubility of available initiators. Photoinitiated radical polymerization may be initiated by both cleavage (Type I) and H abstraction type (*Type II*) initiators. Because of their vital role in photopolymerization, photoinitiators are the subject of particularly extensive research. Most of this research has focused on *Type I* photoinitiators, which upon irradiation undergoes an  $\alpha$ -cleavage process to form two radical species. *Type II* photoinitiators are a second class of photoinitiators and are based on compounds whose triplet excited states are reacted with a hydrogen donor thereby producing an initiating radical.

Electrically conducting polymers have received growing interest because of their wide range applications in the areas such as rechargeable batteries, membranes, optical displays, and electro chromic devices. These materials are often termed as synthetic metals due to the fact that they combine chemical and mechanical properties of the polymers with the electronic properties of the metals and semiconductors. Polypyrrole is one of the polymers among a general type of conducting polymers that include polyacetylenes, polythiophene, polyanilines, polyphenylenes, polycarbazoles, polyquinolines, and polyphthalocyanines.

The “click”-type reactions, 1,3-dipolar azide-alkyne, [3 + 2], or Diels–Alder cycloadditions, [4 + 2], were applied, as a novel route, for the preparation of well-defined graft copolymers, photoinitiating systems with improved properties and reactive precursors for obtaining inorganic–organic conducting composites.

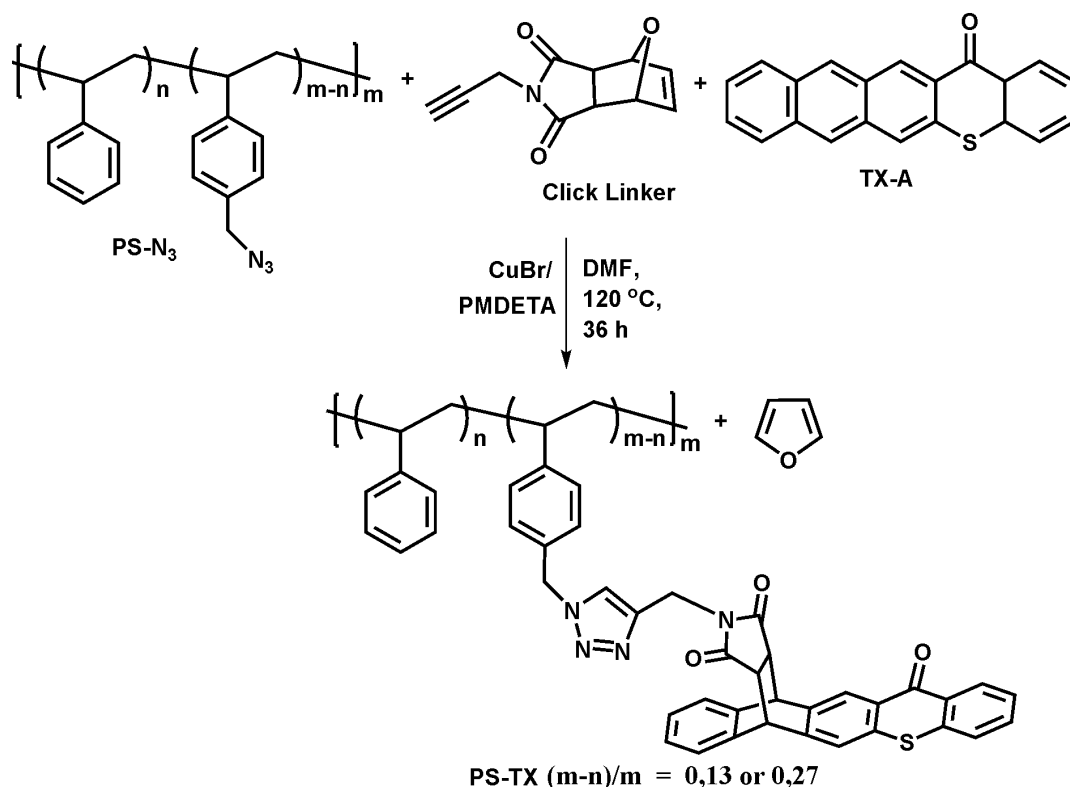
The study presented in the first part of the thesis is aimed at describing the anthracene-maleimide-based DA “click reaction” as a novel route to prepare well-defined graft copolymers. Scheme 1 outlines our synthetic strategy to this various phases of this work, viz., (i) preparing random copolymers of styrene (St) and 4-chloromethylstyrene (CMS) (which is a functionalizable monomer); (ii) attachment of anthracene functionality to the preformed copolymer by the *o*-etherification procedure; (iii) by using efficient DA “click chemistry”, maleimide-functionalized poly(methyl methacrylate) (PMMA-MI) via ATRP of MMA or poly(ethylene glycol) (PEG-MI) via modification of commercial PEG was introduced into copolymers bearing pendant anthryl moieties.



**Figure 1:** General presentation of grafting process by Diels-Alder “Click Chemistry” [12].

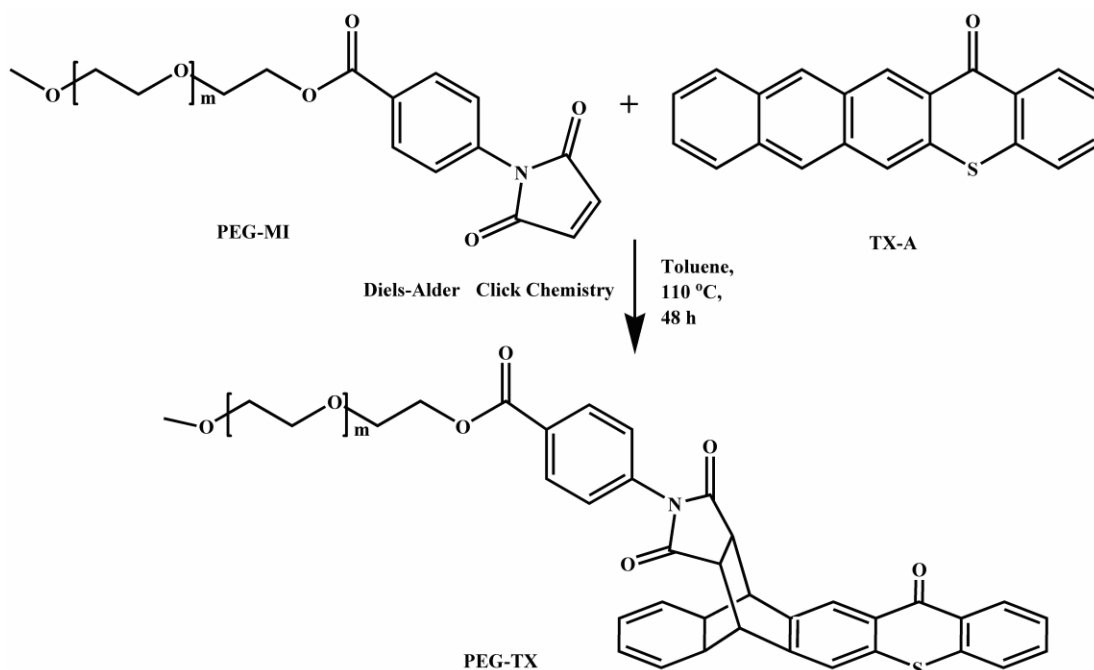
In the second part of the thesis, macrophotoinitiators containing thioxanthone (TX) moieties as side chains were synthesized by using “double click chemistry” strategy; combining in-situ 1,3-dipolar azide-alkyne [3 + 2] and thermoreversible Diels–Alder (DA) [4 + 2] cycloaddition reactions. For this purpose, thioxanthone-anthracene (TX-A), N-propargyl-7-oxynorbornene (PON), and polystyrene (PS) with side-chain azide moieties (PS-N<sub>3</sub>) were reacted in N,N-dimethylformamide (DMF) for 36 h at 120 °C. In this process, PON acted as a “click linker” since it contains both protected maleimide and alkyne functional groups suitable for 1,3-dipolar azide-alkyne and Diels-Alder click reactions, respectively. This way, the aromaticity of the central phenyl unit of the anthracene moiety present in TX-A was transformed into TX chromophoric groups. The resulting polymers possess absorption characteristics similar to the parent TX. Their capabilities to act as photoinitiator for the polymerization of mono and multifunctional monomers, namely methyl methacrylate (MMA) and 1,1,1-tris(hydroxymethyl)propane triacrylate (TPTA) were also examined.





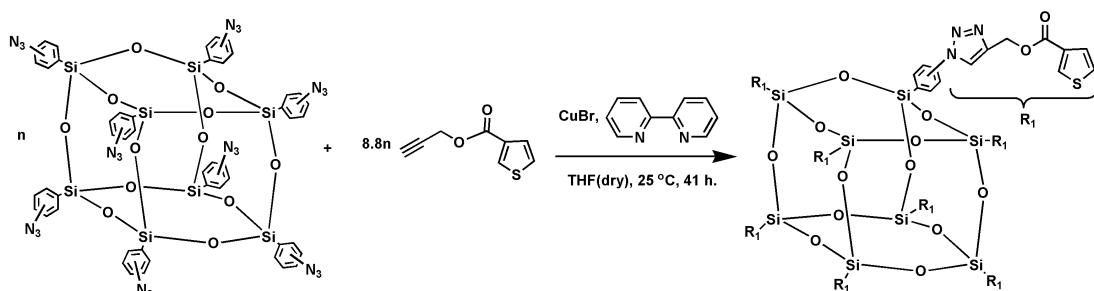
**Figure 2:** Side-chain functionalization of PS-N<sub>3</sub> with anthracene-thioxanthone (TX-A) in the presence of *N*-propargyl-7-oxynorbornene (PON) as click linker via double click chemistry.

As a part of our continuing interest in developing photoinitiating systems via “click chemistry”, in the third part of the thesis, we synthesized a novel water-soluble poly(ethylene glycol) (PEG) macrophotoinitiator containing TX end group via Diels–Alder click reaction. The final polymer poly(ethylene glycol)-thioxanthone (PEG-TX) and the intermediates were characterized in detail by spectral analysis. PEG-TX shows one-component character possessing both the light absorbing (TX) and hydrogen donating (PEG) sites in the same structure and was demonstrated by photopolymerization of several hydrophilic vinyl monomers, such as acrylic acid, acrylamide, 2-hydroxyethyl acrylate, and 1-vinyl-2-pyrrolidone.



**Figure 3:** Synthesis of one-component polymeric photoinitiator by Diels-Alder click chemistry.

Finally, we introduce a new approach for improving the electrochromic properties of polypyrrole by attaching polypyrrole chains onto thiophene possessing OPS nanocages which are efficiently synthesized via click chemistry. Our initial desire was to synthesize octa(azidophenyl) silsesquioxane (ON<sub>3</sub>PS) cube from the corresponding octa(aminophenyl)-silsesquioxane (ON<sub>3</sub>PS) via their diazoniumsalts and the use of “click chemistry” as a facile route for introduction of electroactive molecule “propargylthiophene” to octa(phenyl)silsesquioxane (OPS). With this approach, not only properties of polypyrrole but also other polymers prepared by the copolymerization of functional POSS with the wide variety of monomers may be tuned easily. our main goal was to report the synthesis of azide functionalized octaphenylsilsesquioxane (ON<sub>3</sub>PS) and subsequent use of “click” chemistry as a facile route toward functionalization of silsesquioxanes.



**Figure 4:** Synthesis of OThiophene PS by Click Chemistry.

## KOMPLEKS MAKROMOLEKÜLER VE ELEKTRO-/FOTO- AKTİF YAPILARDA “KLİK KİMYASI”

### ÖZET

Başarılı bir polimerizasyon sürecinin sonrasında elde edilen polimerlerin modifikasyonu makromoleküler bilimin önemli bir görevidir. “Klık” tipi reaksiyonlar, özellikle metal katalizli azid/alkin “klick” reaksiyonu (terminal asetilen ve azidler arasında gerçekleşen Huisgen 1,3-dipolar siklokatılma reaksiyonunun bir varyasyonu) veya Diels-Alder (DA), [4 + 2] sistemi, (genel olarak bir dien ile dienofilin molekül içi veya moleküller arası reaksiyonu) bu çaba yolunda önemli bir katkı sağlamaktadır.

Bu yaklaşım malzeme bilimi açısından muazzam bir potansiyel taşımaktadır. “Klık” kimyasının temel özellikleri; yüksek verim, fonksiyonel gruplara karşı yüksek tolerans, basit ürün izolasyonu, yan ürün eksikliği, üstün regio-selektivite ve hafif/basit reaksiyon koşullarıdır. “Klık” tipi reaksiyonların hızlı gelişiminden bu yana, ilgili strateji makromoleküler mühendisliği alanına hızla entegre edilmiş ve lineer ile kompleks yapılar arasında değişen polimerlerin sentezinde yaygın olarak kullanılmıştır.

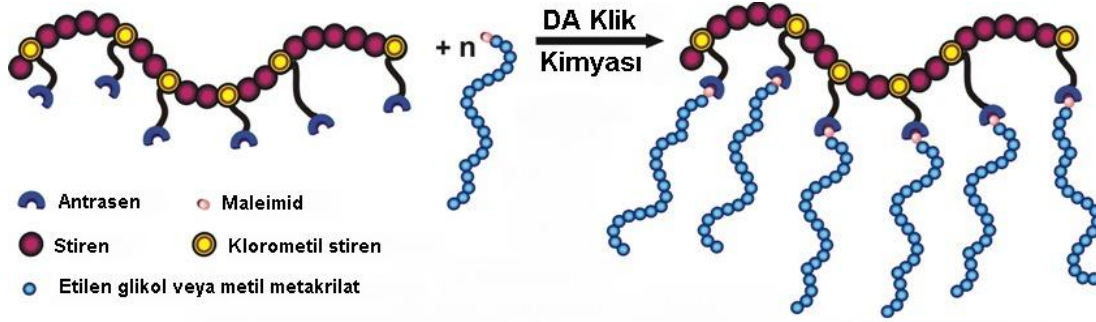
Fotobaşlatılmış serbest radikal polimerizasyonu çeşitli malzemeler üzerindeki kaplamanın kürlenmesi, yapıştırıcılar, matbaa mürekkepleri ve fotorezistler gibi bir dizi uygulama için ticari ölçekte yaygın olarak kullanılır. Işınla kürlenme sektörünün gelişimi bu teknolojiyi destekleyen sürekli yeniliklere bağlıdır. Fotobaşlatılmış serbest radikal polimerizasyon sistemleri geniş bir yelpazede örneğin dalga boyu seçicilik, çözünürlük vb. gibi endüstriyel uygulama için gereksinimleri artık karşılamaktadır. Günümüzde fotobaşlatıcılarla ilgili yapılan araştırmaların büyük bir bölümü, yeni başlatıcıların tanıtımı veya mevcut başlatıcıların çözünürlüklerini geliştirme kaygısı taşımaktadır. Fotobaşlatılmış radikal polimerizasyon bölünme (*Tip I*) ve H-ayırma tipi (*Type II*) fotobaşlatıcılar tarafından başlatılır. Fotopolimerizasyondaki hayati roller nedeniyle, özellikle fotobaşlatıcılar geniş araştırmaya tabidir. Bu araştırmanın çoğu, *Tip I* fotobaşlatıcılara odaklanmıştır. Birinci tip fotobaşlatıcılar, aydınlatma sonucu  $\alpha$ -bölünme süreci ile 2 tür radikal vermek üzere fotoparçalanmaya uğrarlar. *Tip II* fotobaşlatıcılar ikinci tip fotobaşlatıcılardır ve aydınlatma sonucu triplet uyarılmış hal  $\alpha$ -hidrojen verici bileşiklerle reaksiyona girerek başlatıcı radicali oluşturur.

Şarz edilebilen piller, membranlar, optik göstergeler ve elektro kromik aletler gibi çok geniş bir alandaki uygulamalarından dolayı elektriği ileten polimerler gittikçe büyüyen bir araştırma konusu olmuştur. İletken polimerler, polimerlerin mekanik ve kimyasal özellikleri ile metal ve yarı metallerin elektronik özelliklerini kapsadığından sentetik metaller olarak da adlandırılırlar. Polipirol iletken polimerlerin önemli bir türüdür. Ayrıca, poliasetilen, politiyofen, polianilin, polifenilen, polikarbazol, polikinolin ve polifitalosiyen iletken polimerlerden bazılarıdır .

“Klik” tipi reaksiyonlar, 1,3-dipolar azid-alkin, [3 + 2], ya da Diels-Alder siklokatalıma [4 + 2] reaksiyonları, iyi-tanımlı aşırı copolimerlerin hazırlanmasında, gelişmiş özellikleri ile fotobaşlatıcı sistemlerinin ve inorganik-organik iletken kompozitler elde etmek için reaktif öncülerin sentezinde yeni bir rota olarak uygulanmıştır.

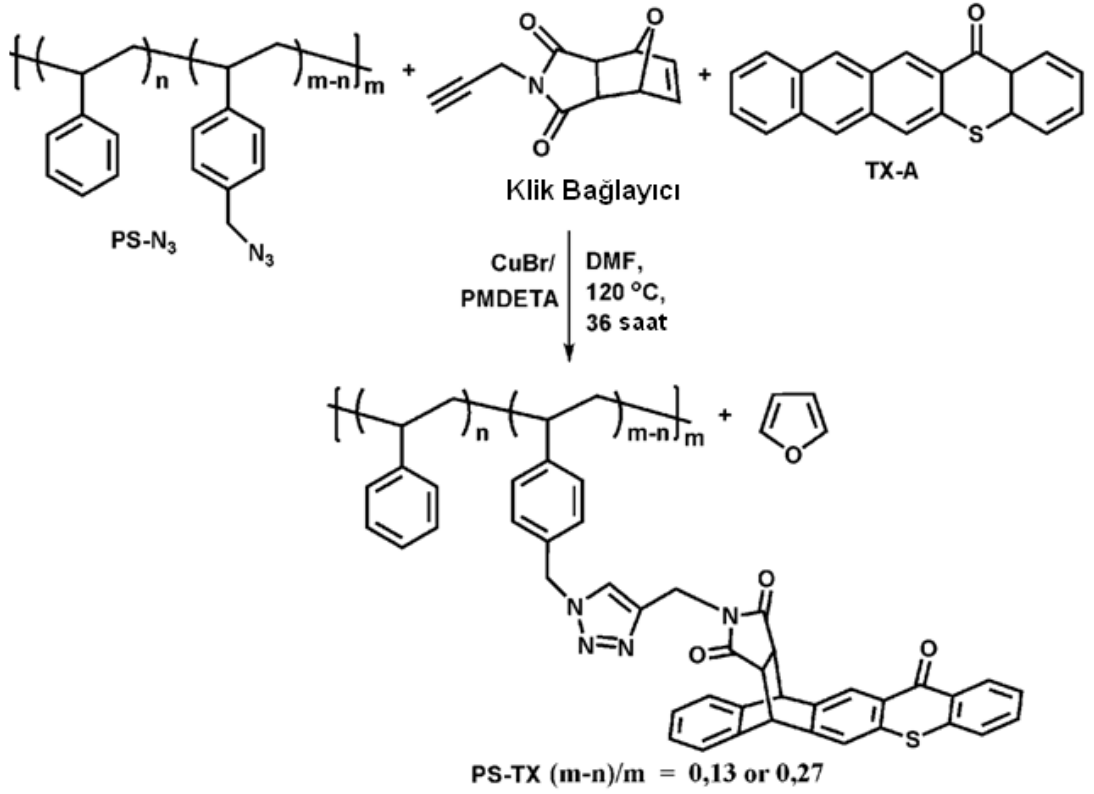
Tezin ilk bölümünde sunulan çalışma, iyi-tanımlı bir aşırı copolimerler hazırlamak için yeni bir rota olarak antrasen-maleimid bazlı DA “klick reaksiyonunu” açıklamayı hedeflemektedir.

Şekil 1 çalışmanın değişik evrelerini içeren sentetik stratejisini özetlemektedir; (i) stiren (St) ve 4-fonksiyonlanabilen bir monomer olan klorometilstiren’in (CMS) rastgele copolimerlerinin hazırlanması; (ii) antrasen fonksiyonlitesinin sentezlenen copolimerlere o-eterifikasyon prosedürü ile bağlanması; (iii) MMA’nın ATRP metodu ile maleimid-fonksiyonlandırılmış poli(metil metakrilat) (PMMA-MI) veya ticari PEG’in modifikasyonu ile elde edilen maleimid-fonksiyonlandırılmış poli(etilen glikol) etkin DA “klick kimyası” ile antiril yan gruplarına sahip copolimerlere katılmıştır.



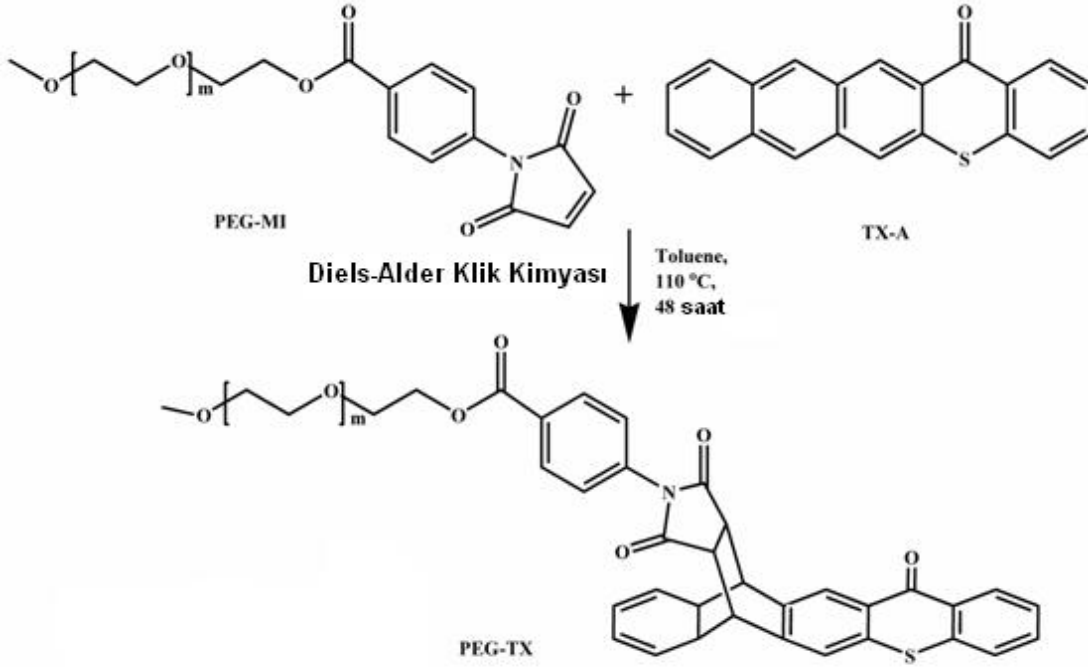
**Şekil 1:** Diels-Alder “Klick Kimya”sı metodu ile aşılama prosesinin genel gösterimi.

Tezin ikinci bölümünde, yan zincirinde tioksanton (TX) içeren makrofotobaşlatıcılar. aynı anda 1,3-dipolar azid-alkin [3 + 2] ve ısıl-tersinir Diels–Alder (DA) [4 + 2] siklokatalıma reaksiyonlarını uygulayarak "çift klik kimya"sı stratejisi ile sentezlenmiştir. Bu amaçla, tioksanton-antrasen (TX-A), N-propargil-7-oxynorborene (PON) ve yan zincirinde azid içeren polistiren (PS) (PS-N<sub>3</sub>) N, N-dimetilformamid (DMF) içerisinde 120 ° C'de 36 saat reaksiyona sokulmuştur. Bu proseste, PON "klick bağlayıcı"olarak hem korumalı maleimid hem de alkin fonksiyonel grupları ile sırasıyla 1,3-dipolar azid-alkin ve Diels-Alder klik reaksiyonlarını gerçekleştirmiştir. Bu şekilde, TX-A yapısında bulunan antasenin merkezi fenil biriminin aromatisitesi TX kromoforik grubuna dönüşmüştür. Sonuç polimerlerin absorpsiyon özellikleri temel TX'la benzerdir. Yapıların fotobaşlatıcı olarak yetenekleri metil metakrilat (MMA) ve 1,1,1-tris(hidroksimetil)propan gibi mono ve çok fonksiyonlu monomerler üzerinde incelenmiştir.



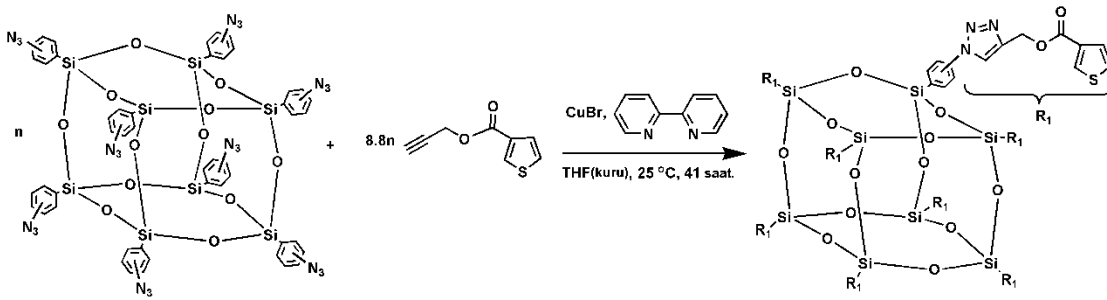
**Şekil 2:** Klik bağlayıcı olarak kullanılan *N*-propargil-7-oksinorborn (PON) varlığında çift klik kimyası metodu ile antrasen-tioksanton ile (TX-A) PS-N<sub>3</sub>'in yan-zincir fonksiyonlandırılması.

“Klik Kimyası” metodu ile fotobaşlatıcı sistemleri geliştirme konusundaki sürekli ilgimizin bir parçası olarak, tezin üçüncü bölümünde suda çözünebilen ve TX uç grubu içeren poli(etilen glikol) (PEG) makrofotobaşlatıcısı Diels-Alder klik reaksiyonu ile sentezlenmiştir. Sonuç polimer poli(etilen glikol)-tioksanton (PEG-TX) ve ara yapılar detaylı spectral analizlerle karakterize edilmiştir. PEG-TX hem ışık absorblayan (TX) hem de hidrojen verici (PEG) özelliklere aynı yapı içerisinde sahip olup, tek bileşenli karakter gösterir. Makrofotobaşlatıcı akrilik asit, akrilamid, 2-hidroksi akrilat ve 1-vinil-2-pirolidon gibi çeşitli hidrofilik vinil monomerlerin fotopolimerizasyonunda kullanılmıştır.



**Şekil 3:** Tek bileşen karakterli polimerik fotobaşlatıcının Diels-Alder klık kimyasıyla sentezlenmesi.

Son olarak, polipirolün elektrokromik özelliklerini geliştirmek için, klık kimyası metodu ile tiyofen içeren OPS nano kafes yapılarına etkin bir şekilde polipirol takılarak yeni bir yaklaşım tanıtıldı. Bizim ilk hedefimiz octa(aminofenil) silsesquioxane ( $ONH_2PS$ ) küplerinden diazonyum tuzları üzerinden octa(azidofenil) silsesquioxane ( $ON_3PS$ ) sentezlemek ve elektroaktif bir molekül olan “propargiltiyofen”i basit ve etkin bir yol olan “klık kimyası” metoduyla yapıya takmaktır. Bu yaklaşım, sadece polipirol değil aynı zamanda geniş bir yelpazedeki monomerlerin fonksiyonel POSS ile kopolimerizasyonu sonucu oluşacak polimerlere de kolaylıkla uygulanabilir.



**Şekil 4:** Klık kimyası metoduyla OTiyofenPS sentezi.

## 1. INTRODUCTION

The development of materials with enhanced properties at the molecular level is the premier challenge of the 21st century. In an effort to meet this challenge, “click” chemistry, the recent advanced of Cu(I)-catalyzed Huisgen 1,3-dipolar cycloaddition of azides and terminal alkynes to form the five-membered (1,2,3)-triazole heterocycle, has been proposed by Sharpless et al.[1,2] This approach brings an enormous potential in material science. The key features in “click” chemistry is represented by quantitative yields, high tolerans of functional groups, simple product isolations, lack of by-product, superior regioselectivity, and mild and simple reaction conditions. The development and the application of click chemistry in polymer and material science are extensively reviewed in recent articles [3].

There has been revitalized interest in the development and applications of novel polymeric photoinitiators. This is mainly associated with the advantages derived from their macromolecular nature. In comparison with their low-molecular weight analogues, the presence of the polymer chain in the polymeric photoinitiator in many cases improves compatibility in the formulation and reduces the migration onto the film surface. Moreover, odor and toxicity problems do not occur with macrophotoinitiators owing to the low volatility of the large molecules. Polymeric photoinitiators [4,5] can be defined as macromolecular systems that possess chromophoric groups either in the main or side chain, which may be accomplished in two ways: (i) synthesis and polymerization of monomers with photoreactive groups and (ii) introduction of photoactive groups into polymer chains. In the latter case, macrophotoinitiators were synthesized by using functional initiators and terminators in a particular polymerization or by reacting functional groups of a preformed polymer with other functional groups of low-molecular weight compounds possessing also photoreactive groups. Macrophotoinitiators, analogous to the low-molecular weight photoinitiators, are divided into two classes, according to their radical generation mechanism, namely cleavage type (*Type I*) and hydrogen abstraction-type (*Type II*) macrophotoinitiators. Most of this research has focused on

*Type I* photoinitiators, which upon irradiation undergoes an  $\alpha$ -cleavage process to form two radical species. *Type II* photoinitiators are a second class of photoinitiators and are based on compounds whose triplet excited states are reacted with a hydrogen donor there by producing an initiating radical.

Electrically conducting polymers [6] such as polyacetylene, polypyrrole, polythiophene and polyaniline have been the subject of intensive research due to their useful electronic properties and for their application in optoelectronic and display devices, and as active electrode materials in primary and secondary batteries. The factor that has motivated much of the work on the synthesis of conducting polymers is the need to find newer materials having a wide range of physical properties such as flexibility and processibility, and conductivity close to that of metals to suit many technological applications.

The incorporation of electroactive sites into polymers is proposed to be a versatile route to improve the physical properties of the conducting polymers. Various controlled polymerizations has been previously used for the preparation of such macromonomers. Obviously, these macromonomers were further used in electropolymerization in conjunction with the low molar mass monomers such as pyrrole and thiophene.

The study presented in this thesis is aimed at describing the (I)-catalyzed azide-alkyne (CuAAC) and Diels-Alder (DA) cycloaddition “click” reactions as a novel route to prepare well-defined graft copolymers [7], polymeric photoinitiators [4,8] and reactive precursors for obtaining inorganic–organic conducting composites [9]. The strategy adopted in this study appears to be entirely satisfactory in terms of efficiency and simplicity.



## 2. THEORETICAL PART

### 2.1 Click Chemistry

“Click chemistry” is a chemical term introduced by Sharpless in 2001 [10] and describes chemistry tailored to generate substances quickly and reliably by joining small units together. Click chemistry [11] can be summarized only one sentence: *Molecules that are easy to make*. Sharpless also introduced some criteria in order to fulfill the requirements as reactions that: are modular, wide in scope, high yielding, create only inoffensive by-products, are stereospecific, simple to perform and that require benign or easily removed solvent. Nowadays there are several processes have been identified under this term in order to meet these criterias such as nucleophilic ring opening reactions; non-aldol carbonyl chemistry; thiol additions to carbon-carbon multiple bonds (thiol-ene and thiol-yne); and cycloaddition reactions. Among these selected reactions, copper(I)-catalyzed azide-alkyne (CuAAC) and Diels-Alder (DA) cycloaddition reactions and thiol-ene reactions have gained much interest among the chemists not only the synthetic ones but also the polymer chemists. From this point view, these reactions will shortly be summarized.

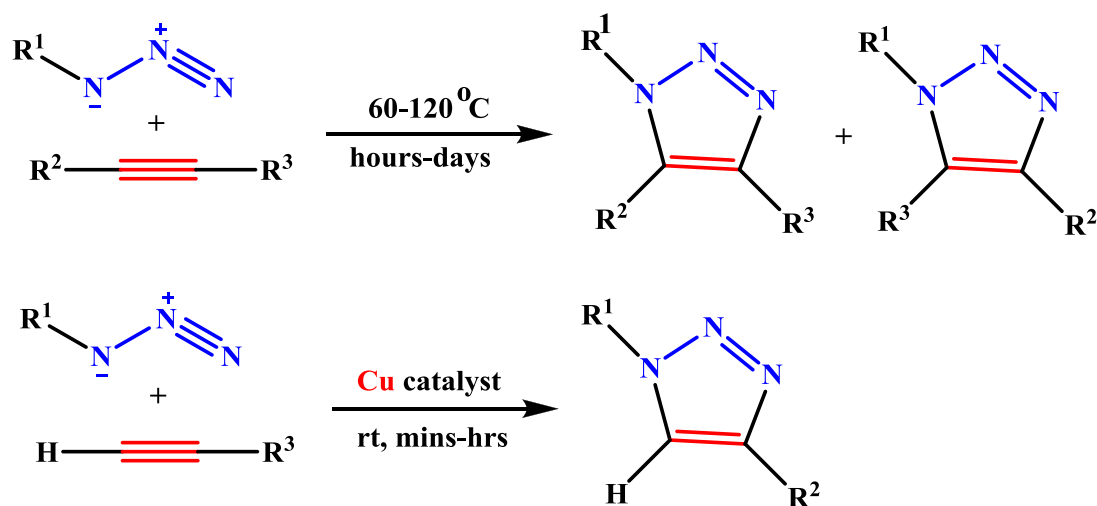
#### 2.1.1 Copper(I)-catalyzed azide-alkyne cycloaddition (CuAAC)

1,3-Dipolar cycloaddition reactions [12] have also been the subject of intensive research, most notably by Rolf Huisgen and co-workers in the 1950s to the 1970s. [13,14], whose work led to the formulation of the general concepts of 1,3-dipolar cycloadditions [12,15]. The process is strongly thermodynamically favored ( $\Delta H^\circ = -45$  to  $-55$  kcal/ mol) due to the high potential-energy content of the two reaction components, but has a relatively high kinetic-energy barrier (ca. 26 kcal/mol for methyl azide and propyne [12,16]) that renders the reaction cycloaddition chemistry has found widespread applications in organic synthesis and has been the subject of several reviews.

Cu(I) catalysis of the Huisgen 1,3-dipolar cycloaddition reaction [17,18] of organic azides and alkynes was introduced in 2001 by Tornøe and Meldal.[19] The Cu(I)

catalysis has transformed this cycloaddition into an essentially quantitative and regioselective “click” reaction, as realized independently by the Meldal and the Sharpless laboratories.[ 20-22]

The **Cu**-catalyzed azide–alkyne 1,3-dipolar cycloaddition (CuAAC) dramatically accelerates the reaction of azides with terminal alkynes (**Figure 2.1**) and exhibits several features. It is very robust, general, insensitive, and orthogonal to most other chemistries used in synthesis of polymers [22].



**Figure 2.1** : General representation of thermal and copper catalyzed cycloaddition [12].

The uncatalyzed thermal cycloaddition of azides to alkynes usually requires prolonged heating and results in mixtures of the 1,4- and 1,5-disubstituted regioisomers. In contrast, CuAAC produces only 1,4-disubstituted-1,2,3-triazoles at room temperature in excellent yields [12].

1. The reaction is not significantly affected by the steric and electronic properties of the groups attached to the azide and alkyne reactive centers. For example, azides carrying a primary, secondary, or tertiary group; electron-deficient or electron-rich group; and aliphatic, aromatic, or heteroaromatic substituent usually react well with variously substituted terminal alkynes [12].
2. The reaction is unaffected by water and by most organic and inorganic functional groups; thus, all but eliminating the need for protecting-group chemistry [12].
3. The rate of the Cu-catalyzed process is approximately  $10^7$  times that of the uncatalyzed version, making the reaction conveniently fast in the temperature range

of 0 to 25 °C. Furthermore, ligand-accelerated-catalysis effects [12, 23] are also significant, resulting in further increases in the reaction rate [12].

4. The 1,2,3-triazole unit that results from the reaction has several advantageous properties:

(i) a high chemical stability (in general, being inert to severe hydrolytic, oxidizing, and reducing conditions, even at high temperature),

(ii) a strong dipole moment (5.2–5.6 D),

(iii) an aromatic character, and

(iv) a good hydrogen-bond-accepting ability [24,25].

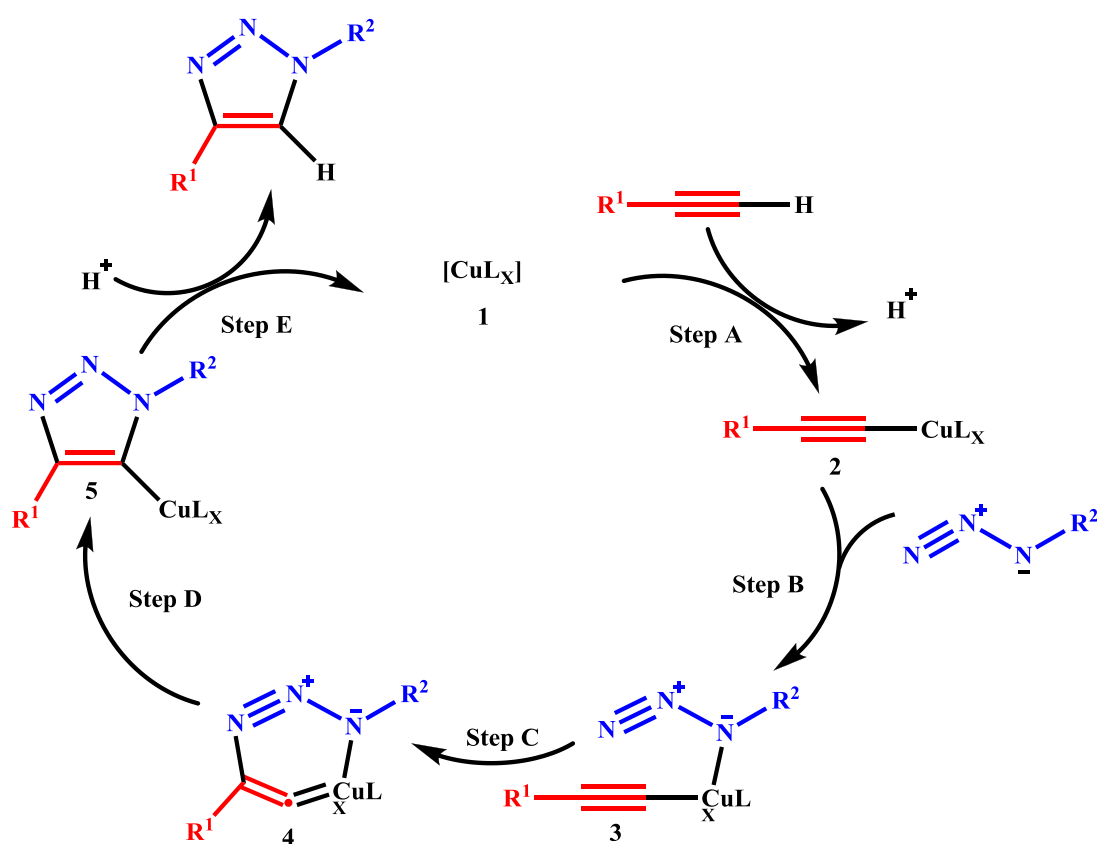
Thus, it can interact productively in several ways with biological molecules, and serve as a replacement for the amide linkage in some circumstances [12].

#### 2.1.1.1 Mechanistic considerations on the Cu(I) catalysis

A mechanistic picture of the copper catalyzed reaction was first proposed by Meldal and co-workers [26] and Sharpless and co-workers, [21,27] and has later been verified by computational methods [28-30].

The intermediacy of copper(I) acetylides in CuAAC was postulated early on based on the lack of reactivity of internal alkynes. Soon thereafter, a computational study of the elementary steps of the sequence was performed. The initial computations focused on the possible reaction pathways between copper(I) acetylides and organic azides (propyne and methyl azide were chosen for simplicity) [31]. The key bond-making steps are shown in Figure 2.2 [12]. The formation of copper acetylide 2 (Step A) was calculated to be exothermic by 11.7 kcal/mol. This is consistent with the well-known facility of this step, which probably occurs through the intermediacy of a  $\pi$ -alkyne–copper complex. The  $\pi$  coordination of an alkyne to copper is calculated to move the pKa of the alkyne terminal proton down by ca. 10 units, bringing it into the proper range to be deprotonated in an aqueous medium. A concerted 1,3-dipolar cycloaddition of the azide to the copper acetylide has a high calculated potential energy barrier (23.7 kcal/mol), thus the metal must play an additional role. In the proposed sequence, the azide is activated by coordination to copper (Step B), forming the intermediate 3. This ligand exchange step is nearly thermoneutral computationally (2.0 kcal/mol uphill when L is a water molecule). The key bond-

forming event takes place in the next step (Step C), when 3 is converted to the unusual 6-membered copper metallacycle 4. This step [12] is endothermic by 12.6 kcal/mol with a calculated barrier of 18.7 kcal/mol, which is considerably lower than the barrier for the uncatalyzed reaction (approximately 26.0 kcal/mol), thus accounting for the enormous rate acceleration accomplished by Cu(I). The CuAAC reaction is therefore not a true concerted cycloaddition, and its regioselectivity is explained by the binding of both azide and alkyne to copper prior to the formation of the C–C bond. The energy barrier for the ring contraction of 4, which leads to the triazolyl–copper derivative 5, is quite low (3.2 kcal/mol). Proteolysis of 5 releases the triazole product, thereby completing the catalytic cycle [12].



**Figure 2.2 :** Proposed catalytic cycle for CuAAC. The density functional theory (DFT) investigation described [12,31,32].

The density functional theory (DFT) investigation described above was soon followed by an examination of the kinetics of the copper-mediated reaction between benzyl azide and phenylacetylene. This study revealed that, with catalytic Cu(I) concentrations under saturation conditions (rate independent of the alkyne concentration), the reaction was second-order in copper [12, 33]

$$\text{rate} = k[\text{alkyne}]^0[\text{azide}]^{0.2\pm 0.1}[\text{Cu}]^{2.0\pm 0.1} \quad (2.1)$$

The second-order dependence on Cu(I) is not unreasonable since most copper(I) acetylides are highly aggregated species, [22,44] and the second copper atom might be present, and in fact required, in the metallacycle-forming step. A recent DFT study suggests that this is indeed the case [22,45].

### 2.1.1.2 The Cu(I) Source

The formation of triazoles from azides and terminal alkynes catalyzed by Cu(I) is an extraordinarily robust reaction, which could be performed under a wide variety of conditions and with almost any source of solvated Cu(I) [36,37].

Provided the reactants are maintained in solution or even as a mixture in a glassy state [38] or aggregate [39,40] and the Cu(I) has not been removed by disproportion or oxidation to Cu(II), the product is usually formed in very high yields. The most important factor seems to be that of maintaining the [Cu(I)] at a high level at all times during reaction [36]. This is why the use of a Cu(II) source with addition of a reducing agent in a large excess has been one of the preferred methods. The presence of reducing agent renders the reaction much less susceptible to oxygen, and such reactions have often been carried out under open-air conditions. However, as detailed below, this is not always without problems, due to potential oxidative side reactions [36].

CuBr is by far the most common source for Cu(I) used for triazole mediated polymerization and in polymer ligation particularly in combination with the promoter PMDETA [22]. Similar conditions are often used in the ATRP polymerizations and may be the origin of this preference; however, the conditions seem robust and lead to high molecular weights when employed for e. g. polymerizations based on repetitive triazole formation [22,41]. The purities of the copper halide have a large influence on both reaction rate and completion of the reaction.[22, 42–45] CuBr is most soluble in hydrolytic solvents, and recently the superior performance of CuBr in aqueous in vivo ligation has been demonstrated.[22, 44,46]

Tornøe and Meldal [47] originally used CuI due to its partial solubility in solvents of intermediate polarity such as acetonitrile, THF, acetone, pyridine and DMSO and is particularly suited for anhydrous conditions [22,48,49]. CuI was employed in a highly optimized protocol for repetitive triazole formation on solid support. Here

high concentration of piperidine and addition of a reducing agent was found to be essential for the quantitative formation of peptide-like triazole based oligomers [22, 50]. The use of polymer bound CuI described by Girard et al.[51] is an attractive alternative that allows catalyst recycling.

Aqueous conditions introduced originally by Rostovtsev *et al.* [52] are extremely useful in biochemical ligations and may be employed for connection of water soluble polymers through triazole ligation [22]. The most common aqueous conditions employ CuSO<sub>4</sub> and a reducing agent such as ascorbate or tris(2-carboxyethyl)phosphine (TCEP) or the use of Cu(0) (wire, turnings, powder or nanoparticles) with or without addition of CuSO<sub>4</sub> [22].

As the reductant, ascorbic acid and/or sodium ascorbate proved to be excellent [53] for they allow preparation of a broad spectrum of 1,4-triazole products in high yields and purity at 0.25 ± 2 mol% catalyst loading. The reaction appears to be very forgiving and does not require any special precautions. It proceeds to completion in 6 to 36 hours at ambient temperature in a variety of solvents, including aqueous tert-butyl alcohol or ethanol and, very importantly, water with no organic co-solvent. Although most experiments were performed at near neutral pH values, the catalysis seems to proceed well at pH values ranging from approximately 4 to 12. In other words, this is a very robust catalytic process, which is so insensitive to the usual reaction parameters as to strain credulity [54].

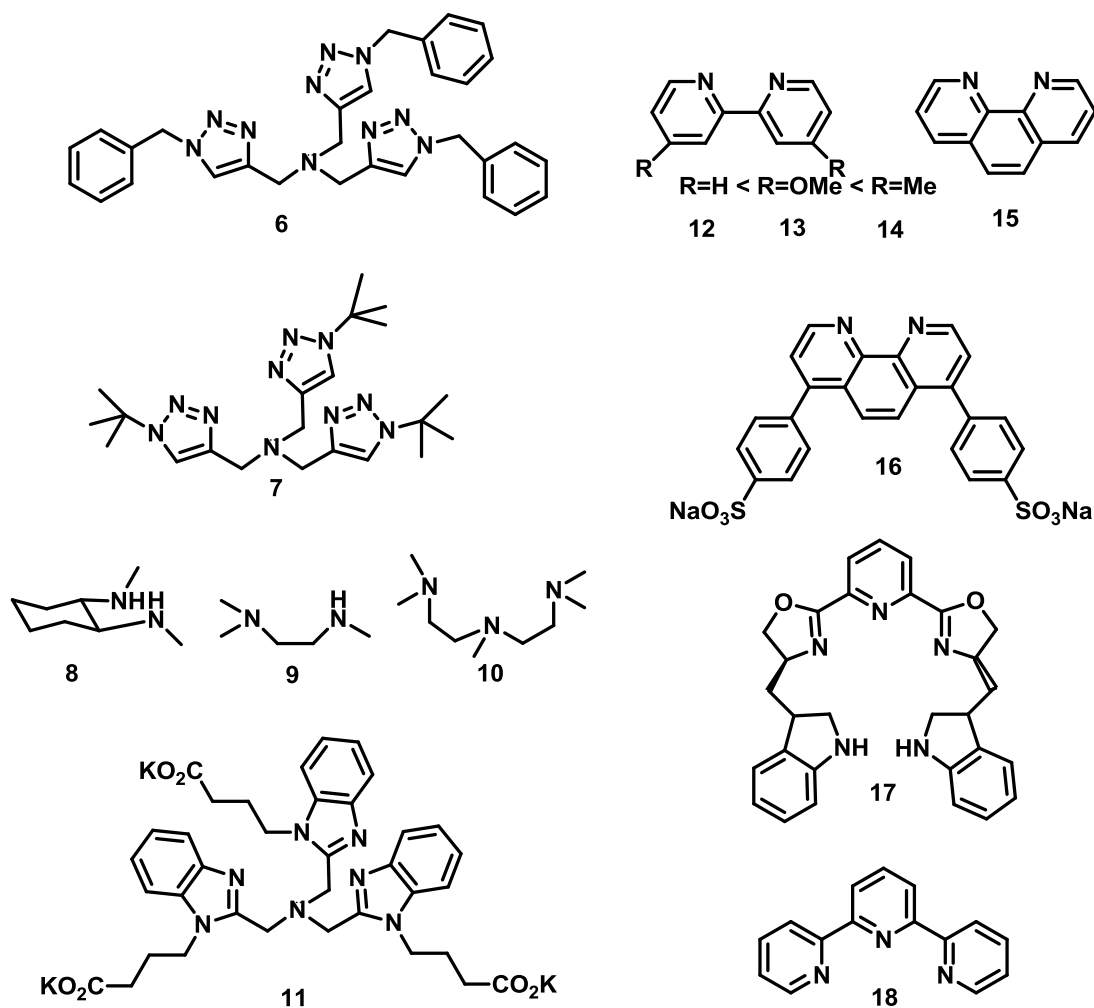
A large difference is observed between the dependence of base in the application of CuSO<sub>4</sub> and Cu(I)-halide salts [36]. While the catalytically active Cu(I) species is directly generated by reduction with ascorbate and immediately forms Cu-acetylides, the CuI and CuBr salts require at least an amine base (TBTA and other nitrogen heterocycles do not provide sufficient basicity) or high temperature to form the Cu-acetylide complexes [36]. This difference may be due to the fact that e.g. CuI initially occurs in stable clusters (e.g. Cu<sub>5</sub>I<sub>5</sub> in CH<sub>3</sub>CN) and that these require a certain concentration of acetylide anion before the reactive complex can form [36]. Ultrasonication greatly enhances the CuI catalyzed reaction even in absence of base [55].

There is a range of other Cu(I) sources that have been introduced for increased solubility in organic solvents ([Cu(CH<sub>3</sub>CN)<sub>4</sub>] PF<sub>6</sub>, (EtO)<sub>3</sub>P:CuI, Cu(CH<sub>3</sub>CN)<sub>4</sub>OTf) or for improved reactivity (Cu(OAc)<sub>2</sub>) as compared to CuSO<sub>4</sub> [22,56].

It should be remembered that the noncatalyzed Huisgen reaction occurs at elevated temperature and in the case of reactive substrates even at ambient temperature with significantly prolonged reaction times [36]. However, Cu(I) catalyzes the reaction with a rate enhancement of  $\sim 10^7$  even in the absence of auxiliary ligands and provides a clean and selective conversion to the 1,4 substituted triazoles even under microwave or elevated temperature conditions [36]. The use of microwave irradiation has significantly shortened reaction times, to minutes, with excellent yields and purities and exclusive formation of the 1,4 isomer [36, 57].

### **2.1.1.3 The influence of ligands on Cu(I) catalysis**

Although ligands are by no means required for the catalytic effect of Cu(I) in triazole formation, they are often employed both to enhance the rate of reaction and to protect the Cu(I) from oxidation in the presence of adventitious oxygen [36]. There may be a range of mechanistic effects of the use of ligands that coordinate the Cu(I) catalysts in the triazole formation. The protection from oxidation of the catalyst is of course important to maintain a good concentration of the catalytically active complexes throughout reaction [36]. However, the direct effects on catalysis can be considerable. These effects can be due to a direct influence on the catalytic complex involved in the reaction; that is, the ligand is coordinated to Cu(I) during the catalytic process [36]. While this is the general understanding, it is important in all mechanistic considerations to keep in mind the second order kinetics observed with respect to [Cu(I)] that is not easily explained in a model with a ligand, e.g. 6 or 7 that saturate the coordination of Cu(I) with four chelating lone-pairs [36]. In fact, a rate reducing effect has been observed by addition of tetravalent ligands to click-polymer reactions catalyzed by CuBr, 8 and particularly so by ligands containing multiple pyridines. The ligands, which have been found to be the most effective in catalysis, are presented in Figure 2.3 [36].



**Figure 2.3 :** Effective ligands used to promote the Cu(I) catalyzed triazole formation [36].

TBTA, 6, and bathophenanthroline, 15, are mostly used for organic synthesis and bioconjugations while PMEDTA, 10, is predominant in polymer chemistry [36].

One aspect of the catalysis is the presence of a variety of Cu(I)-ligand clusters in the reaction medium [22]. The equilibrium between these clusters is slow and may depend significantly on the exact reaction conditions at all times. When purified CuI is dissolved in acetonitrile, the major component according to ESI-MS is initially  $\text{Cu}_4\text{I}_5^-$ , however, this is in equilibrium with smaller quantities of  $\text{CuI}_2^-$ – $\text{Cu}_7\text{I}_8^-$ . If the more catalytically active cluster is different from  $\text{Cu}_5\text{I}_5$ , presence of a ligand could affect rate of reaction [22]. The presence of ligands may have an effect on both the equilibrium distribution and the rate of equilibration amongst the clusters to substantially enhance the rate of reaction on its own by promoting the presence of the most active clusters [22].



Interestingly, the catalytic effect of e.g. the bathophenanthroline disulfonate ligand 16 is optimal with addition of 2 equiv of catalyst while addition of excess is suppressing the catalytic effect in a [Cu(I)] dependent manner [36, 58]. Similar effects are observed with the most popular ligand TBTA introduced by Sharpless [36,59]. Recently, the oligobenzimidazole ligands e.g. 18 corresponding to TBTA in architecture were shown to be extremely efficient to protect Cu(I) against disproportionation and effect catalysis [36,60]. More than 1 active species was involved in catalysis according to the response to variations in salt and the pH of the reaction.

#### **2.1.1.4 Reactivity of the alkyne and azide substrates**

The unhindered terminal coordination of the two reactants to the catalytic Cu(I) cluster as a starting point for the reaction provide for catalysis of triazole formation almost independently of the substrate substitutions [22]. Most significant are the electronic effects that influence the formation of the Cu(I) acetylides and the establishment of the transition state of the reaction. However, the reaction partners can usually be forced to form the triazole [22, 61].

With increasing size of both alkyne and azide substrates in e.g. conjugation of azide containing proteins with large fragments of DNA containing alkyne with the inherently more dilute reaction conditions used in such reactions, conversions have been observed to decrease and be less than optimal [36,62].

This indicates that there could be limiting cases where the utility of this ligation reaction may not be optimal although new improved conjugation conditions are continuously being developed [22,63].

Organic azides are considerably more reactive than the azide anion itself, as explained above. This has allowed the development of one-pot procedures in which  $\text{NaN}_3$  is first reacted with an arylhalide followed by formation of a 1,4-substituted triazole [36,64].

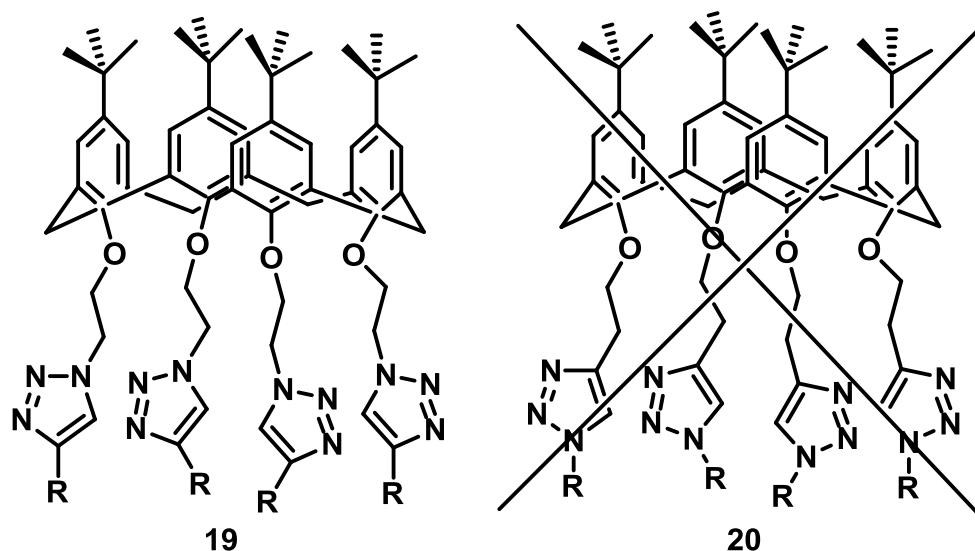
The azides are generally reactive, and only carboxylazides and sulfonylazides require special attention due to substrate instability [36,65]. Somewhat lower reactivity is observed for perfluoroalkylmethylazides [36,66]. A special situation is that of substituted allylic azides, since these are very prone to 1,3-sigmatropic rearrangements at significant rates exceeding those of triazole formation [36,67]. The

allylic azides have a preference for triazole formation from the primary and secondary azides compared to the tertiary, thus indicating some steric effect on the rate of triazole formation. On the other hand, only little difference was observed in the rate difference between primary and secondary azides, indicating again the terminal coordination of azide to Cu in the transition state [36].

Similarly to the Huisgen reaction, [68]  $\alpha$ -carbonyl-alkynes are more reactive than alkyl-alkynes, while the aromatic alkynes are similar or marginally less reactive. Keeping the reactants soluble throughout the reaction is a key requirement for a successful outcome [36,69]. Direct substitution of the alkyne with heteroatoms gives some substrate instability, particularly toward hydrolysis, but they do react to give triazoles under appropriate conditions [36].

#### **2.1.1.5 Proximity effects in the efficiency and rate of the triazole formation**

Several groups have reported significant rate enhancements in the formation of triazole when the azides are linked together on a polymer [36,70], dendrimer, or calixarene [36,71]. The effect is much less pronounced if it is the alkynes that are grouped together on a scaffold, and in the particular case of high density of alkyne, even suppression of triazole formation can be observed [36,71]. This effect was also studied from a mechanistic point of view, [72] as reviewed by Bock et al [73]. The proximity effects are particularly large in an arrangement of scaffolded azides where the catalytic Cu(I) complex leaving a completed cycle of triazole formation and already recruiting and coordinating the next alkyne from the solution encounters a very high local azide concentration in preparation of, e.g., 19 (Figure 2.4) [72,73]. In contrast, complete failure was observed in producing the triazole product, 20, from scaffolded alkyne, and this is most likely due to three important effects [36]. The alkyne is ideally situated to engage in Cu (I) catalyzed homocoupling, the alkyne is also reactive as an electrophile in coupling to the newly formed Cu(I)- coordinated neighbouring triazole, and finally, the presence of four alkynes may saturate the coordination sphere of the catalytic Cu(I) complex [36]. The formation of by products by the first two routes probably prohibits the use of increased temperature as a means to overcome reduced catalysis. Although this is a special case of preorganization of alkyne, it should call for special consideration in situations with high density of alkyne [36].

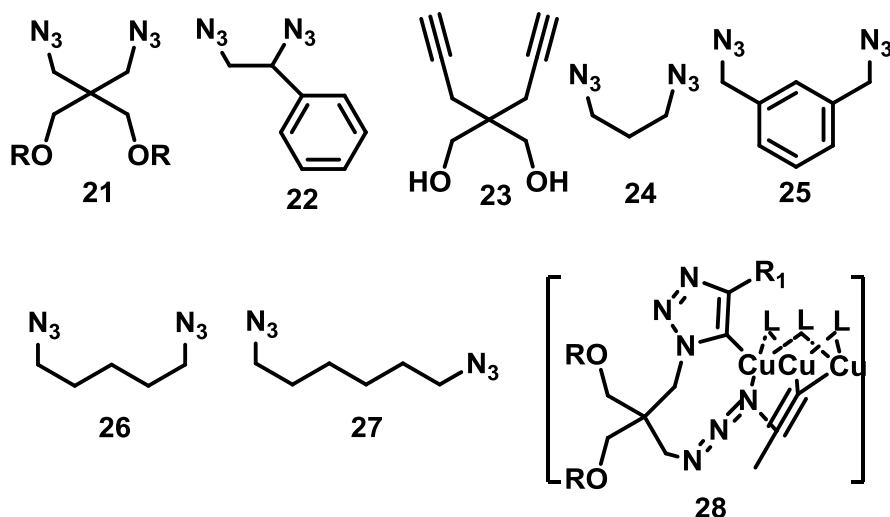


**Figure 2.4 :** Proximity effects in the efficiency and rate of the triazole formation on calixarenes [36].

For calixarenes decorated with azidoethyl ethers the Cu(I) catalyzed reaction with alkynes forms four triazoles simultaneously in a total yield of 80% while the same calixarene decorated with alkynes failed to give the expected product [36, 72,73].

In polymers containing multiple statistically distributed azides, where molecular tumbling is slow and a decrease in reactions rate is expected as compared to the rate of small molecules monomers, considerable rate enhancements (e. g. fourfold) can be observed [22]. This demonstrates the generality of the conformation independent pseudo-concentration effect for templated azides [22,74].

Extreme rate enhancement was observed for formation of the second triazole in compounds 21 and 22 (Figure 2.5) that results in near complete suppression of the monotriazole [36]. Whether this is of a similar nature as the general effect above or if transfer of the second azide to prebound acetylene occurs intramolecularly in a complex such as 28 in Figure 2.5 has not yet been determined. In any event, a high degree of preorganization of intermediates is required for significant suppression of monotriazole, since even structurally similar diazides such as 24 show an almost statistical distribution of products. It is important to note that the situation with bis-alkyne 23 is completely different from that of the bisazide 21, since the formation of the acetylide does not seem to be rate determining in the Cu(I) catalyzed triazole formation and a statistical distribution of products is to be expected [36].



**Figure 2.5** : Bis-azide compounds [36].

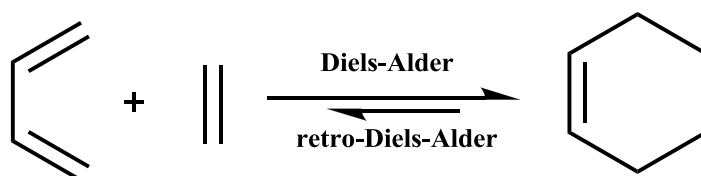
Bis-azides 21 and 22 gave considerable rate enhancement for formation of the second triazole. Compounds 23-27 do not have this ability to any significant extent. The rate enhancement could occur via intramolecular coordination of the second azide to the Cu(I) cluster, leaving the first formed triazole [36].

### 2.1.2 Diels-Alder reaction

The Diels-Alder (DA) reaction is one of the most common reactions used in organic chemistry and is named for Otto Diels and Kurt Alder who received the Nobel Prize in 1950 for their discovery [75].

This reaction is one of the most powerful tools used in the synthesis of important organic molecules. The DA reaction, shown in its general form in Figure 2.6, involves a straightforward [4+2] cycloaddition reaction between an electron-rich diene (furan and its derivatives, 1,3 cyclopentadiene and its derivatives etc.) and an electron-poor dienophile (maleic acid and its derivatives, vinyl ketone etc.) to form a stable cyclohexene adduct [76,77].

The DA cycloaddition reaction not only forms carbon-carbon bonds but also heteroatom-heteroatom bonds (hetero-Diels-Alder, HDA) and is widely used synthetically to prepare six-membered rings [78]. Interesting features of DA reactions (retro-Diels-Alder, rDA) are thermally reversible and the decomposition reaction of the cyclic system can be controlled by temperature [79].



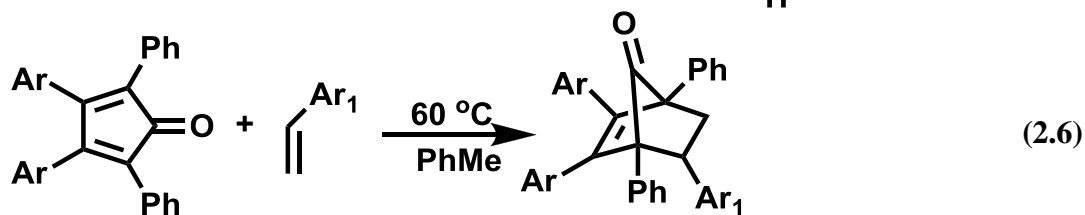
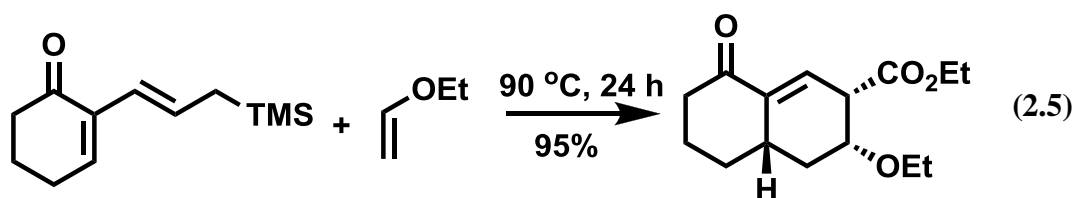
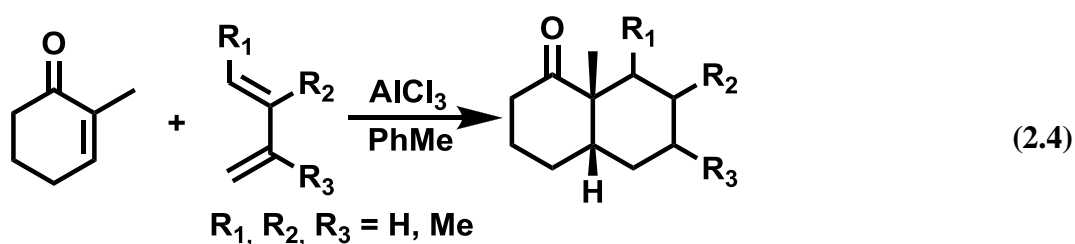
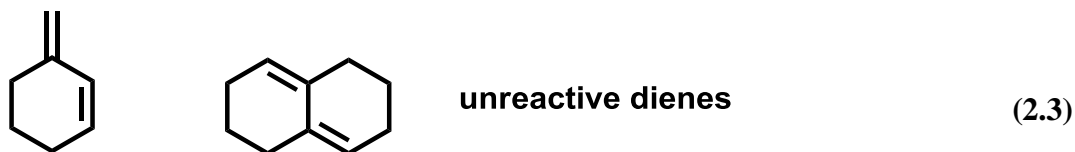
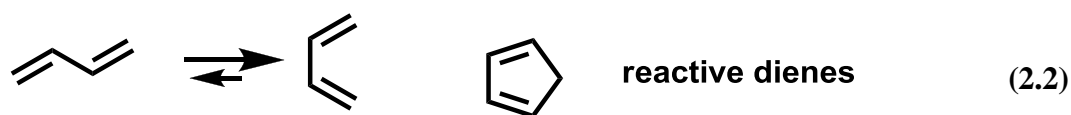
**Figure 2.6 :** General mechanism of Diels-Alder/retro Diels-Alder reactions of dienophile and diene.

### 2.1.2.1 Diene and dienophile

A great variety of conjugated dienes have been used and many of them have been classified in Table 2.1 [80]. Conjugated dienes react providing that the two double bonds have or can assume a *cisoid* geometry (reaction 2.2). A *transoid* diene (reaction 2.2) would give an energetically very unfavorable six-membered ring having a *trans* double bond. Cyclic dienes are generally more reactive than the open chain ones [90]. The electronic effects of the substituents in the diene influence the rate of cycloaddition [80,81]. Electron-donating substituted in the dienes accelerate the reaction with electron-withdrawing substituted dienophiles (*normal electron-demand Diels-Alder reaction*) (reaction 2.3) [80,82], whereas electron withdrawing groups in the diene accelerate the cycloaddition with dienophiles having electron-donating groups (*inverse electron demand Diels-Alder reaction*)(reaction 2.4) [90,93]. Diels-Alder reactions which are insensitive to the substituent effects in the diene and/or dienophile are classified as *neutral*.

**Table 2.1** Representative dienes [80].

Open chain	Outer ring	Inner-outer ring	Across ring	Inner ring

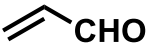

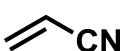

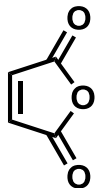
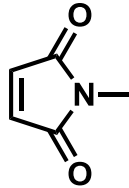
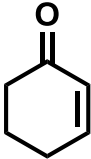
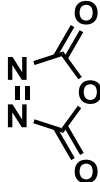
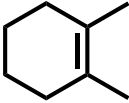

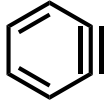
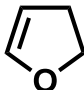
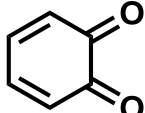


$\text{Ar} = \text{C}_4\text{H}_4\text{Y}$  (Y = H, p-OMe, p-NMe<sub>2</sub>)

$\text{Ar}_1 = \text{C}_6\text{H}_4\text{Y}$  (Y = H, p-OMe, p-NMe<sub>2</sub>, p-Cl, p-NO<sub>2</sub>, m-NO<sub>2</sub>)

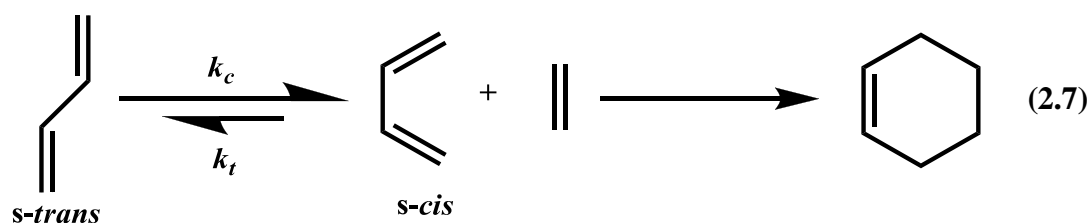
Dienophiles are molecules possessing a double or triple bond. They are more numerous and more varied than dienes [80,84]. Typical dienophiles are illustrated in Table 2.2 [80].

**Table 2.2** Representative dienophiles [80].

Acyclic			Cyclic		
					
$(\text{NC})_2=(\text{CN})_2$	$\text{MeO}_2\text{CCH}=\text{CHCO}_2\text{Me}$				
$\text{H}_2\text{C}=\text{C}=\text{CHMe}$	$\text{HC}\equiv\text{CO}_2\text{Me}$				
$\text{Me}_2\text{C}=\text{S}$	$\text{Ph-N}=\text{O}$	$\text{ArN}=\text{NCN}$			
$\text{O}=\text{O}$	$\text{S}=\text{S}$				

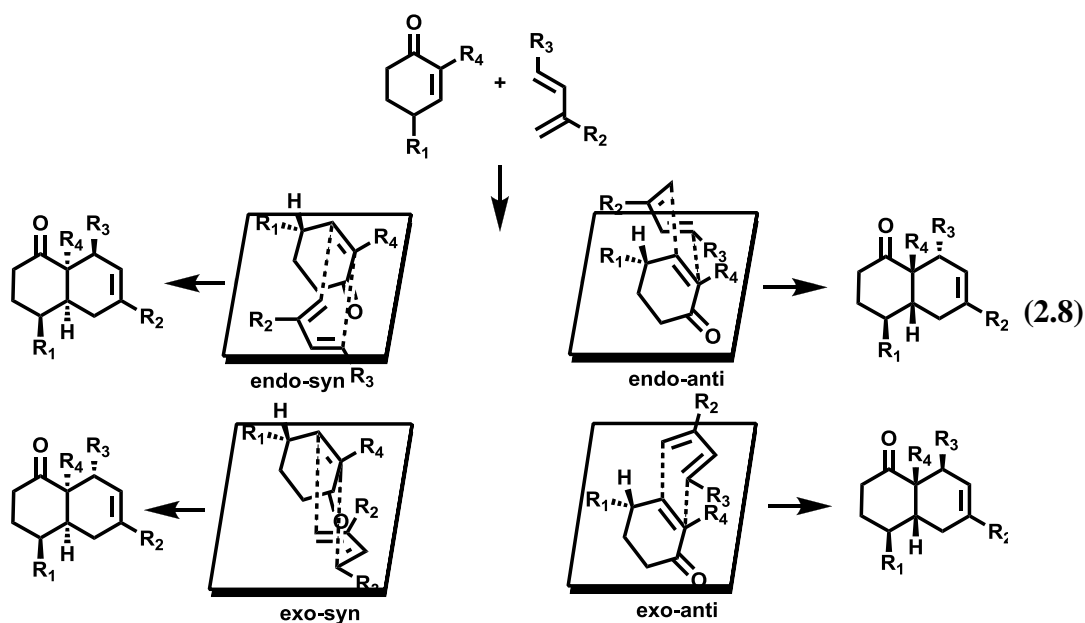
### 2.1.2.2 Stereochemistry of Diels-Alder reaction

There are stereochemical and electronic requirements for the DA reaction to occur smoothly. Many dienes can exist in a *s-cis* and *s-trans* conformation, where  $k_c$  and  $k_t$  are velocity coefficients. The diene must be in an *s-cis* conformation instead of an *s-trans* conformation to allow maximum overlap of the orbitals participating in the reaction (reaction 2.7) [11].



The “s” in *s-cis* and *s-trans* refers to “sigma”, and these labels describe the arrangement of the double bonds around the central sigma bond of a diene. Dienes often exist primarily in the lower energy *s-trans* conformation, but the two conformations are in equilibrium with each other. The *s-cis* conformation is able to react in the DA reaction and the equilibrium position shifts towards the *s-cis* conformer to replenish it [21]. Over time, all the *s-trans* conformer is converted to the *s-cis* conformer as the reaction proceeds. Dienes such as cyclopentadiene that are permanently “locked” in the *s-cis* conformation are more reactive than those that are not [11].

The stereochemistry of the substituents in the new stereogenic centers of the adduct is fixed by two possible suprafacial approaches named *endo* and *exo*[80]. The *endo* mode of attack is the spatial arrangement of reactants in which the bulkier sides of the diene and dienophile lie one above the other, while in the *exo* mode of addition the bulkier side one component is under the small side of the other. If one also considers the regioselectivity and the face selectivity of the reaction, a considerable number of isomers can, in principle, be produced. Reaction 2.8 gives two general pictures. However, the Diels-Alder cycloaddition is known to be a highly selective reaction, and consequently only one or a very limited number of isomers are actually obtained [80].

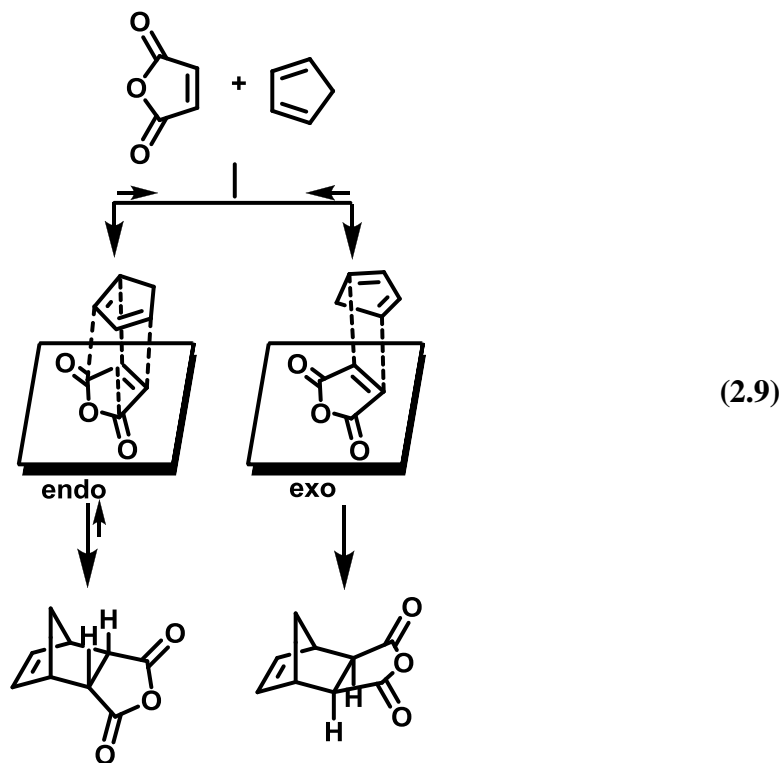


The *exo* addition mode is expected to be preferred because it suffers fewer steric repulsive interactions than the *endo* approach; however, the *endo* adduct is usually the major product because of stabilizing secondary orbital interactions in the transition state (reaction 2.9) [80]. The *endo* preference is known as Alder's rule. Atypical example is the reaction of cyclopentadiene with maleic anhydride which, at room temperature, gives the *endo* adduct which is then converted at 200 °C to the thermodynamically more stable *exo* adduct through a retro Diels-Alder reaction followed by re-addition (reaction 2.9) [80].

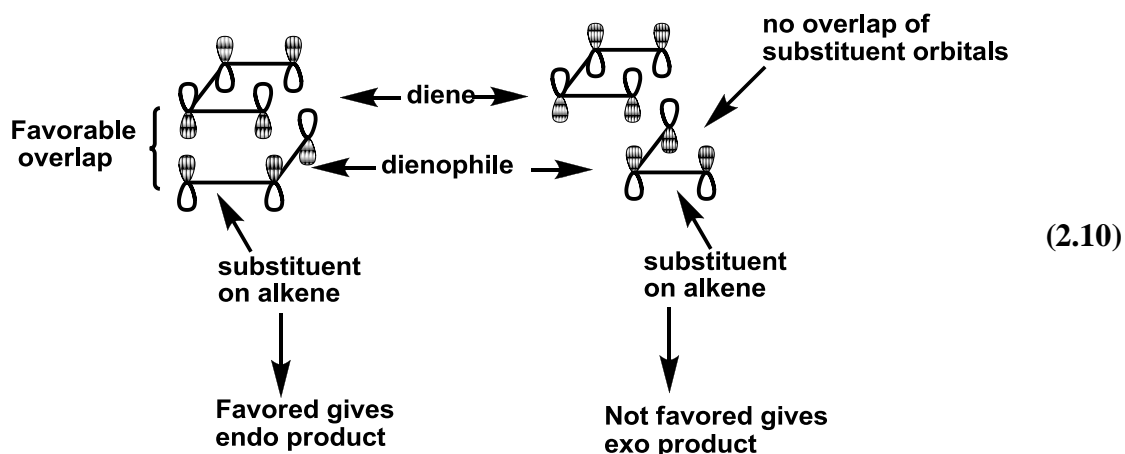


The generally observed endo preference has been justified by secondary orbital interactions, [85a,86,87] by inductive or charge-transfer interactions [88] and by the geometrical overlap relationship of the  $\pi$  orbitals at the primary centers [80,89].

The exo-endo diastereoselectivity is affected by Lewis acid catalysts, and the ratio of two stereoisomers can be explained on the basis of the FMO theory [80,85b,90].



Hoffmann and Fukui shared the 1981 Nobel Prize in chemistry for their molecular orbital explanation of this and other organic reactions. In the illustration below, notice the favorable overlap (matching light or dark lobes) of the diene and the substituent on the dienophile in the formation of the *endo* product (reaction 2.10) [11]:

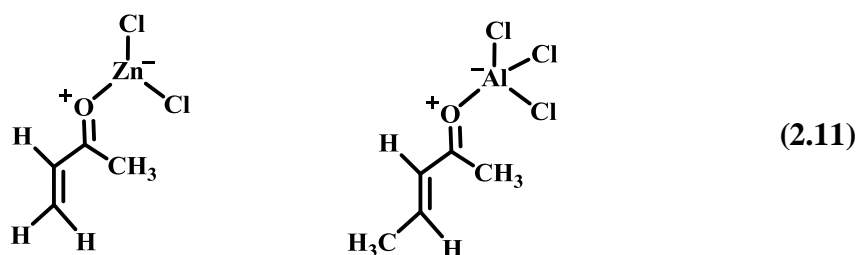


Oftentimes, even though the *endo* product is formed initially, an *exo* isomer will be isolated from a DA reaction. This occurs because the *exo* isomer, having less steric strain than the *endo*, is more stable, and because the DA reaction is often reversible under the reaction conditions [11]. In a reversible reaction, the product is formed, reverts to starting material, and forms again many times before being isolated. The more stable the product, the less likely it will be to revert to the starting material. The isolation of an *exo* product from a DA reaction is an example of an important concept: thermodynamic vs kinetic control of product composition. The first formed product in a reaction is called as the kinetic product. If the reaction is not reversible under the conditions used, the kinetic product will be isolated [11]. However, if the first formed product is not the most stable product and the reaction is reversible under the conditions used, then the most stable product, called the thermodynamic product, will often be isolated [11].

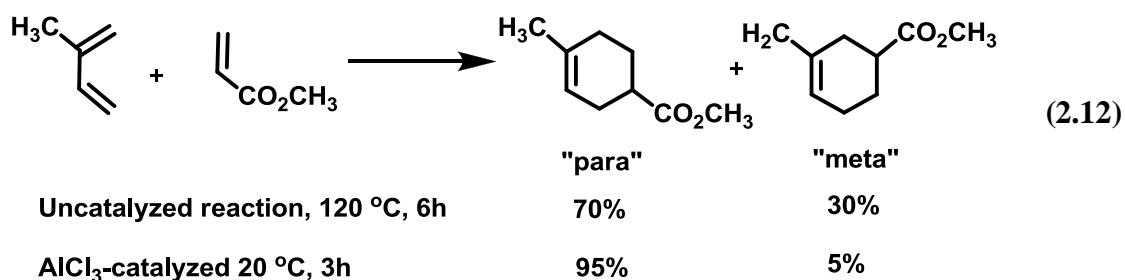
### 2.1.2.3 Catalysis of Diels-Alder reactions by Lewis acids

The discovery that Lewis acids can promote Diels-Alder reactions has become a powerful tool in synthetic organic chemistry [80]. Yates and Eaton [91] first reported the remarkable acceleration of the reactions of anthracene with maleic anhydride, 1,4-benzoquinone and dimethyl fumarate catalyzed by aluminum chloride. The presence of the Lewis-acid catalyst allows the cycloadditions to be carried out under mild conditions, reactions with low reactive dienes and dienophiles are made possible, and the stereoselectivity and site selectivity of the cycloaddition reaction can be modified [80,92]. Consequently, increasing attention has been given to these catalysts in the order to develop new region- and stereoselective synthetic routes based on the Diels-Alder reaction [80].

DA reactions are catalyzed by many Lewis acids, including  $\text{SnCl}_4$ ,  $\text{ZnCl}_2$ ,  $\text{AlCl}_3$ , and derivatives of  $\text{AlCl}_3$  such as  $(\text{CH}_3)_2\text{AlCl}$  and  $(\text{C}_2\text{H}_5)_2\text{AlCl}$  [93]. A variety of other Lewis acids is effective catalysts. The types of dienophiles that are subject to catalysis are typically those with carbonyl substituents. Lewis acids form complexes at the carbonyl oxygen (reaction 2.11) and this increases the electron-withdrawing capacity of the carbonyl group [11,94].



This complexation accentuates both the energy and orbital distortion effects of the substituent and enhances both the reactivity and selectivity of the dienophile relative to the uncomplexed compound [95]. Usually, both regioselectivity and *exo*, *endo* stereoselectivity increases. Part of this may be due to the lower reaction temperature. However, the catalysts also shift the reaction toward a higher degree of charge transfer by making the electron-withdrawing substituent more electrophilic (reaction 2.12) [11].



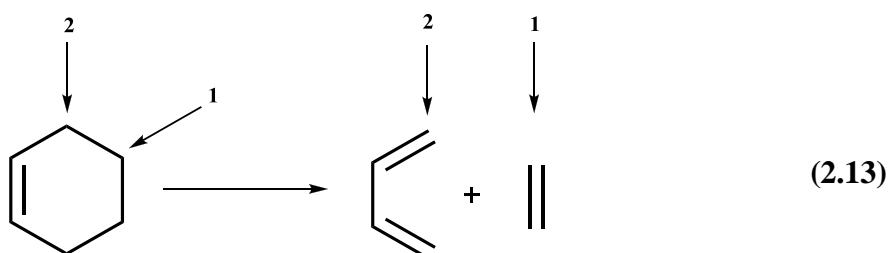
The solvent also has an important effect on the rate of DA reactions. The traditional solvents were nonpolar organic solvents such as aromatic hydrocarbons. However, water and other polar solvents, such as ethylene glycol and formamide, accelerate a number of DA reactions [11,96-99]. The accelerating effect of water is attributed to “enforced hydrophobic interactions” [97]. That is, the strong hydrogen bonding network in water tends to exclude nonpolar solutes and forces them together, resulting in higher effective concentrations [11].

#### 2.1.2.4 Retro Diels-Alder reaction

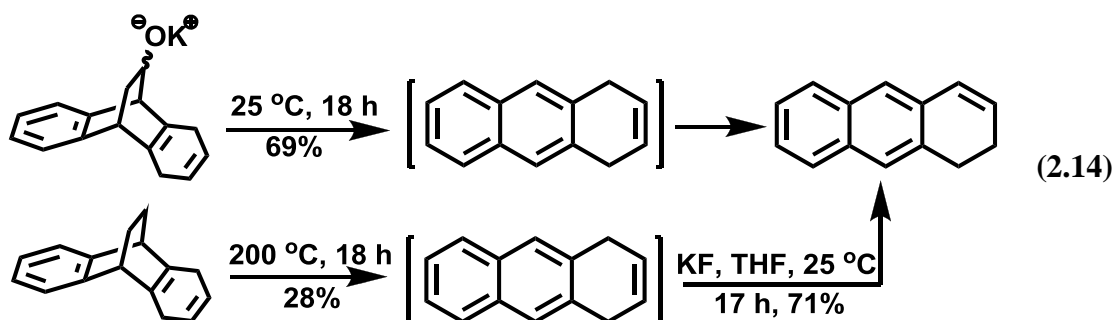
The Diels-Alder reaction is reversible and the direction of cycloaddition is favored because two  $\pi$  bonds are replaced by two  $\sigma$ -bonds [80]. The cycloreversion occurs when the diene and/or dienophile are particularly stable molecules ( i.e. formation of an aromatic ring, of nitrogen, of carbon dioxide, of acetylene, of ethylene, of nitriles, etc.) or when one of them can be easily removed or consumed in a subsequent reaction [80].

The retro Diels-Alder reaction usually requires high temperatures in order to surmount the activation barrier of the cycloreversion. Moreover, the strategy of retro Diels-Alder reaction in organic synthesis to mask a diene fragment or to protect a double bond [80,100].

The retro Diels-Alder reaction is strongly accelerated when an oxide anion substituent is incorporated at positions 1 and 2 of the six-membered ring which has to be cycloreversed, namely at one terminus carbon of the original diene or at one  $sp^2$  carbon of the dienophile [80,101] (Equation 2.13).



An example of the effect of oxide-anion associated with the  $2\pi$  component (i.e. position 1, Equation 2.14) is illustrated in Equation 2.18 [102]. The potassium salt of 1,4-dihydro-11-hydroxy-9,10-dihydro-9,10-ethanoanthracene undergoes more facile debridging (removal of ethylene) than the 11-deoxygenerated parent compound [80].

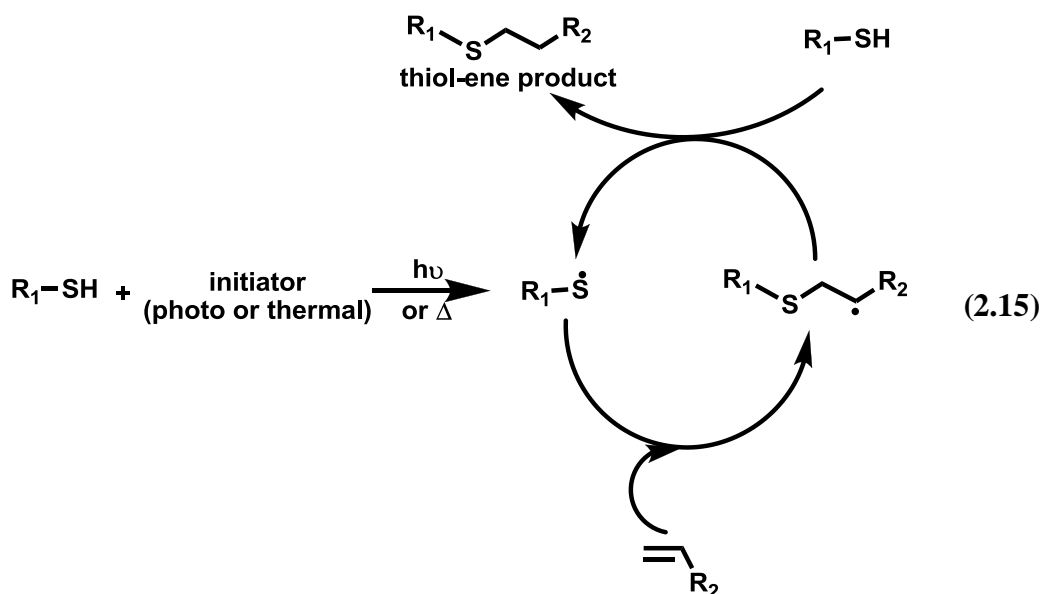


### 2.1.3 Thiol-ene reaction

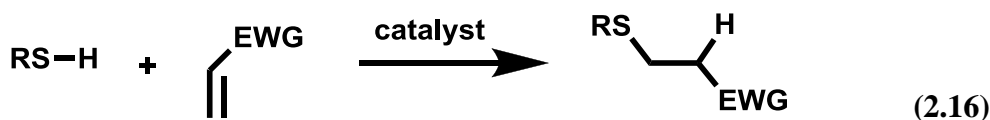
The thiol-ene reaction, well-known for over 100 years, [103] is, simply, the hydrothiolation of a  $C=C$  bond (reaction 2.15). Hoyle and Bowman groups have been most widely employed this method for preparing near-perfect networks and films which is arguably the latest and newest attempts in polymer/materials fields [104]. The click status of this reaction is due to its highly efficient and orthogonal character to a wide range of functional groups, as well as for being compatible with

water and oxygen. The thioether linkage, formed after thiol-ene reaction shows greater stability to a wide range of chemical environments, such as strong acid and basic media as well as oxidizing and reducing conditions [11].

Generally, the thiol-ene reaction has been conducted under radical conditions, photochemically and thermally induce [103-106]. Under such conditions, it proceeds via a typical chain process with initiation, propagation and termination steps. Initiation involves the treatment of a thiol with an initiator, under irradiation or heat, resulting in the formation of a thiyl radical,  $RS\cdot$ , plus other byproducts (reaction 2.15). Simple thermolysis of the S–H bond can also be employed as a means of generating thiyl radicals [11]. Propagation is a two step process involving first the direct addition of the thiyl radical across the C=C bond yielding an intermediate carbon-centred radical followed by chain transfer to a second molecule of thiol to give the thiol-ene addition product, with anti-Markovnikov orientation, with the concomitant generation of a new thiyl radical. Possible termination reactions involve typical radical–radical coupling processes [11].

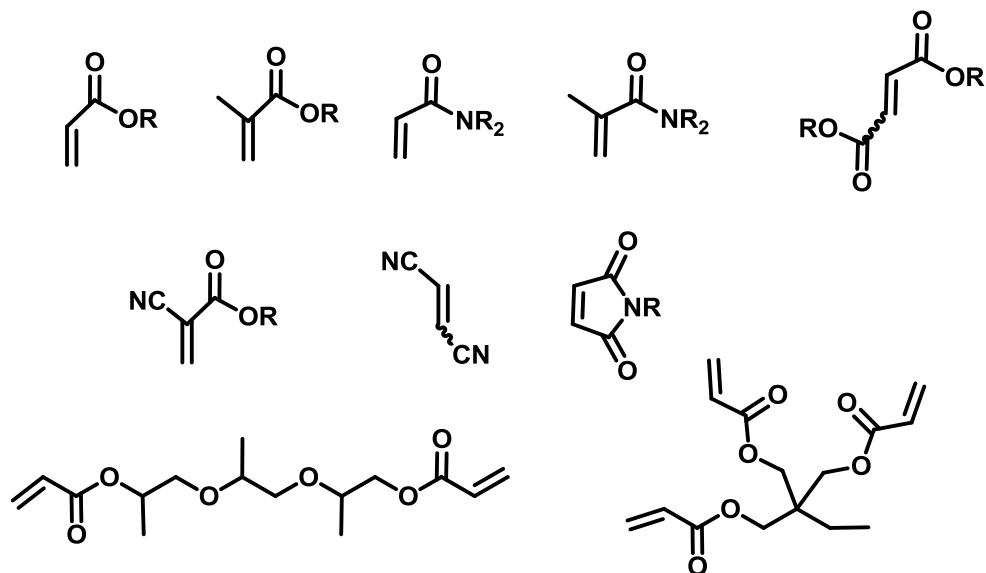


In addition to the radical mediated thiol-ene reactions, hydrothiolations can be readily accomplished under mild base or nucleophilic catalysis such as  $NEt_3$ , primary/secondary amines or certain phosphines [107]. Such reactions are slightly less versatile than the radical-mediated thiol-ene reaction since to be effective the C=C must be activated, *i.e.* electron deficient (reaction 2.16) [11].



**EWG (Electron Withdrawing Group) = ester, amide, cyano**

Figure 2.7 shows some examples of suitable activated ene substrates, and includes (meth)acrylates, fumarate esters and maleimide derivatives [11].



**Figure 2.7 :** Examples of activated substrates susceptible to hydrothiolation via a base/nucleophile-mediated process [11].

Maleimides are common activated substrates for such thiol-ene reactions and deserve a special comment. Due to the presence of two activating carbonyl groups in a *cis*-conformation coupled with ring-strain/bond angle distortion, the C=C bond in maleimides is especially reactive and as such, thiol-ene reactions occur extremely rapidly [11]. Indeed, the high efficiency of these reactions is evident from their widespread use as a bioconjugation tool [11,108-112].

## 2.2 Photopolymerization

In recent years, photoinitiated polymerization has received revitalized interest as it congregates a wide range of economic and ecological anticipations [113]. For more than 30 years, photopolymerization has been the basis of numerous conventional applications in coatings, adhesives, inks, printing plates, optical waveguides, and microelectronics [114,115,116-118]. Some other less traditional but interesting applications, including production of laser videodiscs, curing of acrylate dental

fillings [119], and fabrication of 3D objects [120] are also available. Many studies involving various photopolymerization processes have been continuously conducted in biomaterials [121] for bones and tissue engineering, microchips, optical resins and recoding media, surface relief gratings, anisotropic materials, polymeric photo-optical control materials, clay and metal nanocomposites, photoresponsive polymers, liquid crystalline materials, interpenetrated networks, microlenses, multilayers, surface modification, block and graft copolymerization, two-photon polymerization, spatially controlled polymerizations, topochemical polymerization, solid-state polymerization, living/ controlled polymerization, interfacial polymerization, mechanistically different concurrent polymerizations, pulsed laser polymerization, polymerizations in microheterogeneous media, and so forth [113]. Interest has also grown in identifying the reactive species involved in the polymerization process by laser flash photolysis, time-resolved fluorescence and phosphorescence, and electron spin resonance spectroscopy as well as monitoring the polymerization itself by different methods including real time IR spectroscopy, in-line NIR reflection spectroscopy, differential scanning calorimetry, in situ dielectric analysis, and recently developed optical pyrometry [122].

Photopolymerization is typically a process that transforms a monomer into polymer by a chain reaction initiated by reactive species (free radicals or ions), which are generated from photosensitive compounds, namely photoinitiators and/or photosensitizers, by ultra violet-visible (UV-Vis) light irradiation [113,123]. The wavelength or range of wavelengths of the initiating source is determined by the reactive system including the monomer(s), the initiator(s), and any photosensitizers, pigments or dyes which may be present. An active center is produced when the initiator absorbs light and undergoes some type of decomposition, hydrogen abstraction, or electron transfer reaction [113]. Upon generation of active centers, photopolymerizations propagate and terminate in the same manner as traditional (i.e. thermal) polymerizations. Although photopolymerization can be initiated radically, cationically and anionically, much effort has been devoted to free radical and cationic systems mainly due to the availability of a wide range of photoinitiators and the great reactivity of monomers [113].

### 2.2.1 Photoinitiated free radical polymerization

Photoinitiated free radical polymerization is one of the most widely employed route in industrial applications because of its applicability to a wide range of formulations based on acrylates, unsaturated polyesters, and polyurethanes and the availability of photoinitiators having spectral sensitivity in the near-UV or visible range [113].

It consists of four distinct steps:

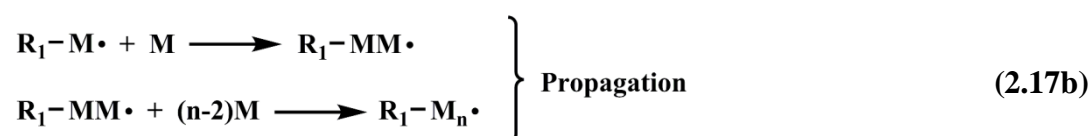
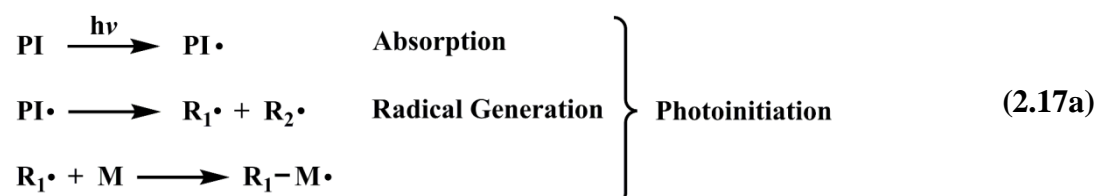
*i) photoinitiation step* involves absorption of light by a photosensitive compound or transfer of electronic excitation energy from a light absorbing sensitizer to the photosensitive compound. Homolytic bond rupture leads to the formation of a radical that reacts with one monomer unit [113].

*ii) propagation step* involves repeated addition of monomer units to the chain radical produces the polymer backbone [113].

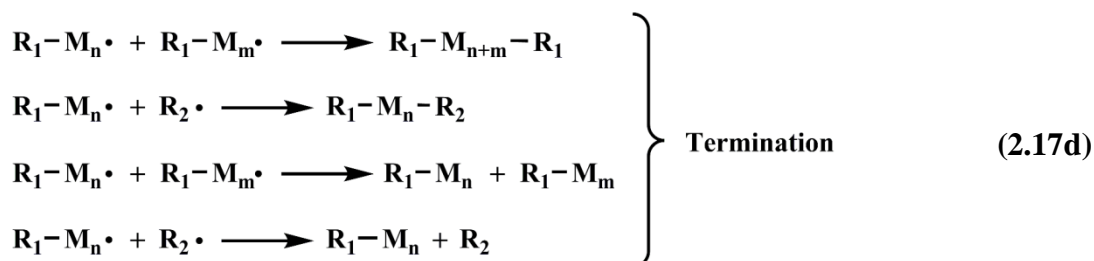
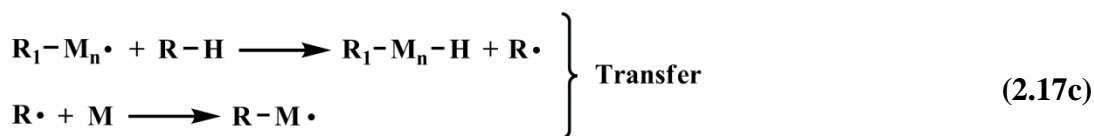
*iii) chain transfer step* involves termination of growing chains by hydrogen abstraction from various species (e.g., from solvent) and formation of new radicals capable of initiating other chain reactions [113].

*iv) termination step* involves termination of chain radicals by disproportionation or recombination reactions. Termination can also occur by recombination or disproportionation with any other radical including primary radicals produced by the photoreaction [113].

The role that light plays in photopolymerization is restricted to the very first step, namely the absorption and generation of initiating radicals. The reaction of these radicals with monomer, propagation, transfer and termination are purely thermal processes; they are not affected by light [113].

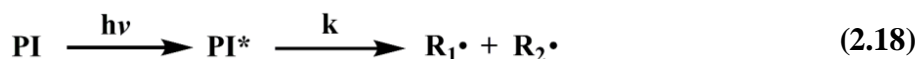






### 2.2.1.1 Type I photoinitiators (unimolecular photoinitiator system)

Photoinitiators termed unimolecular are so designated because the initiation system involves only one molecular species interacting with the light and producing free-radical active centers. These substances undergo a homolytic bond cleavage upon absorption of light (reaction 2.18). The fragmentation that leads to the formation of radicals is, from the point of view of chemical kinetics, a unimolecular reaction (equation 2.17) [113].



$$\frac{d[\text{R}_1\cdot]}{dt} = \frac{d[\text{R}_2\cdot]}{dt} = k[\text{PI}^*] \quad (2.19)$$

The number of initiating radicals formed upon absorption of one photon is termed as quantum yield of radical formation ( $\Phi_{\text{R}\cdot}$ ) (equation 2.20).

$$\Phi_{\text{R}\cdot} = \frac{\text{Number of initiating radicals formed}}{\text{Number of photons absorbed by the photoinitiator}} \quad (2.20)$$

Theoretically, cleavage type photoinitiators should have a  $\Phi_{\text{R}\cdot}$  value of two since two radicals are formed by the photochemical reaction [113]. The values observed, however, are much lower because of various deactivation routes of the photoexcited initiator other than radical generation. These routes include physical deactivation such as fluorescence or non-radiative decay and energy transfer from the excited

state to other, ground state molecules, a process referred to as quenching. The reactivity of photogenerated radicals with polymerizable monomers is also to be taken into consideration. In most initiating systems, only one in two radicals formed adds to monomer thus initiating polymerization[113]. The other radical usually undergoes either combination or disproportionation. The initiation efficiency of photogenerated radicals ( $f_p$ ) can be calculated by the following formula:

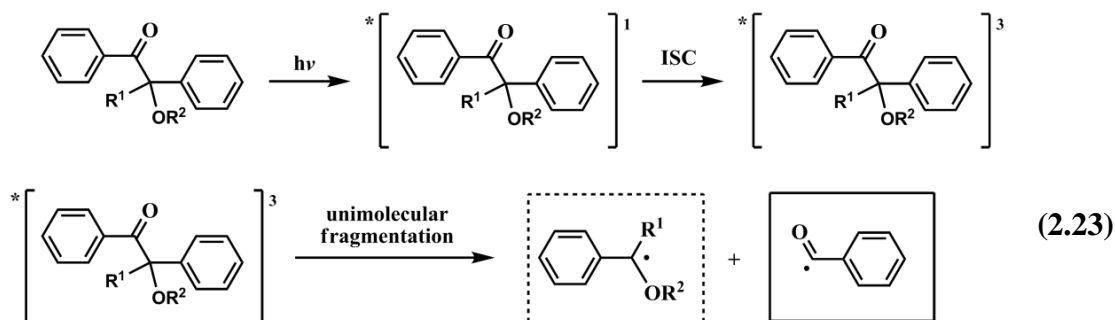
$$f_p = \frac{\text{Number of chain radicals formed}}{\text{Number of primary radicals formed}} \quad (2.21)$$

The overall photoinitiation efficiency is expressed by the quantum yield of photoinitiation ( $\Phi_p$ ) according to the following equation:

$$\Phi_p = \Phi_R \cdot x \cdot f_p \quad (2.22)$$

Regarding the energy necessary, it has to be said that the excitation energy of the photoinitiator has to be higher than the dissociation energy of the bond to be ruptured. The bond dissociation energy, on the other hand, has to be high enough in order to ensure long term storage stability.

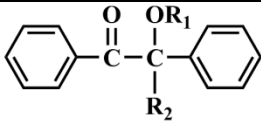
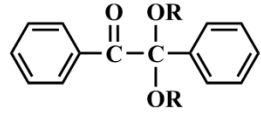
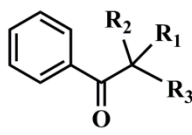
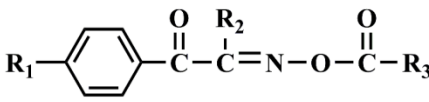
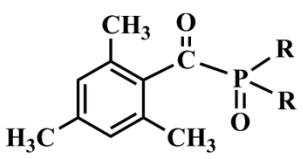
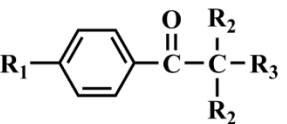
Initiating radicals, formed by direct photofragmentation process ( $\alpha$  or less common  $\beta$  cleavage) of *Type I* photoinitiators upon absorption of light, are capable of inducing polymerization. The photoinitiator forms an excited singlet state, which then undergoes rapid intersystem crossing to form a triplet state. In the triplet state, two radicals (benzoyl and benzyl radicals) are generated by  $\alpha$ -cleavage fragmentation. The benzoyl radical is the major initiating species, while, in some cases, the benzyl radical may also contribute to the initiation [113].



$R^1 = \text{H, alkyl, substituted alkyl}$   
 $R^2 = \text{H, alkyl, substituted alkyl}$

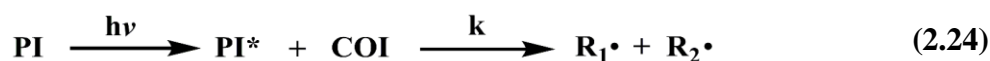
The majority of *Type I* photoinitiators are aromatic carbonyl compounds with appropriate substituents. Benzoin ether derivatives, benzil ketals, hydroxylalkylphenones,  $\alpha$ -aminoketones and acylphosphine oxides are the most efficient ones (Table 2.2) [113, 124-127].

**Table 2.3:** Structures of typical *Type I* radical photoinitiators [113].

Photoinitiators	Structure	$\lambda_{\max}$ (nm)
Benzoin ethers	 $R_1 = \text{H, alkyl}$ $R_2 = \text{H, substituted alkyl}$	323
Benzil ketals	 $R = \text{CH}_3, \text{C}_3\text{H}_7, \text{CH}_2$	365
Acetophenones	 $R_1 = \text{OCH}_3, \text{OC}_2\text{H}_5$ $R_2 = \text{OCH}_3, \text{H}$ $R_3 = \text{C}_6\text{H}_5, \text{OH}$	340
Benzyl oximes	 $R_1 = \text{H, SC}_6\text{H}_5$ $R_2 = \text{CH}_3, \text{C}_6\text{H}_{13}$ $R_3 = \text{C}_6\text{H}_5, \text{OC}_2\text{H}_5$	335
Acylphosphine Oxides	 $R = \text{C}_6\text{H}_5, \text{OCH}_3$	380
Aminoalkyl phenones	 $R_1 = \text{SCH}_3, \text{morpholine}$ $R_2 = \text{CH}_3, \text{CH}_2\text{Ph}, \text{C}_2\text{H}_5$ $R_3 = \text{N(CH}_3)_3, \text{morpholine}$	320

### 2.2.1.2 Type II photoinitiators (bimolecular photoinitiator systems)

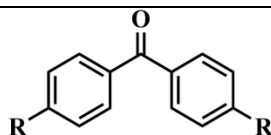
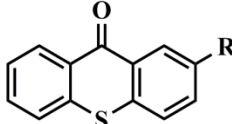
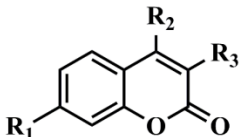
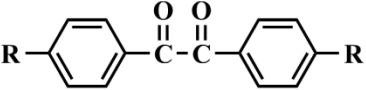

The excited states of certain compounds do not undergo *Type I* reactions because their excitation energy is not high enough for fragmentation (i.e., their excitation energy is lower than the bond dissociation energy). The excited molecule can, however, react with another component of the polymerization mixture (co-initiator (COI)) to produce initiating radicals (reaction 2.24) [113]. In this case, radical generation follows second-order kinetics (equation 2.25).



$$\frac{d[\text{R}_1\cdot]}{dt} = \frac{d[\text{R}_2\cdot]}{dt} = k[\text{PI}^*][\text{COI}] \quad (2.25)$$

Typical *Type II* photoinitiators include aromatic carbonyls such as benzophenone and derivatives [128-131], thioxanthone and derivatives [132-136], benzyl [129], quinines [139], and organic dyes [137-142], whereas alcohols, ethers, amines, and thiols are used as hydrogen donors [113]. Recently, thiol and carboxylic acid derivatives of thioxanthenes have been reported to initiate photopolymerization without co-initiators as they contain functional groups with H-donating nature [143-145]. Alternative approach concerns the attachment of both chromophoric and hydrogen donating groups into polymer chains [146-160]. This way, the odor and toxicity problems observed with the conventional photoinitiators and amine hydrogen donors were overcome. A novel thioxanthone based photoinitiator have also been developed possessing anthracene group that does not require an additional hydrogen donor for radical formation and initiates the polymerization of both acrylate and styrene monomers in the presence of air [113,161]. In addition, TX-A possesses excellent optical absorption properties in the near-UV spectral region, ensuring efficient light absorption. Quite recently, thioxanthone-fluorene carboxylic acid (TX-FLCOOH) and its sodium salt (TX-FLCOONa) were synthesized as efficient photoinitiators in visible light [162]. In fact, photoinitiators with higher wavelength absorption characteristics are desired as they cost lower energy and are defined to be “green” [113]. Typical photoinitiators for *Type II* system are listed in Table 2.4.

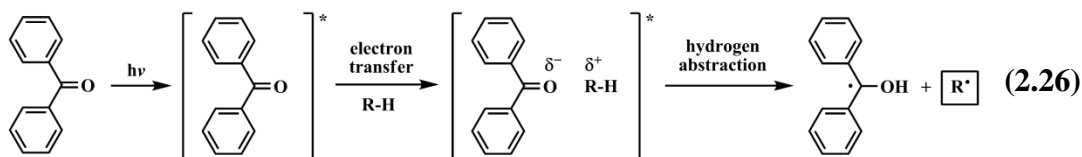
**Table 2.4:** Structures of typical *Type II* photoinitiators [113].

Photoinitiator	Structure	$\lambda_{\max}$ (nm)
Benzophenones	 R = H, OH, N(C <sub>2</sub> H <sub>5</sub> ) <sub>2</sub> , C <sub>6</sub> H <sub>5</sub>	335
Thioxanthenes	 R = H, Cl, isopropyl	390
Coumarins	 R <sub>1</sub> = N(C <sub>2</sub> H <sub>5</sub> ) <sub>2</sub> , N(CH <sub>3</sub> ) <sub>2</sub> R <sub>2</sub> = CH <sub>3</sub> , cyclopentane R <sub>3</sub> = benzothiazole, H	370
Benzils	 R = H, CH <sub>3</sub>	340
Camphorquinones	 R <sub>1</sub> = CH <sub>3</sub> , H R <sub>2</sub> = H, CH <sub>3</sub>	470

Radical generation by *Type II* initiating systems has two distinct pathways:

### Hydrogen abstraction from a suitable hydrogen donor

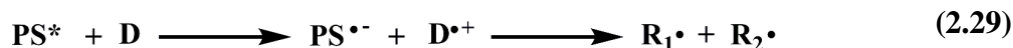
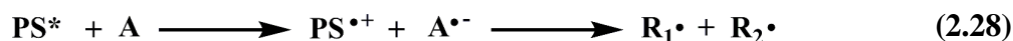
Bimolecular hydrogen abstraction is limited to diaryl ketones [163]. The free radical generation process is the H-abstraction reaction of triplet photoinitiator from hydrogen donors (R-H) such as amines and alcohols. The radical derived from the donor can initiate the polymerization, whereas ketyl radicals stemming from aromatic carbonyl compound are usually not reactive toward vinyl monomers because of bulkiness, the delocalization of the unpaired electrons, or both [113]. The overall process is depicted in the example of benzophenone in reaction 2.26.



R = amines, alcohols, ethers, thiols

### Photoinduced electron transfer reactions and subsequent fragmentation

Photoinduced electron transfer is a more general process, which is not limited to a certain class of compounds and is more important as an initiation reaction comprising the majority of bimolecular photoinitiating systems [113]. The photoexcited compounds (sensitizer) can act as either an electron donor with the coinitiator as an electron acceptor or vice-versa. The radical ions obtained after the photoinduced electron transfer can generally undergo fragmentation to yield initiating radicals (2.27-2.29).



The electron transfer is thermodynamically allowed, if Gibbs Energy Change ( $\Delta G$ ) calculated by the Rehm-Weller equation (2.30) is negative [164].

$$\Delta G = F [E_{1/2}^{\text{ox}} (\text{D}/\text{D}^{\bullet+}) - E_{1/2}^{\text{red}} (\text{A}/\text{A}^{\bullet-})] - E_S + \Delta E_c \quad (2.30)$$

where

F = Faraday constant

$E_{1/2}^{\text{ox}} (\text{D}/\text{D}^{\bullet+})$ ,  $E_{1/2}^{\text{red}} (\text{A}/\text{A}^{\bullet-})$  = redox potentials of the donor and acceptor

$E_S$  = excitation state of the reactive state of the sensitizer;  $E_S = h\nu$

$\Delta G$  = Coulombic stabilization energy

Electron transfer is often observed for aromatic ketone/amine pairs and always with dye/coinitiator systems. Dyes comprise a large fraction of visible light photoinitiators because their excited electronic states are more easily attained. Co-initiators, such as tertiary amines, iodonium salts, triazines, or hexaarylbisimidazoles, are required since dye photochemistry entails either a photo-reduction or photo-oxidation

mechanism [113]. Numerous dye families are available for selection of an appropriate visible initiation wavelength; examples of a thiazine dye (with an absorption peak around 675 nm), acridine dyes (with absorption peaks around 475nm), xanthene dyes (500–550 nm), fluorone dyes (450–550 nm), coumarin dyes (350–450 nm), cyanine dyes (400–750 nm), and carbazole dyes (400 nm) [165-168]. The oxidation or reduction of the dye is dependent on the co-initiator; for example, methylene blue can be photo-reduced by accepting an electron from an amine or photo-oxidized by transferring an electron to benzyltrimethyl stannane [166]. Either mechanism will result in the formation of a free-radical active center capable of initiating a growing polymer chain.

### **2.2.1.3 Monomers**

Unsaturated monomers, which contain a carbon–carbon double bond (C=C), are used extensively in free radical photopolymerizations. The free-radical active center reacts with the monomer by opening the C=C bond and adding the molecule to the growing polymer chain. Most unsaturated monomers are able to undergo radical polymerization because free-radical species are neutral and do not require electron-donating or electron-withdrawing substituents to delocalize the charge on the propagating center, as is the case with ionic polymerizations [113]. Commercial consideration in formulation development is therefore given to the final properties of the polymer system, as well as the reactivity of the monomer. Acrylate and methacrylate monomers are by far most widely used in free-radical photopolymerization processes. These monomers have very high reaction rates, with acrylates having an even faster reaction rate than their methacrylate counterparts [113,169]. This makes them especially amenable for high speed processing needed in the films and coatings industry.

Multiacrylates increase the mechanical strength and solvent resistance of the ultimate polymer by forming cross-linked networks rather than linear polymer chains, whereas monoacrylates reduce the viscosity of the prepolymer mixture for ease of processing [169,170]. One of the drawbacks of acrylate and methacrylate systems is their relatively large polymerization shrinkage. Shrinkage is caused by the formation of covalent bonds between monomer molecules. When a covalent bond is formed between two monomer molecules, the distance between them is approximately half as much as that between two molecules experiencing van der Waal's forces in

solution [113]. This shrinkage causes stresses in the polymer parts, which can affect their ultimate performance, especially in applications such as stereo lithography, dentistry, and coatings. One way to overcome this disadvantage is to develop oligomeric acrylates. These oligomers contain 1 to 12 repeat units formed through step-growth polymerization; the ends are then capped with two or more (meth)acrylate functional groups [113].

Diallyldiglycolcarbonate has been used for many years in optical components such as lenses [171]. Acrylamide is used in stereo lithography and to prepare holographic materials [172-174]. N-vinylpyrrolidinone is copolymerized with acrylates and methacrylates for cosmetic and biomedical applications [175]. Norbornene is copolymerized with thiols for optical fiber coatings [176].

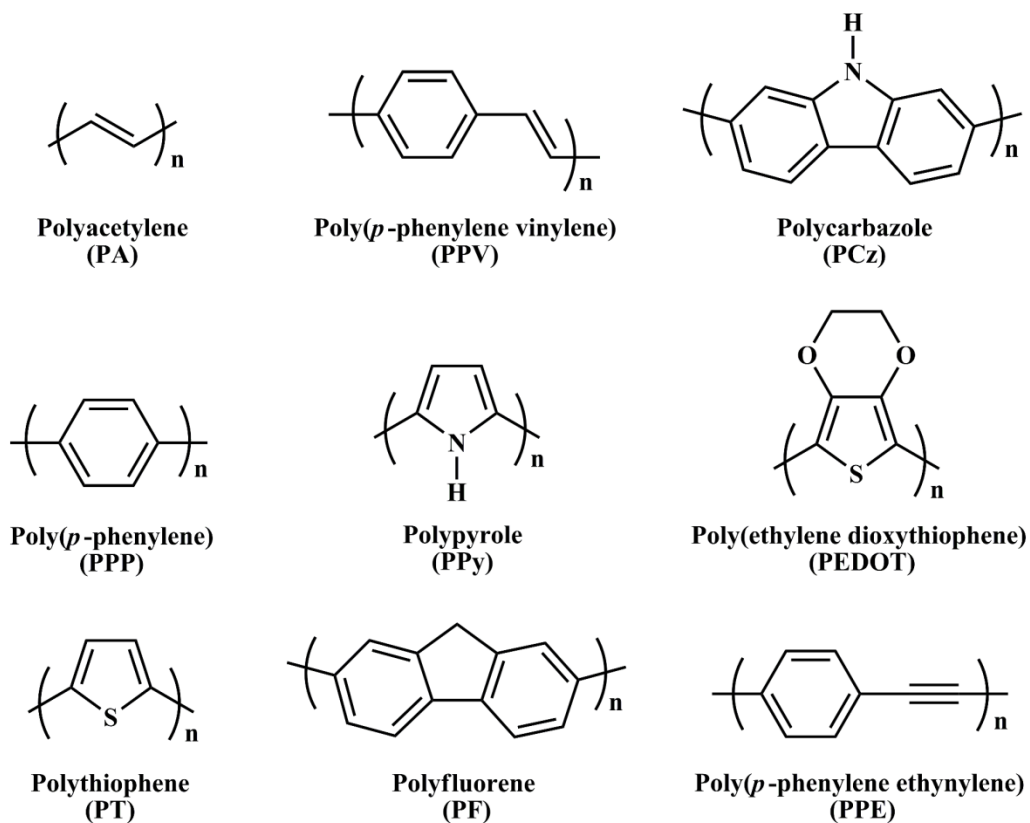
### **2.3 Conducting polymers (CP)**

Conducting polymers are a relatively new class of materials whose interesting metallic properties were first reported in 1977, with the discovery of electrically conducting polyacetylene [177].

MacDiarmid, Shirakawa, and Heeger demonstrated that chemical doping of polyacetylene with oxidizing agents (e.g., I<sub>2</sub>, FeCl<sub>3</sub>, and AsF<sub>5</sub>) results in increased electronic conductivity by several orders of magnitude [178-180].

They were awarded the 2000 Nobel Prize in Chemistry for this work. Many of these polymers, especially those with a conjugated  $\pi$ -bond system, often yield higher conductivity once having undergone the doping process [181]. Since the discovery of polyacetylene there has been much research into conducting polymers and many new conducting polymers have been synthesised [182]. The most important, and common, of these are polyacetylene (PA), poly(*p*-phenylene) (PPP), polythiophene (PT), poly(*p*-phenylene vinylene) (PPV), polypyrrole (PPy), polyfluorene (PF), polycarbazole (PCz), poly(ethylene dioxythiophene) (PEDOT) and poly(*p*-phenylene ethynylene) (PPE) (Figure 2.8).



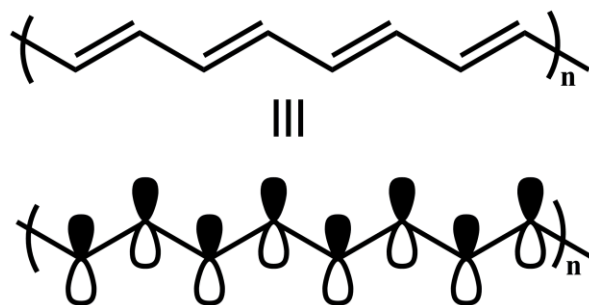


**Figure 2.8 :** Structures of typical conductive polymers [182].

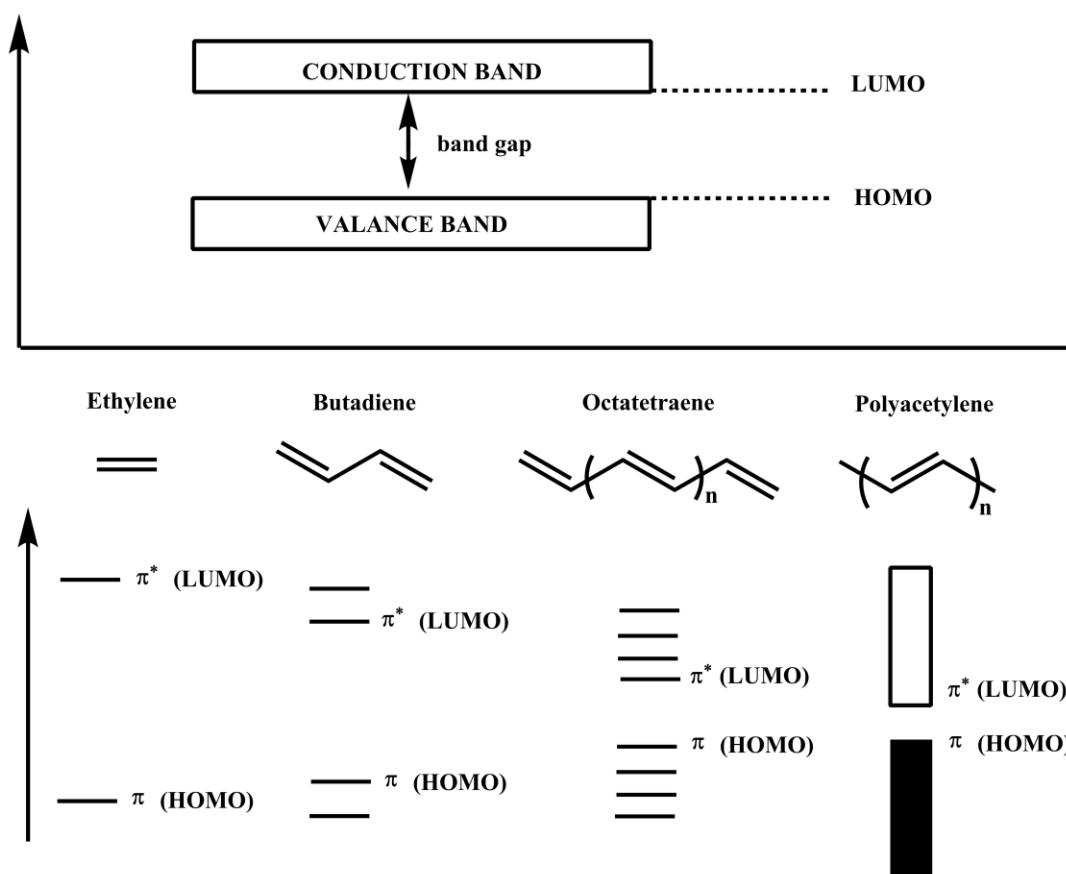
For these materials the fundamental prerequisite for conduction is the existence of extended conjugated systems containing delocalized  $\pi$ -electrons arising from their alternating structure of single and double bonds along polymer chains [183].

### 2.3.1 Band theory

The utilization of the conjugated construction affords polymer chains possessing extended  $\pi$ -systems, and it is this feature alone that separates CPs from their other polymeric counterparts [182]. Using this generic, lowest energy (fully bonding) molecular orbital (MO) representation as shown by the  $\pi$ -system model, the picture of primary concern that is generated by these networks consists of a number of  $\pi$  and  $\pi^*$  levels (Figure 2.9). However, unlike the discrete orbitals that are associated with conjugated organic molecules, the energy of the polymers' MOs are so close in energy that are indistinguishable [182]. In fact, for long chains orbital separation is so small that band formation occurs as illustrated by the MO diagram (Figure 2.10).



**Figure 2.9 :** The  $\pi$ -system model [182].

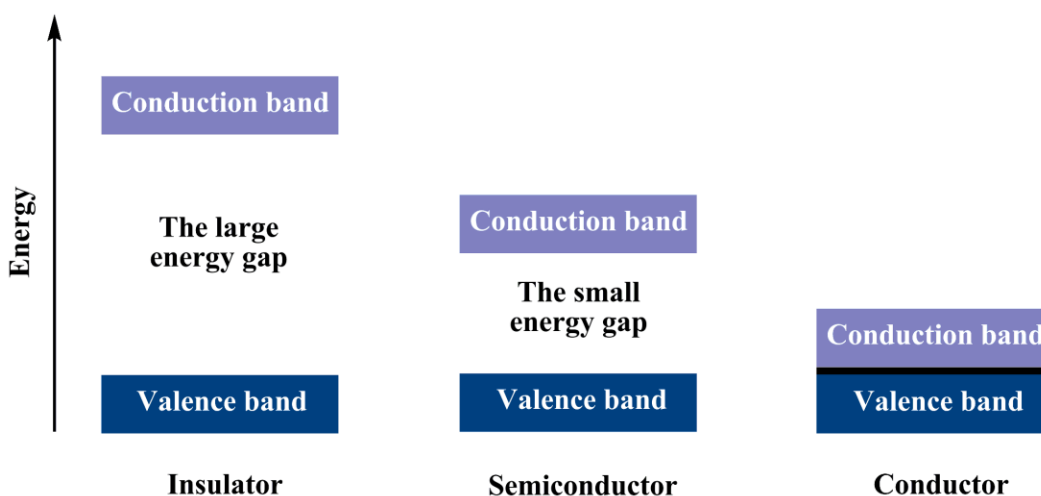


**Figure 2.10 :** Molecular orbital (MO) diagram [182].

The electrical properties of any material are based on the material's electronic structure. The presumption that CPs form bands through extensive molecular orbital overlap leads to the assumption that their electronic properties can be explained by band theory [182].

The degeneration of the molecular orbital of double bonds gives a HOMO band and a LUMO band, as an analogue to the valence band and the conduction band in inorganic semiconductors. The energy difference between these two bands is called the band gap [182].

Figure 2.11 shows the band structures of insulators, semiconductors and conductors.



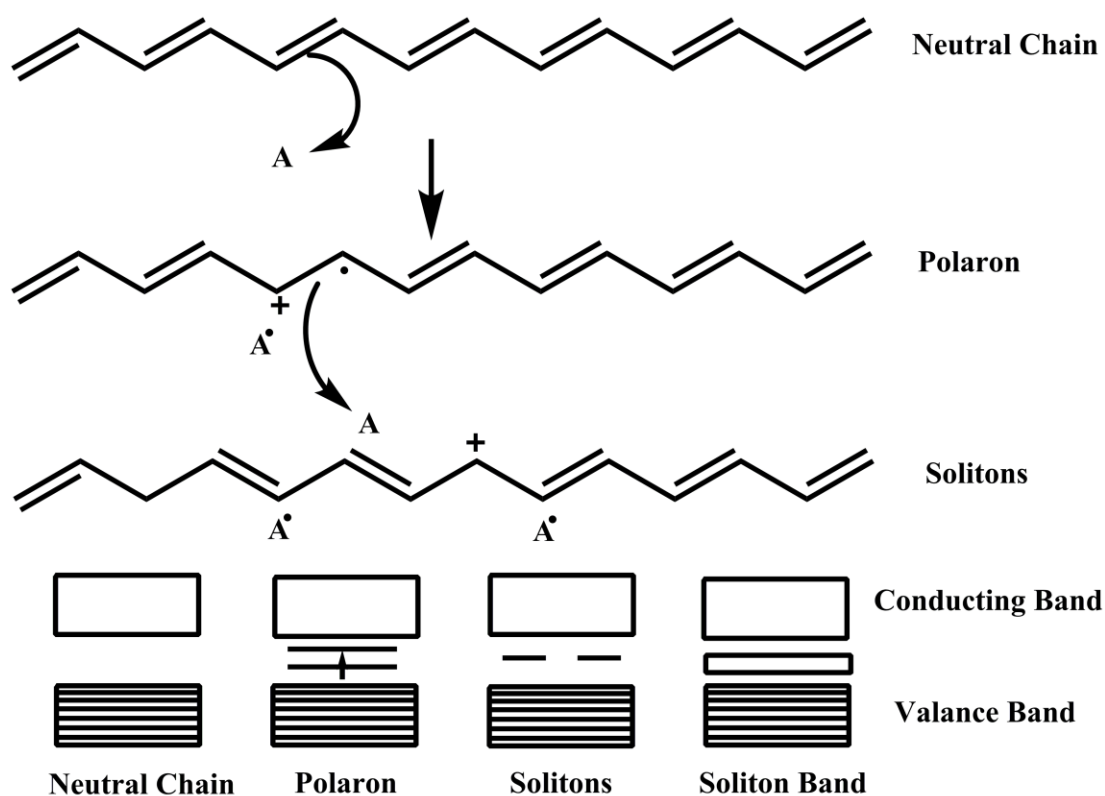
**Figure 2.11** : Band structures of insulator, semiconductor and conductor [113].

Conductors (metals) are materials that possess partially filled bands, and this characteristic is the key factor leading to the conductive nature of this class of materials. Semiconductors, on the other hand, have filled (valence bands) and unfilled (conduction bands) bands that are separated by a range of forbidden energies (known as the ‘band gap’). The conduction band can be populated, at the expense of the valence band, by exciting electrons (thermally and/or photochemically) across this band gap. Insulators possess a band structure similar to semiconductors except here the band gap is much larger and inaccessible under the environmental conditions employed [182].

Conjugated polymers are considered as insulators or sometimes as semiconductors in their neutral state [182]. Charge injection (doping) into a conjugated polymeric system leads to wide varieties of semiconductors and conductors. Doping introduces charge carriers into the polymer, thus every repeating unit can essentially be an active redox site. Therefore, conjugated polymers can be doped with an oxidant (p-type) or with a reductant (n-type). In the oxidative doping two new states are produced within the energy gap between the valence and the conduction bands, and the presence of these bands gives rise to new low-energy transitions in the doped material. On the other hand, in the reductive doping electrons are injected into the conduction band and these electrons serve as the charge carriers. Upon doping the charge carriers are allowed to move along the shared intramolecular  $\pi$  bonds. The

charge carrier delocalization along the polymer backbone increases the effective conjugation length of the polymer and extends into a three dimensional system through inter-chain charge transfer. After doping, the electrical conductivity through mobility of either holes or electrons increases dramatically and the doped conjugated polymers behave as conductors [182].

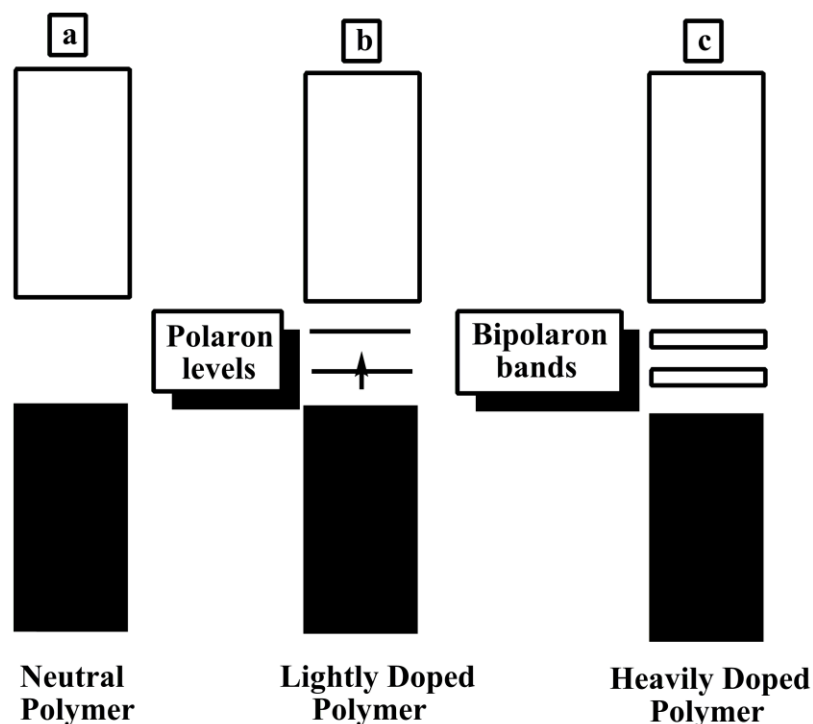
Polyacetylene turns out to be a special case when considering its neutral and doped forms. Comparison of the two neutral forms, shown in Figure 2.12, reveals them to be structurally identical, and thus, their ground states are degenerate in energy. Two successive oxidations on one chain could yield radical cations that, upon radical coupling, become non-associated charges termed positive ‘solitons’ [182].



**Figure 2.12 :** Neutral and doped forms of polyacetylene [182].

In contrast to polyacetylene, the other CP not show evidence of soliton formation. In this instance, the oxidation of the CP is believed in the destabilization (raising of the energy) of the orbital from which the electron is removed. This orbital’s energy is increased and can be found in the energy region of the band gap as shown in Figure 2.13. Initially, if only one electron per level is removed a radical cation is formed and is known as a ‘polaron’ (Figure 2.13b). Further oxidation removes this unpaired

electron yielding a dicationic species termed a ‘bipolaron’(Figure 2.13c). High dopant concentrations create a bipolaron-‘rich’ material and eventually lead to band formation of bipolaron levels. Such a theoretical treatment, thereby, explains the appearance, and subsequent disappearance, of the EPR signal of a CP with increased doping as the neutral polymer transitions to the polaronic form and subsequently to the spinless bipolaronic state [182].



**Figure 2.13 :** Band structures of a) neutral polymer b) lightly doped polymer c)heavily doped polymer [182].

### 2.3.2 Synthesis of conjugated polymers

Conducting polymers can be prepared either chemically or electrochemically [184].

The latter is generally preferred because it provides a better control of film thickness and morphology, and cleaner polymers when compared to chemical oxidation. The chemical oxidation method usually leads to fine powders, while electrochemical synthesis provides free-standing films on electrode [182].

### 2.3.3 Electrochemical polymerization

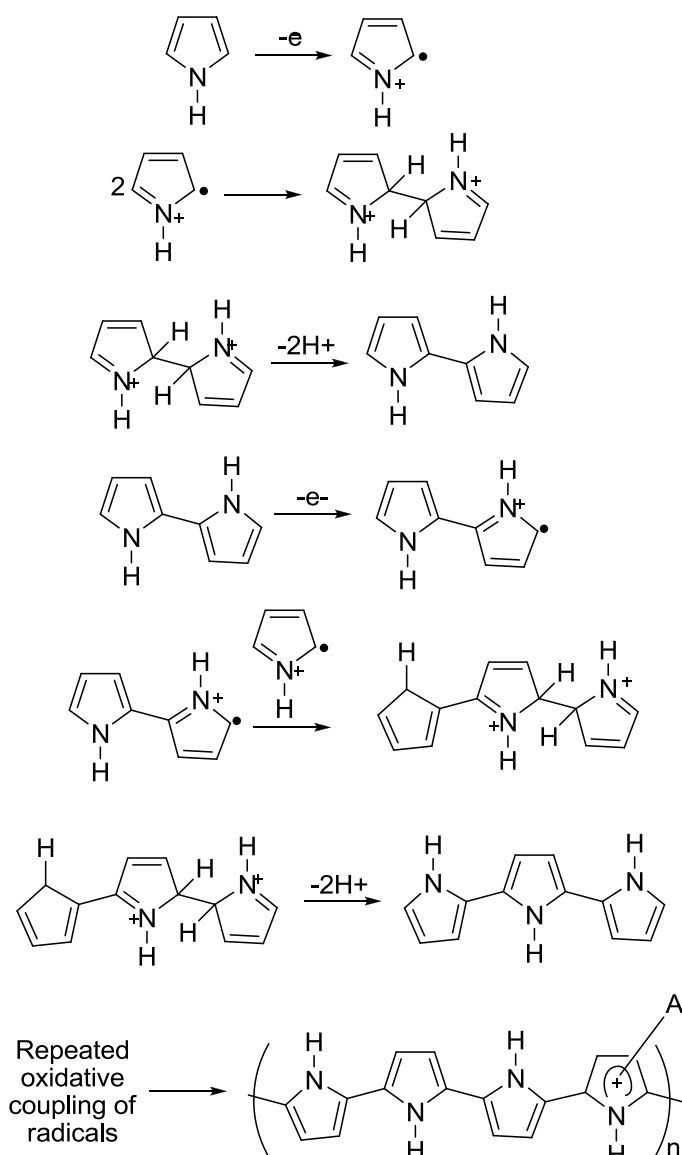
Electrochemical preparation of conjugated polymers was firstly described by Diaz in 1981 [185]. In the first step oxidation, radical cation of the monomer is formed. The second involves the coupling of two radical cations to produce a dihydrodimer

dication which leads to a dimer after loss of two protons and rearomatization (2.65). In this coupling process the formation of the dihydro dimer is the key driving force. The dimer has lower oxidation potential than the monomer and, consequently it is readily oxidized to lead to further couplings [182]. Subsequent electrochemical and chemical steps proceed until the oligomer becomes insoluble in the electronic medium and precipitates onto the electrode surface. Coupling is generally a second order reaction between radical cations followed by fast proton release as shown for pyrroles (2.65). The coupling rate increases as the oligomer length is increased and the activation energy increases linearly with the inverse of the oligomer length [182,186].

#### **2.3.4 Oxidative chemical polymerization**

Oxidative chemical polymerization is very simple method to prepare conducting polymers [182,187]. In this method, a stoichiometric amount of oxidizing reagent is used to form polymer that is in its doped or conducting form.  $\text{FeCl}_3$  is generally employed as a chemical oxidant in the polymerization of the heterocyclic monomers [188,189]. Reduction of the synthesized monomer to the neutral state is achieved by addition of a strong base such as ammonium hydroxide or hydrazine. Benzene can also undergo oxidative polymerization with  $\text{AlCl}_3/\text{CuCl}_2$  to yield poly (p-phenylene) [190].

Electrochemical polymerization involves short reaction times, small amounts of monomers, and yields polymers in their oxidized state in the form of electrode supported, stable films, which possess favorable opto-electronic properties [9]. However, the polymer obtained by electrochemical polymerization possesses a regioirregular structure [191-193]. This method is useful for the preparation of conducting polymer films for electronic devices such as electro-analytical sensors composed of a receptor for a particular compound anchored on a conducting polymer film. On the other hand, electropolymerization is not regarded as a method suitable for the large-scale production of conducting polymers [194].



### 2.3.5 Electrochemical techniques

The electrochemical techniques generally employed in the electrochemical synthesis of conducting polymers are potentiostatic or galvanostatic electrolysis. They have advantages over chemical oxidative polymerization [182].

Polymerization carried out via electrochemical techniques is simple, selective, and reproducible. Reactions are done at room temperature. Thickness of the films can be controlled and it is also possible to produce homogenous polymers. Films are directly formed at the electrode surface. Moreover, graft and block copolymers can be easily obtained [182].

### **2.3.5.1 Constant-current electrolysis (Galvanostatic)**

Constant-current, or controlled-current, electrolysis (CCE) is very simple and carried out in a cell containing two electrodes. In this method, current is kept constant throughout the electrolysis and potential is allowed to vary. In a typical experiment, a direct current of fixed magnitude between the anode and cathode is passed for the necessary time. This may be done by using current sources either with a variable voltage in series with the cell (as resistor) or a fixed voltage source and a variable resistor. Although CCE is simple in application it has some disadvantages. The major disadvantage of constant-current electrolysis is the lack of selectivity. As the potential is a variable parameter, all possible redox processes may take place. Also, the involvement of species present in the system in addition to monomer is inevitable. Therefore, complications may arise in initiation and propagation steps [182].

### **2.3.5.2 Constant-potential electrolysis**

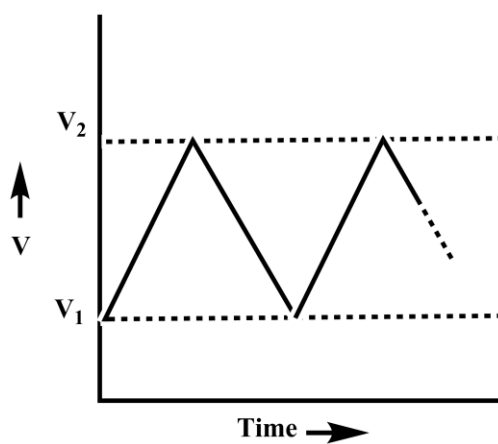
Three- electrode system is employed in constant potential electrolysis. The potential of the working electrode (WE) with respect to that of a reference electrode (RE) is adjusted to a desired value and kept constant by a potentiostat while current is allowed to vary. The voltage between the working and the reference electrodes may be called the polymerization potential. Creation of undesired species is prevented by keeping the potential constant and thus the initiation becomes selective, that is, through the monomer itself [182].

### **2.3.5.3 Cyclic voltammetry (CV)**

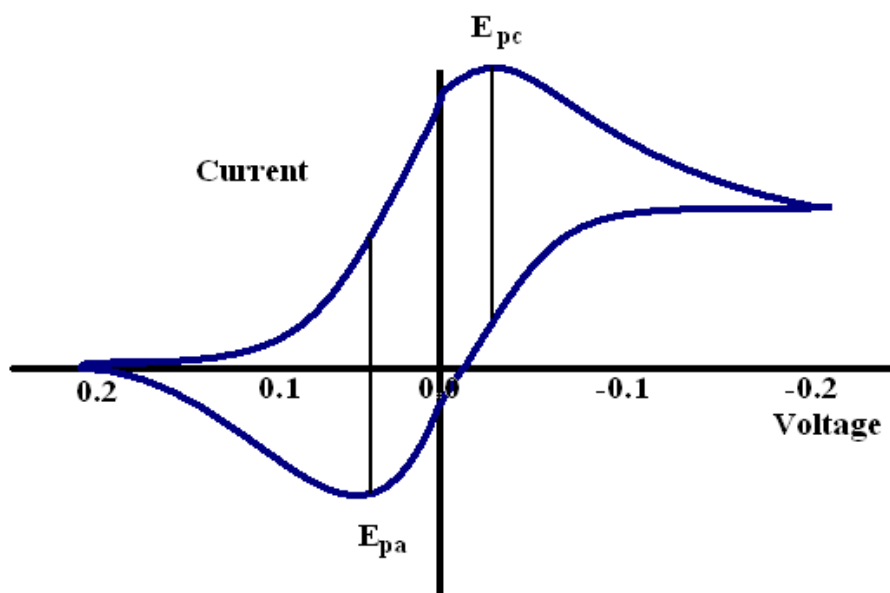
Cyclic voltammetry (CV) is used to find out the electrochemical behavior of electroactive species. In this technique the potential is linearly scanned up to a value suitable for polymer formation and then reversed to its initial value. The voltage applied to the working electrode as a cyclic triangular wave (Figure 2.14) and then current response is plotted as a function of applied potential by recorder (Figure 2.15). The shape of the cyclic voltammogram of a material is highly dependent on relative rates of electron transfer, mass transport, and any chemical reactions at the electrode. The formation of conducting polymer can be clearly followed by cyclic voltammetry. As the polymer coated on the electrode is conductive, this causes the increase of electrode surface area, peak height continuously increases with repetitive scanings. Shortly, the cyclic voltammogram of a material provides to understand its



electroactivity, redox potential, mechanism of the electrochemical reaction [182].



**Figure 2.14** : Triangular wave function [182].



**Figure 2.15** : Cyclic voltammogram of reversible process [182].



### **3. EXPERIMENTAL WORK**

#### **3.1 Materials and Chemicals**

##### **3.1.1 Monomers**

*Styrene (St, 99%, Aldrich):*

It was passed through a basic alumina column to remove the inhibitor before use.

*4-chloromethylstyrene (CMS, ca. 60/40 meta/para isomer mixture, 97%, Aldrich):*

It was distilled under reduced pressure before use.

*Pyrrrole (Py, 99.0%, Sigma-Aldrich):*

It was purified by double distillation

##### **3.1.2 Solvents**

*Tetrahydrofuran (THF, 99.8%, J.T. Baker):*

It was dried and distilled over benzophenone-Na.

*Ethyl acetate ( $\geq 99\%$ , Sigma):*

It was used as received.

*Dichloromethane (DCM, J.T. Baker):*

It was used as received.

##### **3.1.3 Other chemicals**

*Anhydrous magnesium sulfate (99%, Sigma-Aldrich):*

It was used as received.

*Sodium hydroxide, ( $\geq 97.0\%$ , Sigma-Aldrich):*

It was used as received.

*Sulfuric acid (98%, Sigma-Aldrich):*

It was used as received.

*Sodium nitrite*, ( $\geq 99.0\%$  Sigma-Aldrich):

It was used as received.

*Sodium azide* ( $\geq 99.0\%$ , Fluka):

It was used as received.

*Propargylbromide* (~80 volume % in toluene, Fluka):

It was used as received.

*Tetrabutylammonium bromide* (TBAB, Acros Organics % 99):

It was used as received.

*Copper(I)bromide* ( $\geq 97.0\%$ , Riedel-deHaën):

It was used as received.

*2,2'-bipyridine* ( $\geq 99\%$ , Aldrich):

It was used as received.

*4-(Dimethylamino)-pyridinium 4-toluenesulfonate* (DPTS):

It was obtained according to a published procedure [195]

*Tetrabutylammonium tetrafluoroborate* (TBAFB, Aldrich):

It was used as received.

*2,2,6,6-tetramethylpiperidine-N-oxyl free radical* (TEMPO, 99%, Aldrich):

It was used as received.

*N,N,N',N'',N''-Pentamethyldiethylenetriamine* (PMDETA, Aldrich):

It was distilled over NaOH prior to use.

*Poly(ethylene glycol) methyl ether* (Me-PEG, Acros):

It was dried over anhydrous toluene by azeotropic distillation.

*4-(dimethylamino)-pyridine* (DMAP, 99%, Aldrich):

It was used as received.

*Octaphenylsilsesquioxane* (OPS, Aldrich):

It was used as received.

*3-Thiophenecarboxylic acid* (% 99, Acros):

It was used as received.

*2,2'-Azobis(isobutyronitrile)* (AIBN, 98%, Aldrich):

It was recrystallized from ethanol.

*N,N'-Dicyclohexylcarbodiimide* (DCC, 99%, Aldrich):

It was used as received.

*2,6-di-tertbutyl-4-methylphenol* (BHT, 99%, Aldrich):

It was used as received.

## **3.2 Equipment**

### **3.2.1 Photoreactor**

A Rayonet type photoreactor equipped with 16 Philips 8W / O6 lamps emitting light nominally at 350 nm was used.

### **3.2.2 Nuclear magnetic resonance spectroscopy (NMR)**

(a)  $^1\text{H}$  NMR and  $^{13}\text{C}$  NMR measurements were recorded in  $\text{CDCl}_3$  with  $\text{Si}(\text{CH}_3)_4$  as internal standard, using a Bruker AC250 (250.133 MHz) instrument.

### **3.2.3 Infrared spectrophotometer (FT-IR)**

FT-IR spectra were recorded on a Perkin Elmer FTIR Spectrum One B spectrometer.

### **3.2.4 UV-Visible spectrophotometer**

UV-Visible spectra were recorded on a Shimadzu UV-1601 UV-visible spectrophotometer.

### **3.2.5 Gel permeation chromatography (GPC)**

(a) Gel permeation chromatography (GPC) analyses were performed with a set up consisting of a Waters 410 Differential Refractometer, a Waters 515 HPLC Pump and an apparatus equipped with three Waters ultrastyrigel columns (HR series 4, 3, 2 narrow bore), with THF as the eluent at a flow rate 0.3 mL/min. Molecular weights

were calculated on the basis of a calibration curve recorded with mono disperse polystyrene standards.

### **3.2.6 Differential scanning calorimetry (DSC)**

Differential scanning calorimetry (DSC) was performed on Perkin- Elmer Diamond DSC with a heating rate of 10 °C/min under nitrogen flow.

### **3.2.7 Thermal gravimetric analyzer (TGA)**

Thermal gravimetric analysis were performed on Perkin–Elmer Diamond TA/TGA with a heating rate of 10 °C min under nitrogen flow.

### **3.2.8 Fluorescence spectrophotometer**

Fluorescence and phosphorescence measurements were performed on a Jobin Yvon-Horiba Fluoromax-P spectrophotometer.

### **3.2.9 Electrochemical measurements**

A three-electrode cell containing ITO-coated glass slides (Delta Technologies,  $R=8-12 \Omega \text{ sq}^{-1}$ ) as the working electrode, a platinum foil as the counter electrode, and a silver wire as the pseudo-reference electrode were used for electrodeposition of polymer films by potentiodynamic methods. All electrochemistry was performed on a Voltalab PST50 potentiostat/galvanostat Agilent 8453 spectrophotometer was used to perform the spectroelectrochemical studies of the copolymer and the characterization of the devices. Colorimetry measurements were done via Minolta CS-100 spectrophotometer.

## **3.3 Preparation Methods**

3-Acetyl-N-(2-hydroxyethyl)-7-oxabicyclo[2.2.1]hept-5-ene-2-carboxamide (**29**) and 2-bromo-2-methylpropionic acid 2-(3,5-dioxo-10-oxa-4-azatricyclo[5.2.1.0<sup>2,6</sup>]-dec-8-en-4-yl) ethyl ester (**30**) were synthesized as described in the literature [196]. Synthesis of 4-(2-([(3-Acetyl-7-oxabicyclo[2.2.1]hept-5-en-2-yl)carbonyl]amino}ethoxy)-4-oxobutanoic acid (**31**) was kindly synthesized by Hakan Durmaz from Hizal and Tunca group. Its synthesis procedure is given below.

### 3.3.1 Synthesis of 4-(2-[(3-acetyl-7-oxabicyclo[2.2.1]hept-5-en-2-yl) carbonyl]amino)ethoxy)-4-oxobutanoic acid (**31**)

For synthesis of the compound **3**, the above obtained compound, 5.0 g of compound **1** (23.9 mmol) was dissolved in 150 mL of 1,4-dioxane. To this solution Et<sub>3</sub>N (16.58 mL, 119.6 mmol) and DMAP (4.4 g, 35.8 mmol) were added. Then, 9.6 g of succinic anhydride (95.6 mmol) was added to this reaction mixture and stirred overnight at 40 °C. The resulting solution was poured into ice-cold water and extracted with CH<sub>2</sub>Cl<sub>2</sub>. The organic phase was washed with 1 M HCl and was dried over Na<sub>2</sub>SO<sub>4</sub> and then concentrated. The crude product was crystallized from ethanol and white crystalline product was obtained (5.9 g, yield: 80%). M.p. = 122-123 °C (DSC); <sup>1</sup>H NMR (CDCl<sub>3</sub>, δ) 6.50 (s, 2H, CH=CH, as bridge protons), 5.25 (s, 2H, -CHO, bridge-head protons), 4.25 (t, *J* = 5.2 Hz, 2H, NCH<sub>2</sub>CH<sub>2</sub>OC=O), 3.74 (t, *J* = 5.2 Hz, 2H, NCH<sub>2</sub>CH<sub>2</sub>OC=O), 2.87 (s, 2H, CH-CH, as bridge protons), 2.66-2.53 (m, 4H, C=OCH<sub>2</sub>CH<sub>2</sub>C=OOH).

### 3.3.2 Preparation of PEG-maleimide (PEG-MI)

Me-PEG (*M*<sub>na</sub> = 550) (2.0 g, 3.63 mmol) was dissolved in 20 mL of CH<sub>2</sub>Cl<sub>2</sub>. To the reaction mixture compound **3** (3.4 g, 11 mmol), and DPTS (1.2 g, 3.63 mmol) were added successively. After stirring 5 minutes at room temperature, a solution of DCC (2.3 g, 11 mmol) in 10 mL of CH<sub>2</sub>Cl<sub>2</sub> was added to it. Reaction mixture was stirred overnight at room temperature. After filtration off the salt, the solution was concentrated and the viscous brown color product was purified by column chromatography over silica gel eluting with CH<sub>2</sub>Cl<sub>2</sub>/ethylacetate mixture (1:1, vol/vol) and then with CH<sub>2</sub>Cl<sub>2</sub>/ MeOH (0.95: 0.05) to obtain compound **4** as viscous yellow oil (Yield: 2.7 g, 88%). *M*<sub>n,theo</sub> = 840; *M*<sub>n,NMR</sub> = 850; *M*<sub>n,GPC</sub> = 1300; *M*<sub>w</sub>/*M*<sub>n</sub> = 1.01. <sup>1</sup>H NMR (CDCl<sub>3</sub>, δ) 6.50 (s, 2H, CH=CH), 5.25 (s, 2H, CH as bridge-head protons), 4.23 (m, 4H, CH<sub>2</sub>OC=O), 3.75-3.51 (m, OCH<sub>2</sub>CH<sub>2</sub> repeating unit of PEG, C=ONCH<sub>2</sub>, and CH<sub>2</sub>-PEG repeating unit), 3.36 (s, 3H, PEG-OCH<sub>3</sub>), 2.87 (s, CH-CH, as bridge protons) 2.61-2.56 (m, 4H, C=OCH<sub>2</sub>CH<sub>2</sub>C=O).

### 3.3.3 Preparation of PMMA-maleimide (PMMA-MI)

PMMA-MI was prepared by ATRP of MMA. In a 50 mL Schlenk tube, MMA (10 mL, 93.5 mmol), toluene (10 mL), PMDETA (0.4 mL, 1.87 mmol), CuCl (0.19 g, 1.87 mmol) and **30** (0.67 g, 1.87 mmol) were added and the reaction mixture was

degassed by three freeze-pump-thaw cycles and left in vacuum. The tube was then placed in an oil bath at 40 °C for 3h. Afterward the resulted polymerization mixture was diluted with THF, passed through a basic alumina column to remove the catalyst, and then precipitated into hexane. The polymer obtained was dried for 24 h in a vacuum oven at 30 °C.

$[M]_0/[I]_0 = 50$ ;  $[I]_0$ :  $[CuCl]$ :  $[PMDETA] = 1:1:1$ ; conv. % = 18;  $M_{n,theo} = 1250$ ;  $M_{n,NMR} = 2350$ ;  $M_{n,GPC} = 2100$ ;  $M_w/M_n = 1.2$ .

### **3.3.4 General procedure for etherification of chloromethyl moieties (8, 30 and 50%) of poly(styrene-co-chloromethyl styrene) P(S-co-CMS)**

P(S-co-CMS) copolymers containing various amount of CMS moieties were prepared via nitroxide-mediated radical polymerization (NMP) of St and CMS at 125 °C. To a solution of 9-anthracene methanol (1.1 equiv.) in dry 20 mL of THF was added to sodium hydride (60 w % dispersion in oil) (1.1 equiv.) and the reaction mixture was stirred at room temperature under nitrogen for 30 min. A solution of random copolymer (1.0 CMS equiv.), in dry THF was then added to this mixture, and the reaction mixture was refluxed for 12 h in the dark. It was then cooled to room temperature, evaporated to half of its volume and then precipitated into methanol. The light yellow product, P(S-co-CMS) with anthryl pendant groups, was dried for 24 h in a vacuum oven at 30 °C.

### **3.3.5 General procedure for preparation of graft copolymer via DA reaction of PMMA-MI and PS with anthryl pendant groups (PS-Anth)**

A solution of PMMA-MI (1.1 equivalent) in 10 mL of toluene was added to a 10 mL solution of random copolymer (1.0 anthracene equiv.) in of toluene. Catalytic amount of BHT as a radical inhibitor was added. The mixture was bubbled with nitrogen for 30 min. and refluxed for 48 h at 110 °C in the dark. The reaction mixture was evaporated under high vacuum. The crude product obtained was then dissolved in 5 mL of THF and poured into methanol. The white product formed was dried for 24 h in a vacuum oven at 30 °C.



### **3.3.6 General procedure for preparation of graft copolymer via DA reaction of PEG-MI and PS-Anth**

A solution of PEG-MI (1.1 equivalent) in 10 mL of toluene was added to a 10 mL solution of random copolymer (1.0 anthracene equiv.) in toluene. Catalytic amount of BHT as a radical inhibitor was added. The mixture was bubbled with nitrogen for 30 min. and refluxed for 48 h. at 110 °C in the dark. The reaction mixture was evaporated under high vacuum. The crude product obtained was then dissolved in 5 mL of THF and poured into methanol. The pale yellow product was dried for 24 h in a vacuum oven at 30 °C.

### **3.3.7 Preparation of samples for AFM**

Solutions of graft copolymers were prepared in toluene at a concentration of 8 mg/mL. Films were spin-coated at 2000 rpm for 1 min from these solutions on oxidized silicon substrates. Spin-coated films were kept in vacuum oven at low temperatures for solvent evaporation.

### **3.3.8 Synthesis of octa(nitrophenyl)silsesquioxane (ONO<sub>2</sub>PS)**

Octa(nitrophenyl)silsesquioxane was synthesized according to the literature reported by Laine et al [197]. OPS, 5.0 g (4.84 mmol) was added slowly to 30 mL fuming HNO<sub>3</sub> in small portions at 0 °C as done for ONO<sub>2</sub>PS. The obtained product was a light yellow powder (6.13 g, 4.40 mmol, 90%). OPS was slightly soluble in methylene chloride, but the ONO<sub>2</sub>PS product was soluble in THF, chloroform, acetone, methylene chloride etc.

<sup>1</sup>H NMR (DMSO-d<sub>6</sub>): 8.8-7.0 (Ar, 4.0H)

FT-IR (cm<sup>-1</sup>): 1527 (νN=O asym.), 1348 (νN=O sym.), 1304-990 (νSi-O-Si).

### **3.3.9 Synthesis of octa(aminophenyl)silsesquioxane (ONH<sub>2</sub>PS)**

Octa(aminophenyl)silsesquioxane was synthesized according to the literature reported by Laine et al [197]. To a 100 ml Schlenk flask equipped with a condenser and magnetic stirring, was added ONO<sub>2</sub>PS (4.0 g, 2.88 mmol) and 5 wt% Pd/C (488 mg, 0.23 mmol). Distilled THF (40 mL) and triethylamine (25 mL, 179.4 mmol) were added under nitrogen. The mixture was heated to 40 °C, and 99% formic acid (3.0 mL, 7.95 mmol) was added slowly at 40 °C under nitrogen with vigorous stirring with a magnetic stir bar. Carbon dioxide evolved with the addition of formic acid and

the solution separated into two layers. The reaction was run for 20 h. After the required time, the THF layer was separated from the black slurry by decantation. Then, 60 ml of THF was added to the black slurry and the solution was stirred until a black suspension formed. The suspension and the THF solution were passed through a funnel equipped with a glass fiber/celite filter to remove the catalyst. The two THF solutions were combined. The volume was then reduced to 20 mL under reduced pressure. This solution was put in a separatory funnel with 30 mL of water and 50 mL of ethyl acetate. The solution was washed five times with 250 mL aliquots of water to remove triethylammonium formate by-product and then washed with saturated aq. NaCl (40 mL). The organic layer was then dried over 3 g of Na<sub>2</sub>SO<sub>4</sub> to remove water and precipitated by adding into 150 mL of hexane. The precipitate was collected by filtration. The powder was then dissolved in 20 mL of THF and reprecipitated in 150 mL of hexane to remove any remaining triethylamine. The obtained powder was vacuum dried. The ONH<sub>2</sub>PS product obtained from ONO<sub>2</sub>PS was very similar giving light yellow powders in 85% (1.41 g 1.22 mmol), and was soluble in THF, acetone etc.

<sup>1</sup>H NMR (DMSO-d<sub>6</sub>): 7.9-6.1 (Ar, 4.0H), 5.5-4.4 (-NH, 2.0H).

FT-IR (cm<sup>-1</sup>): 3368 (νN-H asym.), 3456 (νN-H sym.), 1304-990 (νSi-O-Si).

### 3.3.10 Synthesis of octa(azidophenyl)silsesquioxane (ON<sub>3</sub>PS)

Octa(nitrophenyl)silsesquioxane was synthesized according to the literature reported by Moses et al [198]. Water (0.3 mL) was placed in a round-bottomed flask equipped with a thermometer and an efficient mechanical stirrer. While stirring, 0.09 ml. of concentrated sulfuric acid was added, followed by 0.5 g (4.33x10<sup>-4</sup> mole) of ONH<sub>2</sub>PS. When all the amine were converted to the brown sulfate, 0.2 ml more of water was added and the suspension was cooled to 0–5 °C in an ice-salt bath. A solution of 0.032 g (4.62x10<sup>-4</sup> mole) of sodium nitrite in 0.2 mL of water was added dropwise over a period of 15 minutes, and the mixture was further stirred for another 45 minutes. A thick precipitate of the sparingly soluble diazonium salt was separated from the initially clear solution during this period. With vigorously stirring, a solution of 0.03 g (4.91x10<sup>-4</sup> mole) of sodium azide in 0.3 ml of water was added, and stirring was continued for 40 minutes. The thick dark brown solid was filtered

with suction and washed with water. The material was allowed to dry in air in a dark place.

$^1\text{H}$  NMR (DMSO- $d_6$ ): 7.8-6.2 (Ar, 4.0 H)

FT-IR ( $\text{cm}^{-1}$ ): 2104 ( $\nu\text{-N}\equiv\text{N}$ ), 1304-990 ( $\nu\text{Si-O-Si}$ ).

### 3.3.11 Synthesis of prop-2-ynyl thiophene-3-carboxylate (*Propargylthiophene*)

In a 250 mL flask, of 3-thiophenecarboxylic acid (2 g, 15 mmol) was dissolved in 100 mL of 0.1 N NaOH. The mixture was heated at 50  $^{\circ}\text{C}$  until a clear solution was formed. To this solution, tetrabutylammonium bromide (0.5 g, 1.55 mmol) was added as a phase transfer catalyst. A solution of propargylbromide (2.04g, 17 mmol) in 20 mL of toluene was added portion wise to the solution. The mixture was kept stirring at 60  $^{\circ}\text{C}$  for 24 h. Then the toluene layer was separated and washed repeatedly with 2 % NaOH (200 mL, 0.1 N) and with water. Evaporating toluene afforded semi-solid. This solid was washed with cold hexane, and dried under vacuum. (Yield: ca. 60%)

$^1\text{H}$  NMR (DMSO- $d_6$ ): 8.14 (1.0H), 7.54 (1.0H), 7.33 (1.0H), 4.86 (1.0H), 2.50 (1.0H).

FT-IR ( $\text{cm}^{-1}$ ): 3293 ( $\nu\equiv\text{C-H}$ ), 2129 ( $\nu\text{C}\equiv\text{C}$ ), 1716 ( $\nu\text{C=O}$ ).

### 3.3.12 General procedure for synthesis of octa(*Thiophenophenyl*)silsesquioxane via click chemistry (*OThiophenePS*)

Octa(azidophenyl)silsesquioxane (0.2 g,  $2.20 \times 10^{-4}$  mol), prop-2-ynyl thiophene-3-carboxylate (0.04g,  $2.42 \times 10^{-4}$  mol), CuBr (0.047 g,  $3.3 \times 10^{-4}$  mmol) and 2,2'-bipyridine (0.057 g,  $3.63 \times 10^{-4}$  mmol) were dissolved in 10 mL of THF in a schlenk tube. The tube was degassed by three freeze-pump-thaw cycles and left in nitrogen. The reaction was carried out for 41 h at room temperature. The solution was filtered. This solution was put in a separatory funnel with 25 mL of diluted  $\text{H}_2\text{SO}_4$  (aq.) solution and 30 mL of ethyl acetate. The solution was washed with 150 ml aliquots of diluted acid solution and then  $\text{NaHCO}_3$  (aq.) solution and finally with water. The organic layer was then dried over  $\text{MgSO}_4$  to remove water and precipitated by adding into hexane. The precipitate was collected by filtration. The obtained dark brown powder was vacuum dried.

$^1\text{H}$  NMR (DMSO- $d_6$ ): 8.14 (1.0H), 7.54 (1.0H), 7.33 (1.0H), 4.86 (1.0H), 2.50 (1.0H).

FT-IR ( $\text{cm}^{-1}$ ): 1716 ( $\nu\text{C=O}$ ), 1716 ( $\nu\text{C=O}$ ).

### 3.3.13 Synthesis of PPy and OPS-PPy

Electrochemical polymerization of **OPS-PPy** was kindly performed by Metin Ak from Levent Toppare group. Its synthesis procedure is given below.

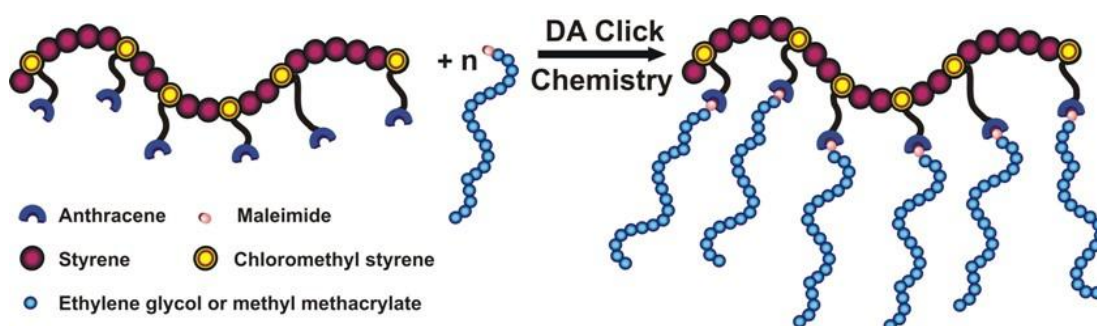
Electrochemical polymerization of **OPS-PPy** was carried out by sweeping the potential between -0.8 V and +1.1 V with 40 mV/s scan rate, in the presence of 50 mg **OThiophenePS** and 10  $\mu\text{L}$  Py in TBAFB (0.1 M) / DCM electrolyte-solvent couple. The working and counter electrodes were Pt wire and the reference electrode was a Ag wire. **OPS-PPy** was washed with DCM in order to remove excess electrolyte and unreacted monomer after the potentiodynamic electrochemical polymerization. PPy was synthesized under the same conditions. For the spectroelectrochemical studies, polymers were synthesized in the same solvent–electrolyte couple on an ITO-coated glass slide using a UV-cuvette as a single-compartment cell equipped with Pt counter electrode, and a Ag wire reference electrode. The electrochromic measurements, spectroelectrochemistry and switching studies of the polymer films were carried out in the same media in the absence of monomer.

## 4. RESULTS AND DISCUSSION

The “click”-type reactions, 1,3-dipolar azide-alkyne, [3 + 2], or Diels–Alder cycloadditions, [4 + 2], were applied, as a novel route, for the preparation of well-defined graft copolymers, developing photoinitiating systems with improved properties and reactive precursors for obtaining inorganic–organic conducting composites.

### 4.1 Anthracene-maleimide-based Diels-Alder “Click Chemistry” as a novel route to graft copolymers

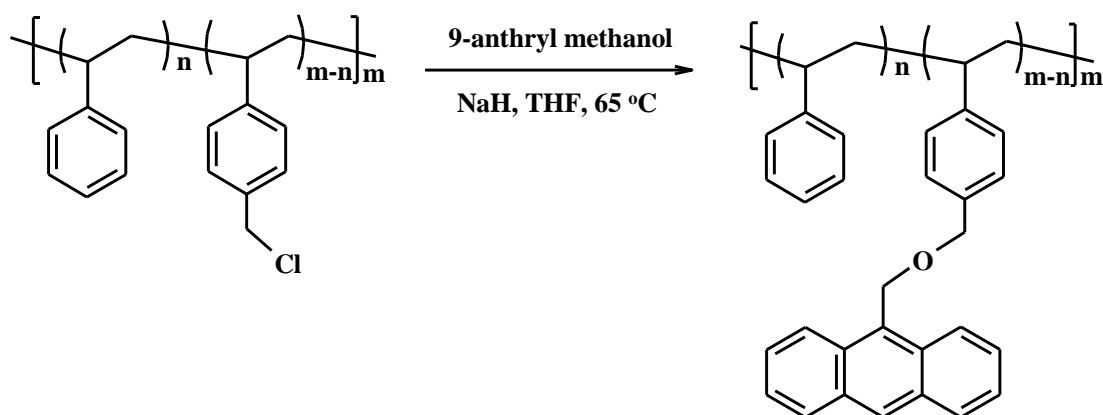
The study presented in this paper [7] aimed at describing anthracene-maleimide based DA “click reaction” as a novel route to prepare well-defined graft copolymers. Figure 4.1 outlines our synthetic strategy to this various phases of this work, viz., (i) preparing random copolymers of styrene (St) and 4-chloromethylstyrene (CMS) (which is a functionalizable monomer); (ii) attachment of anthracene functionality to the preformed copolymer by the *o*-etherification procedure; (iii) by using efficient DA “click chemistry”, maleimide functionalized poly(methyl methacrylate) (PMMA-MI) via ATRP of MMA or poly(ethylene glycol) (PEG-MI) via modification of commercial PEG was introduced into copolymers bearing pendant anthryl moieties. The details of these procedure and the results obtained were discussed below.



**Figure 4.1:** General presentation of grafting process by Diels-Alder click chemistry [7].

P(S-*co*-CMS) copolymers containing 8, 30 and 50% CMS units were prepared via NMP of St and CMS at 125°C. 9-Anthryl methanol was successfully introduced into the preformed P(S-*co*-CMS) copolymer backbone via etherification reaction through nucleophilic substitution of CMS units (Figure 4.2).

P(S-*co*-CMS) copolymers containing 8, 30 and 50% CMS units were prepared via NMP of St and CMS at 125°C. 9-Anthryl methanol was successfully introduced into the preformed P(S-*co*-CMS) copolymer backbone via etherification reaction through nucleophilic substitution of CMS units (Figure 4.2).



**Figure 4.2:** Incorporation of anthryl moieties by etherification process [7].

Copolymer compositions of polymers were determined using  $^1\text{H}$  NMR spectroscopy. The mole fractions of CMS and St were calculated from the ratio of the peak areas around 4.4 ppm, corresponding to two side-chain methylene protons of CMS to the total area between 6.3-7.4 ppm, which was attributed to the total aromatic protons. Similar method was applied for all random copolymers to calculate the mole fractions of CMS and St. The molar compositions of copolymers and number average molecular weights of P(S-*co*-CMS) determined by GPC were presented in Table 4.1.

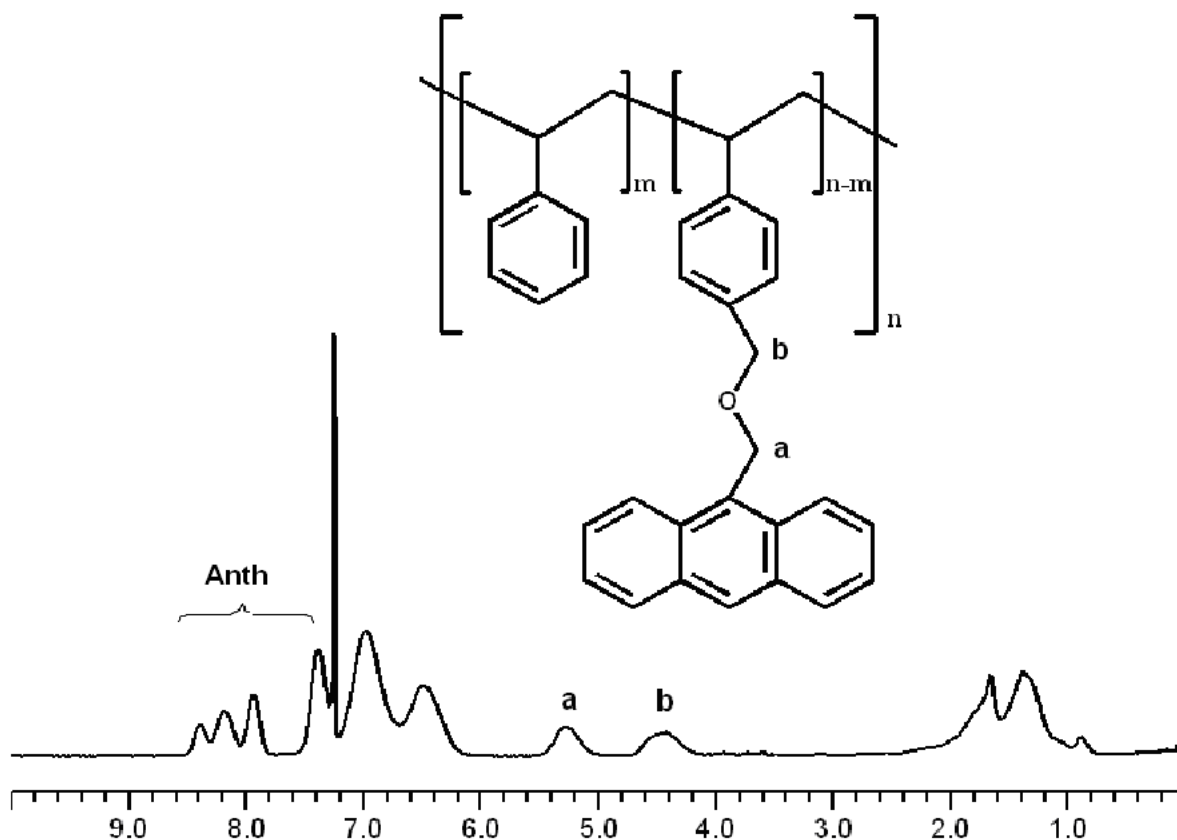
**Table 4.1:** Molecular weights and functionalities of the polymers at various stages [7].

Polymers	$M_n^a$	$M_w/M_n^a$	Functionality (mol %) <sup>b</sup>	
			CMS	Anth
P(S- <i>co</i> -CMS) (8%)	3700	1.38	8.5	-
PS-Anth (8%)	4000	1.51	-	8.5
PS- <i>g</i> -PEG (8%)	4400	1.42	-	-
PS- <i>g</i> -PMMA (8%)	12100	1.26	-	-
P(S- <i>co</i> -CMS) (30%)	4100	1.33	30.0	-
PS-Anth (30%)	4400	1.36	-	30.0
PS- <i>g</i> -PEG (30%)	5700	1.47	-	-
PS- <i>g</i> -PMMA (30%)	18000	1.24	-	-
P(S- <i>co</i> -CMS) (50%)	4200	1.39	50.6	-
PS-Anth (50%)	4800	1.31	-	50.6
PS- <i>g</i> -PEG (50%)	7100	1.40	-	-
PS- <i>g</i> -PMMA (50%)	27000	1.20	-	-

<sup>a</sup>Determined by GPC according to linear polystyrene standards.

<sup>b</sup>Determined from <sup>1</sup>H NMR spectra of the corresponding polymers (see text).

P(S-*co*-CMS) (8%, 30% and 50%) copolymers were modified by etherification procedure as described in the experimental section to obtain copolymers with anthryl pendant groups (PS-Anth). Primarily, the extent of substitution in the etherification was determined. The FTIR and <sup>1</sup>H NMR spectra confirmed the structure. In the NMR spectrum of a typical example, the new signals corresponding to methylene protons CH<sub>2</sub> adjacent to anthracene ring at 5.3 ppm and aromatic protons of anthryl group between 7.3 and 8.5 were detected (Fig. 4.3)



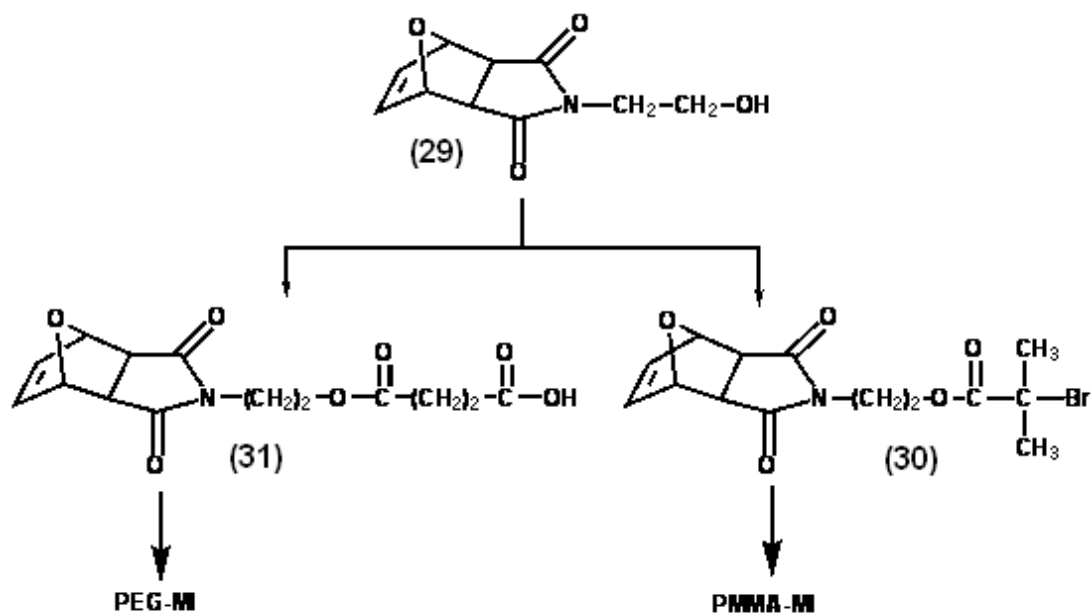
**Figure 4.3:**  $^1\text{H}$  NMR spectrum of PS-Anth (30%) in  $\text{CDCl}_3$  [7].

Moreover, the integrals of methylene protons  $\text{CH}_2$  adjacent to anthryl and phenyl ring on the modified random copolymer were in the ratio of 1:1, indicating complete etherification for each PS-Anth copolymers. The FTIR spectra supports this result showing no absorption around  $1265\text{ cm}^{-1}$ , proving disappearance of  $\text{CH}_2\text{Cl}$  moiety.

Independently, maleimide functionality was introduced into PEG via esterification reaction of monohydroxyl end-functionalized PEG and **31**. The number-average molecular weight ( $M_{n,\text{NMR}}$ ) of PEG-MI was calculated using NMR signals by comparison of the integrals of the vinyl end group signals (6.5 ppm) and that of the  $-\text{CH}_2\text{CH}_2\text{O}$  signal of PEG (3.64 ppm), respectively.  $M_{n,\text{theo}}$  and  $M_{n,\text{NMR}}$  values for PEG-MI are 840 and 850, respectively. In fact, the direct incorporation of maleimide end functionality by ATRP of MMA using maleimide functional initiator can be considered. However, this possibility is disregarded because of the participation of maleimide double bond during the free radical process. Therefore, ATRP of MMA using maleimide protected initiator, **30** was performed to yield polymers with the corresponding functionality. The polymerization temperature was deliberately kept low, i.e.,  $40\text{ }^\circ\text{C}$  so as to prevent possible deprotection during the polymerization. The



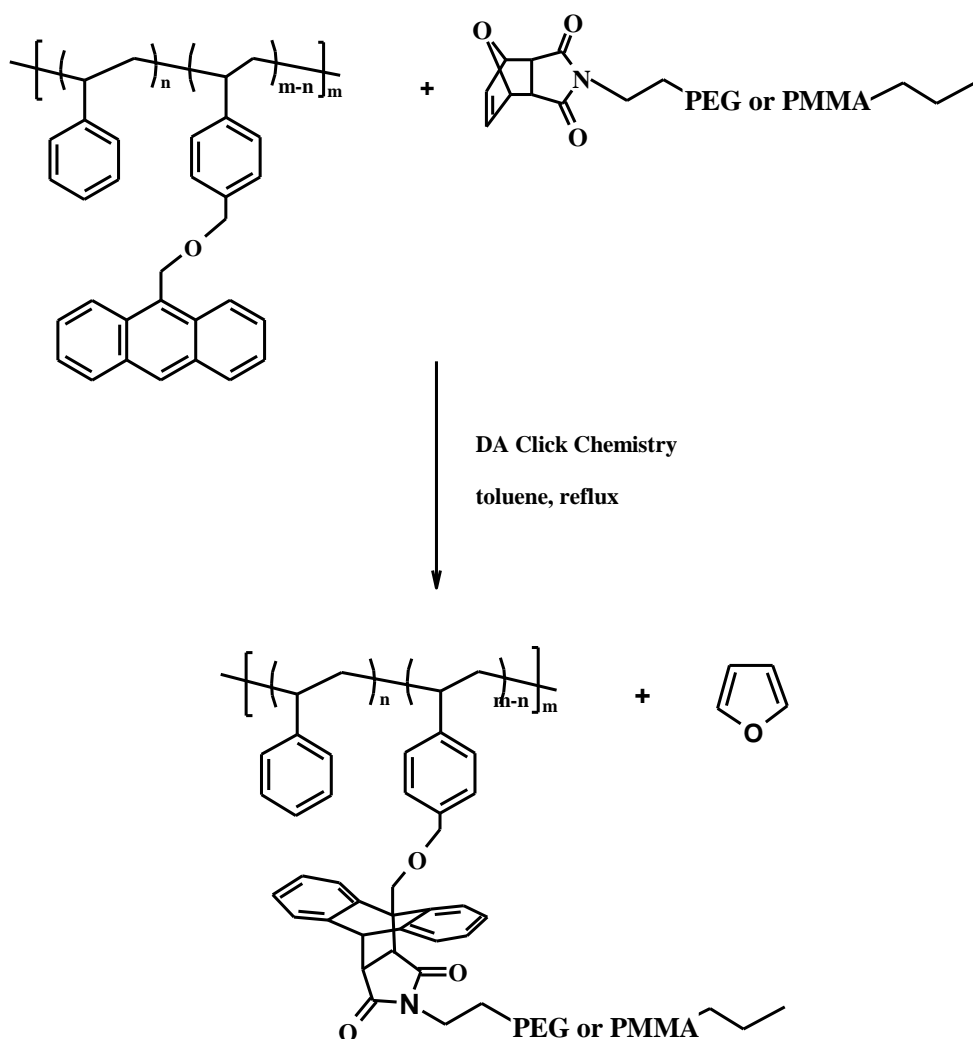
intermediates used for maleimide functionalization of both PEG and PMMA are presented in Figure 4.4.



**Figure 4.4:** Intermediates used for maleimide functionalization [7].

The theoretical MW of PMMA-MI was calculated by using the following equation:  $M_{n,theo} = ([M]_0/[I]_0) \times \text{conversion \%} \times \text{MW of monomer} + \text{MW of } \mathbf{30}$ . In addition,  $M_{n,NMR}$  of PMMA-MI was determined from the ratio of integrated signals at 3.58 ppm ( $\text{OCH}_3$  protons of MMA) to 6.5 ppm (vinyl end protons).  $M_{n,theo}$  and  $M_{n,NMR}$  values of PMMA-MI were calculated as 1250 and 2350, respectively.

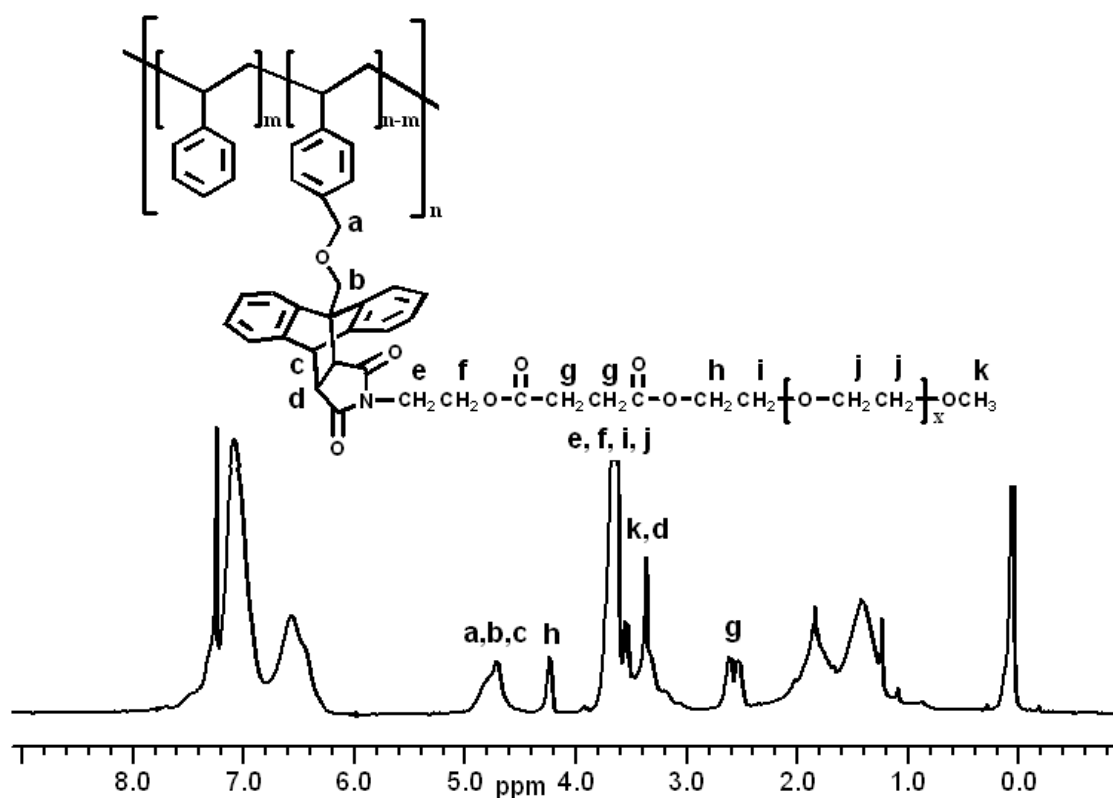
As it will be described below, the combined retro DA and “DA click reaction” utilizing polymers with antagonist functional groups leads to the formation of well-defined graft copolymers, where both main and side chain segments were prepared in a controlled manner. The overall process is presented in Figure 4.5.



**Figure 4.5:** Grafting by *in situ* retro DA and DA processes [7].

Deprotections of maleimide-functionalized polymers (retro DA) were carried out *in situ* during DA “Click Reaction” by heating PS-Anth copolymers with PEG-MI or PMMA-MI in toluene at 110 °C. First, a retro- DA reaction of PEG-MI or PMMA-MI proceeds via releasing of furan to give the deprotected maleimide functionality at the reflux temperature of toluene. Then, at this temperature, efficient DA reaction of the recovered maleimide and copolymers with pendant anthryl units resulted the expected well-defined graft copolymers, PS-*g*-PEG or PS-*g*-PMMA. The copolymerization reaction was completed with quantitative yields without need for additional purification step. The by-product, furan, and excess PEG-MI or PMMA-MI (having relatively low molecular weight), all are completely soluble in methanol which is the precipitating solvent. Evidence for the formation of DA adduct of the resulting PS-*g*-PEG graft copolymer was observed in the  $^1\text{H}$  NMR spectra (Figure 4.6). Also, the efficiency of DA for grafting process was investigated by UV and

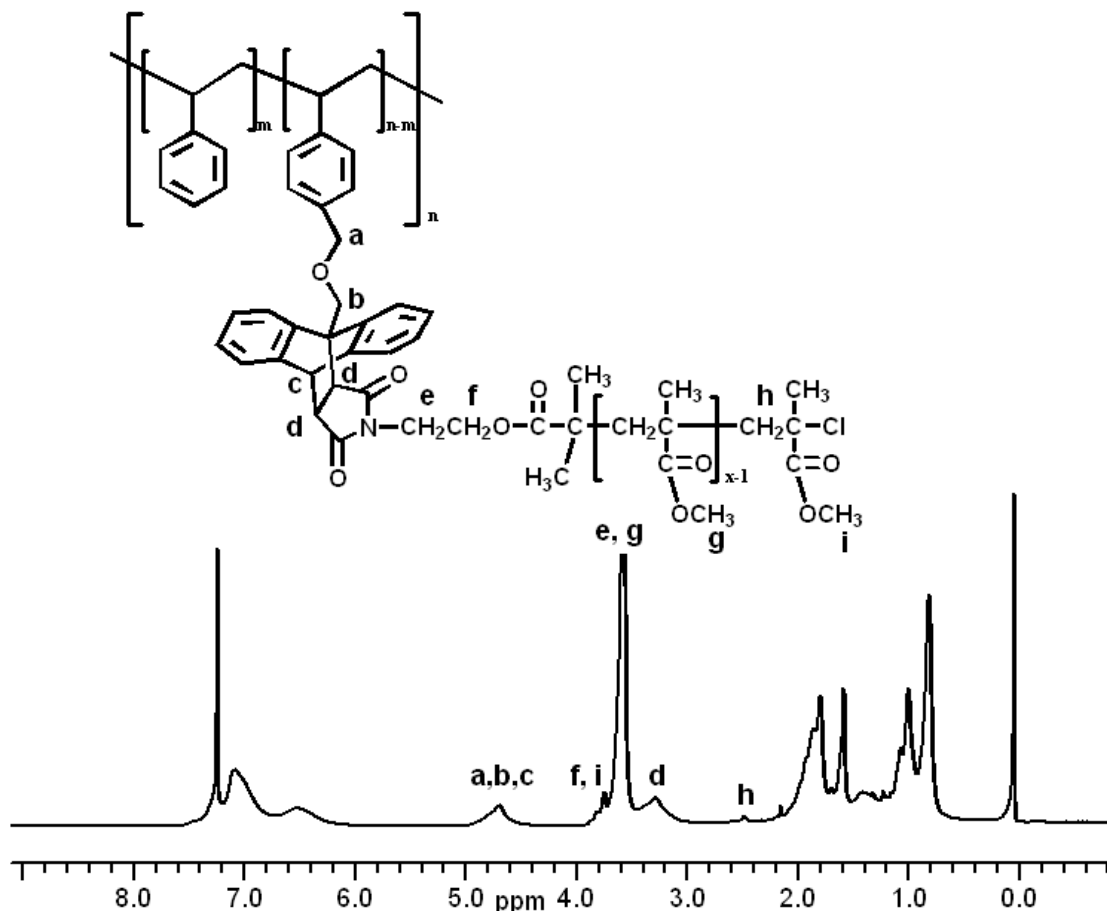
fluorescence spectroscopy (*vide infra*). The peaks between 7.3 and 8.5 ppm, characteristic for aromatic protons of anthracene were completely disappeared. It also revealed that, aromaticity of central phenyl unit of anthracene disappeared as a result of DA cycloaddition, and a new bridgehead proton was appeared. A broad peak at 4.7 ppm, due to the bridgehead proton of cyclo-adduct CH, appeared and it overlapped with the peaks corresponding to methylene protons of CH<sub>2</sub> adjacent to anthracene and phenyl ring. Moreover, a new signal corresponding to CH proton on the fused maleimide ring and OCH<sub>3</sub> methoxy protons of PEG end group was observed at 3.4 ppm. The main chain protons of PEG (OCH<sub>2</sub>CH<sub>2</sub>) and CH<sub>2</sub>CH<sub>2</sub> protons adjacent to nitrogen atom of maleimide gave distinct signal at 3.6 ppm. Obviously, the resulting graft copolymers are amphiphilic in nature and are expected to form aqueous micelles as demonstrated by Schubert and co-workers [199,200] who reported the linking of PEG chains to a hydrophobic backbone via ruthenium-terpyridine complexes. Further studies in this line are in progress and will be reported elsewhere.



**Figure 4.6:** <sup>1</sup>H NMR spectrum of PS-g-PEG (30%) in CDCl<sub>3</sub> [7].

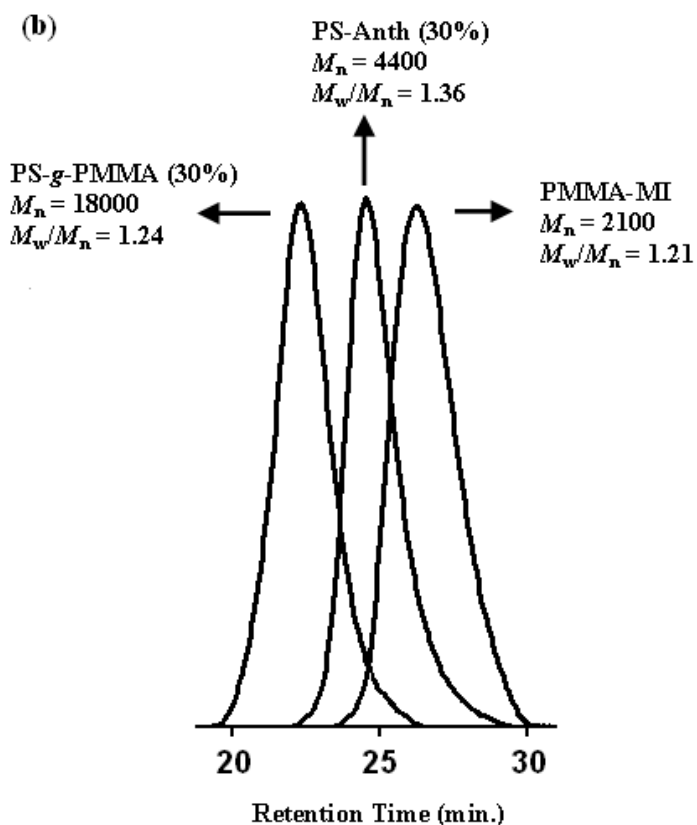
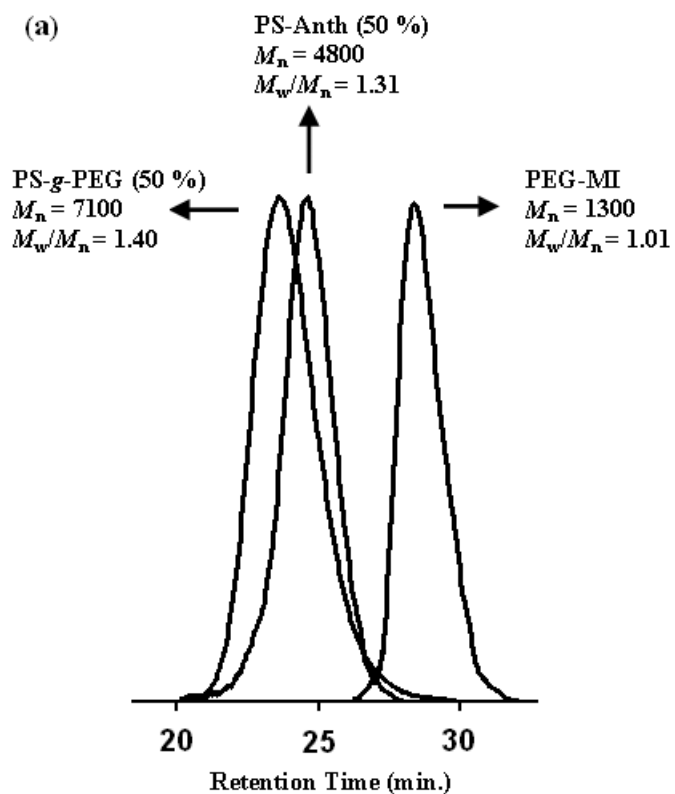
The PS-g-PMMA graft copolymers, prepared by the same procedure, were characterized by <sup>1</sup>H-NMR spectroscopy. These spectra revealed the corresponding

DA cyclo-adduct. Similar chemical shifts were observed (Figure 4.7). The peak of OCH<sub>3</sub> protons of PMMA backbone and CH<sub>2</sub> protons adjacent to the nitrogen of the maleimide appeared at 3.6 ppm. The peaks at 3.7 are attributed to OCH<sub>3</sub> end group of PMMA and CH<sub>2</sub> protons adjacent to ester linkage. Furthermore, two CH protons of the imide ring at 3.3 ppm were also detected.



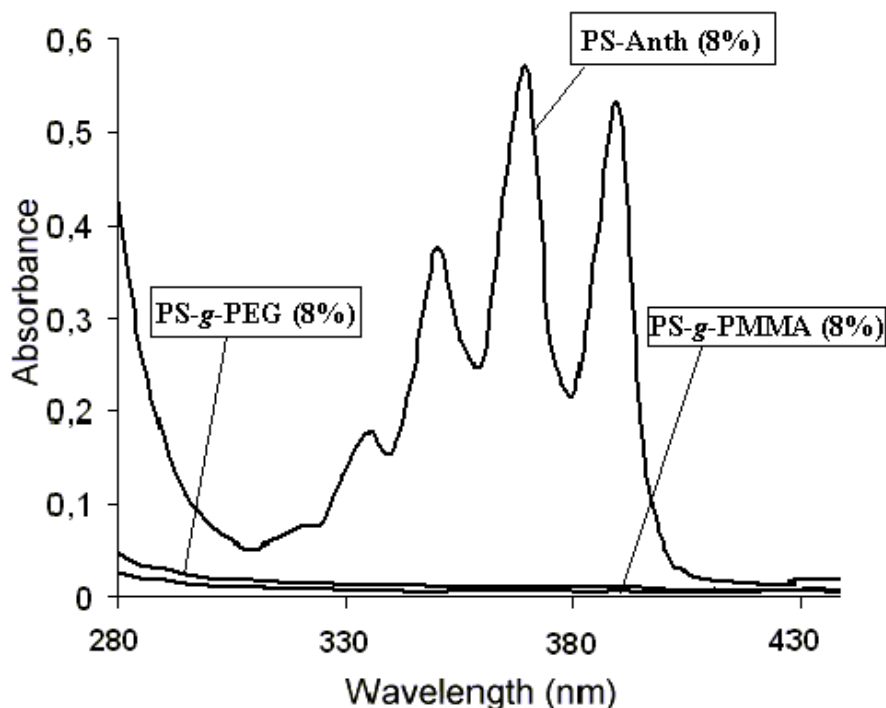
**Figure 4.7:** <sup>1</sup>H NMR spectrum of PS-g-PMMA (30%) in CDCl<sub>3</sub> [7].

Figure 4.8 shows the evolution of GPC traces of the PS-Anth, PS-g-PEG and PS-g-PMMA copolymers with 30 or 50% functionality content. All GPC traces based on linear PS used as standard in GPC calibration were unimodal and narrow. No tailing was observed in the molecular weight of precursors. The shift of PS-Anth and PEG-MI or PMMA-MI precursors to higher molecular weight region revealed that the formation of PS-g-PEG or PS-g-PMMA by DA reaction was achieved efficiently.



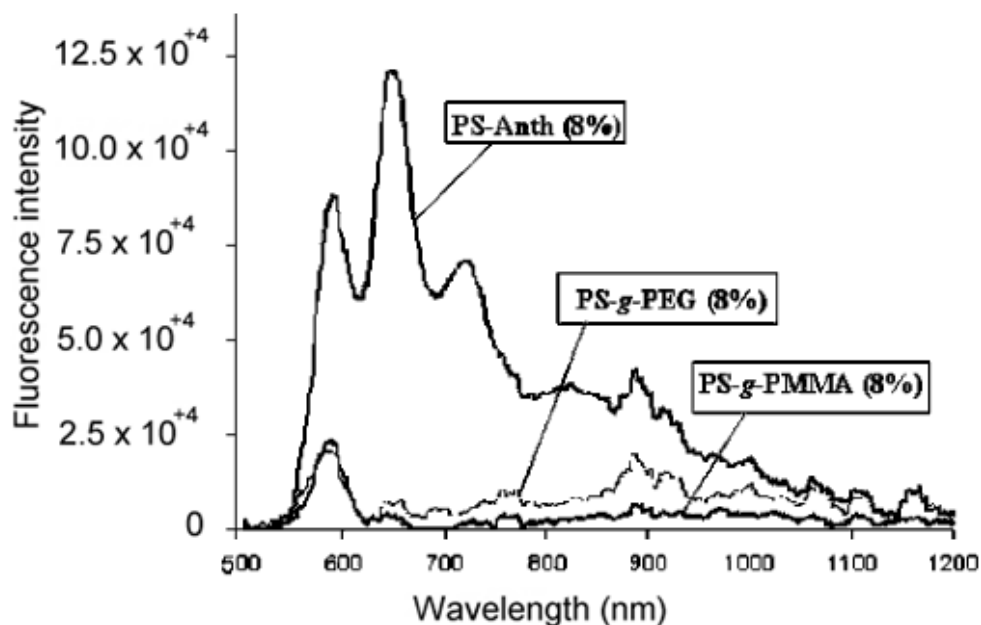
**Figure 4.8:** Evolution of GPC traces: PEG-MI PS-Anth (50%), and PS-g-PEG (50%) (a), and PMMA-MI, PS-Anth (30%), and PS-g-PMMA (30%) (b) [7].

DA adduct formation was also monitored by UV and fluorescence spectroscopy (Figures 4.9 and 4.10). In UV measurement, the characteristic five-finger absorbance of PS-Anth (8%) was observed from 300 to 400 nm, while the corresponding PS-*g*-PEG (8 %) and PS-*g*-PMMA (8 %) showed no absorbance in this region (Figure 4.9). Overall UV measurements clearly pointed out a quantitative DA reaction between anthracene and maleimide moieties.



**Figure 4.9:** Absorption spectra of PS-Anth (8%), PS-*g*-PEG (8%), and PS-*g*-PMMA (8%);  $c = 2 \times 10^{-5}$  M in  $\text{CCl}_4$  [7].

The fluorescence spectrum of diluted solution of PS-Anth (8%) in  $\text{CH}_2\text{Cl}_2$  excited at  $\lambda_{\text{exc}} = 390$  nm showed the characteristic emission bands of the excited (singlet) anthracene at 595, 655 and 725 nm (Figure 4.10). In contrast, PS-*g*-PEG (8 %) and PS-*g*-PMMA (8 %) had no significant emission proving disappearance of anthracene moieties after efficient DA reaction.



**Figure 4.10:** Emission spectra of PS-Anth (8%), PS-g-PEG (8%), and PS-g-PMMA (8%);  $\lambda_{exc.} = 390 \text{ nm}$ ;  $c = 2 \times 10^{-5} \text{ M}$  in  $\text{CCl}_4$  [7].

The glass transition temperatures ( $T_g$ ) of copolymers were determined by DSC under nitrogen atmosphere. As shown in Table 2, the addition of more rigid and bulky anthracene functionality into P(S-co-CMS) copolymers, further increases the  $T_g$ , comparing with those of the pristine polymers.  $T_g$  values for the copolymer series of PS-PEG (8 %, 30%, and 50%) are determined as 79, 75, and 73 °C, respectively. It was obvious that  $T_g$  values gradually decreased depending on the increasing PEG content. Any  $T_g$  for the PEG segment ( $T_g$  of PEG-MI = -44 °C) was not observed, because of the relatively shorter PEG-MI when compared with that of PS-Anth. The first transitions were almost identical to that of PMMA-MI segment ( $T_g$  of PMMA-MI = 78 °C), while the second transitions were increased with the increase of the grafted PMMA concentration, which affected the rigidity of PS backbone. For PS-g-PMMA copolymers, two  $T_g$  values were observed (see Table 2). These thermal data clearly indicated that PS backbone and grafted PMMA segments were phase separated for these studied compositions.

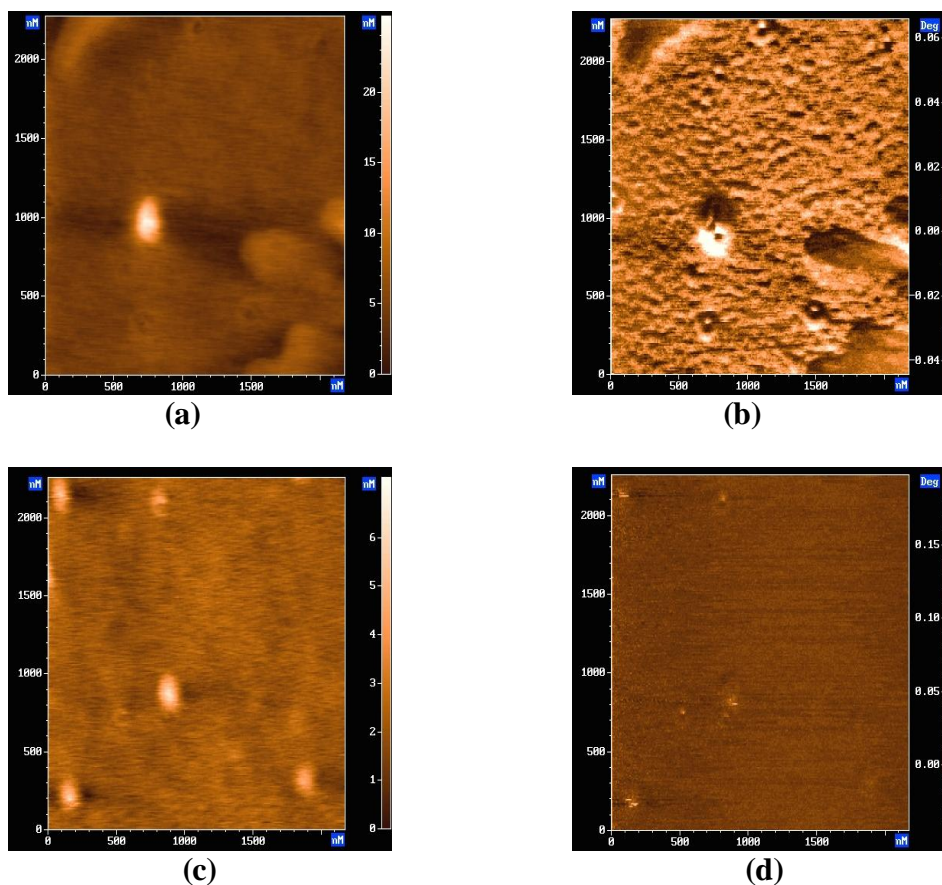
**Table 4.2:** The glass transition temperatures<sup>a</sup> ( $T_g$ ) of the polymers at various stages [7].

Functionality (mol %)	$T_g$ of P(S- <i>co</i> -CMS) (°C)	$T_g$ of PS-Anth (°C)	$T_g$ of PS- <i>g</i> -PEG (°C)	$T_g$ s of PS- <i>g</i> -PMMA (°C)
8	92	96	79	79 and 105
30	98	108	75	80 and 121
50	105	115	73	82 and 130

<sup>a</sup>Determined by DSC under nitrogen at a heating rate of 10 °C/min.

Atomic Force Microscopy (AFM) investigations of the PS-*g*-PMMA (8 %) showed indications of this behavior. While AFM height picture (Figure 4.11a) showed a relatively smooth surface, the corresponding AFM phase picture (Figure 4.11b) showed bright and dark contrast undulations indicating polymers of different viscoelasticity in the material. The length scale of these regions is less than 100 nm. PS-*g*-PEG (8 %) also showed smooth surface features (Figure 4.11c) but any indication of the regions of different viscoelastic materials was not observed. AFM phase picture (Figure 4.11d) showed a uniform phase throughout the surface without any contrast undulations. This is due to the relatively shorter PEG chain compared to PS main chain, in agreement with observation of only one  $T_g$  in DSC measurements for this molecule.

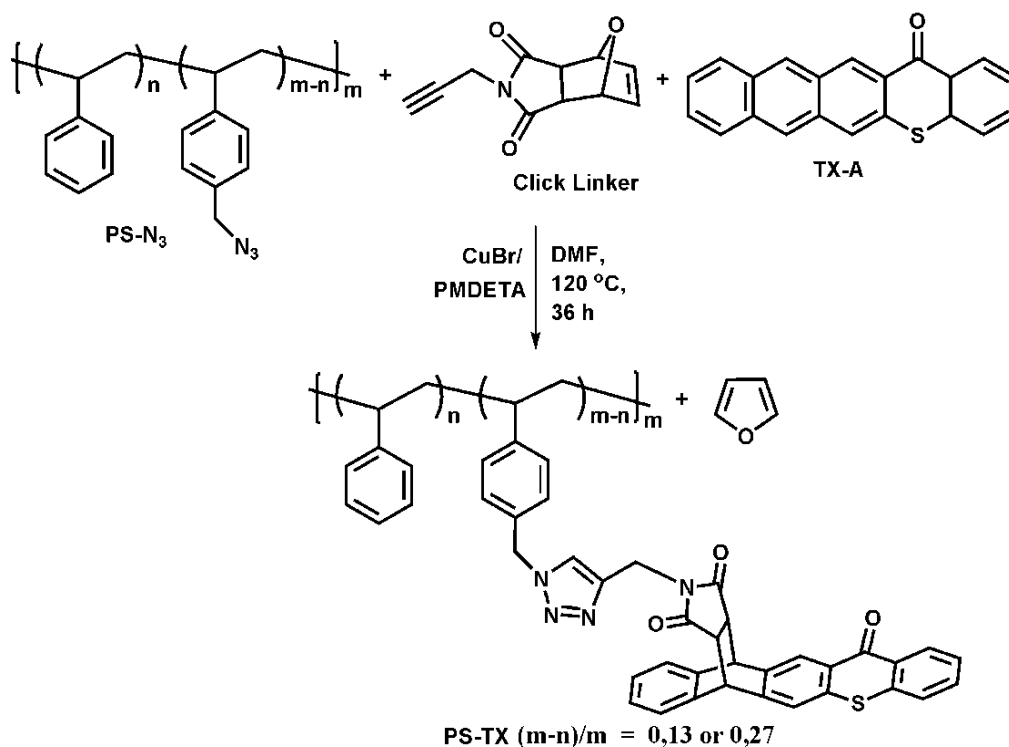




**Figure 4.11:** Atomic force microscopy pictures: height (a) and phase (b) picture of PS-*g*-PMMA (8%); height (c) and phase (d) picture of PS-*g*-PEG (8%). All pictures correspond to an area of 2  $\mu\text{m}$  x 2  $\mu\text{m}$  [7].

## 4.2 Synthesis and characterization of polymeric thioxanthone photoinitiators via double Click Reactions

As part of our continuing interest on the development of photosensitive systems for various synthetic applications, our synthetic approach towards the direct preparation of polymers containing side-chain thioxanthone moieties is based on “double click” chemistry strategy combining *in situ* 1,3-dipolar azide-alkyne [3+ 2] and thermoreversible Diels-Alder [4 + 2] cycloaddition reactions. The overall process is represented in Figure 4.12.

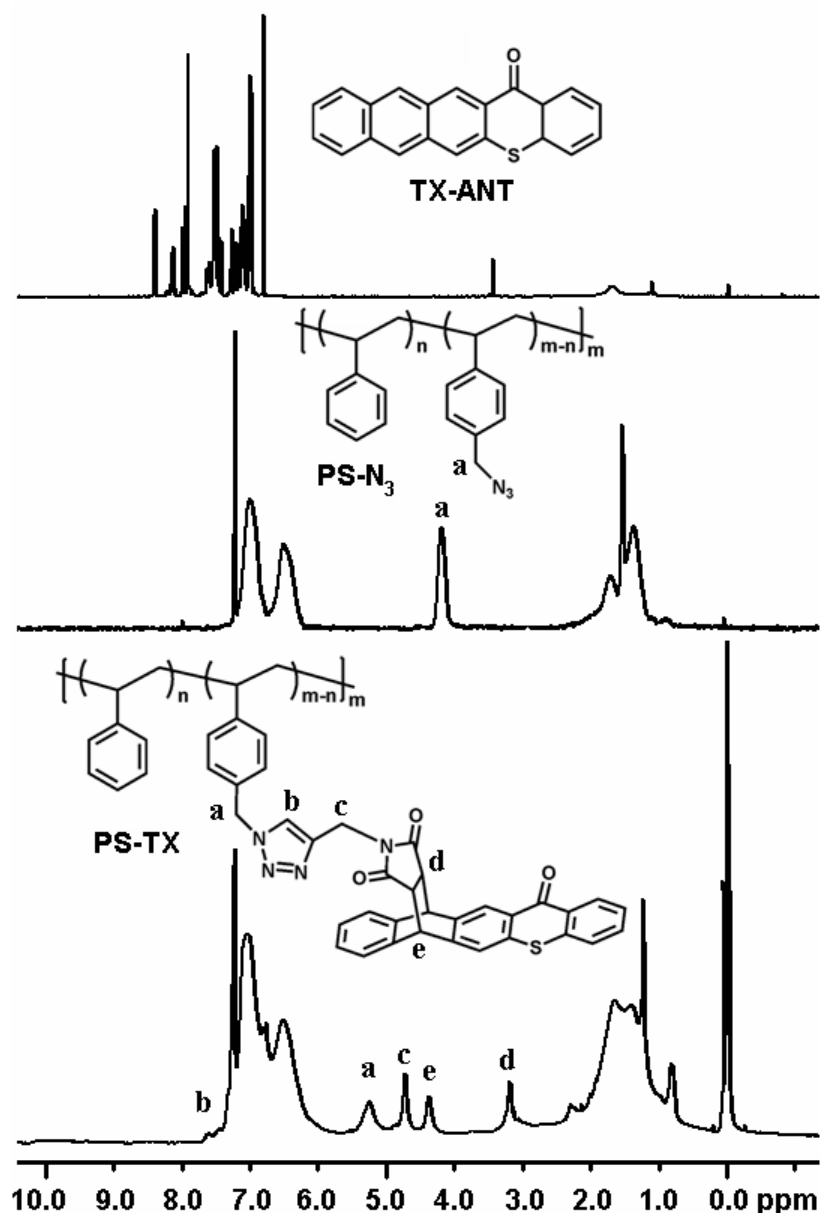


**Figure 4.12:** Side-chain functionalization of PS-N<sub>3</sub> with anthracene-thioxanthone (TX-A) in the presence of N-propargyl-7-oxynorbornene (PON) as click linker via double click chemistry [8].

According to this approach, first poly(styrene-*co*-chloromethylstyrene) P(S-*co*-CMS) copolymers containing two different chloromethylstyrene (CMS) units (13 and 27 mol%) were prepared via nitroxide mediated radical polymerization (NMP). The compositions of copolymers as determined by using <sup>1</sup>H-NMR spectroscopy are in agreement with the expected values and indicate the random copolymer structure. The resulting P(S-*co*-CMS) copolymers were then quantitatively converted into polystyrene-azide (PS-N<sub>3</sub>) in the presence of NaN<sub>3</sub>/DMF at room temperature. In the <sup>1</sup>H NMR spectrum of PS-N<sub>3</sub>, while the signal at 4.50 ppm corresponding to -CH<sub>2</sub>-Cl protons of the precursor P(S-*co*-CMS) disappeared completely, a new signal appeared at 4.25 ppm was attributed to -CH<sub>2</sub> linked to azide groups. The FT-IR spectral analysis also supports this result. The other components of the double click reaction, namely thioxanthone-anthracene (TX-A) [201] and N-propargyl-7-oxynorbornene [8] (PON) were synthesized according to the literature procedures. In the final step of the process, PS-N<sub>3</sub>, TX-A and PON were reacted in one-pot to yield the desired PS-TX macrophotoinitiator. In this step, two independent click reactions occurred simultaneously. While CuBr/PMDETA catalyzed triazole formation was accomplished between the azide of PS-N<sub>3</sub> and the alkyne functional end group of PON, retro-Diels-Alder reaction proceeded concomitantly between

PON and anthracene moiety of TX-A after deprotection of the maleimide group. Notably, PON acts as a “click linker” in the process, as it contains suitable functional groups for the two click reactions involved. The possible by-products, i.e., furan and excess TX-A or PON are completely soluble in the precipitating solvent methanol. Consequently, the side chain modification was completed with quantitative yields without additional purification steps.

Evidence for the occurrence of the double click reactions was obtained from  $^1\text{H}$  NMR, UV and fluorescence spectroscopy.

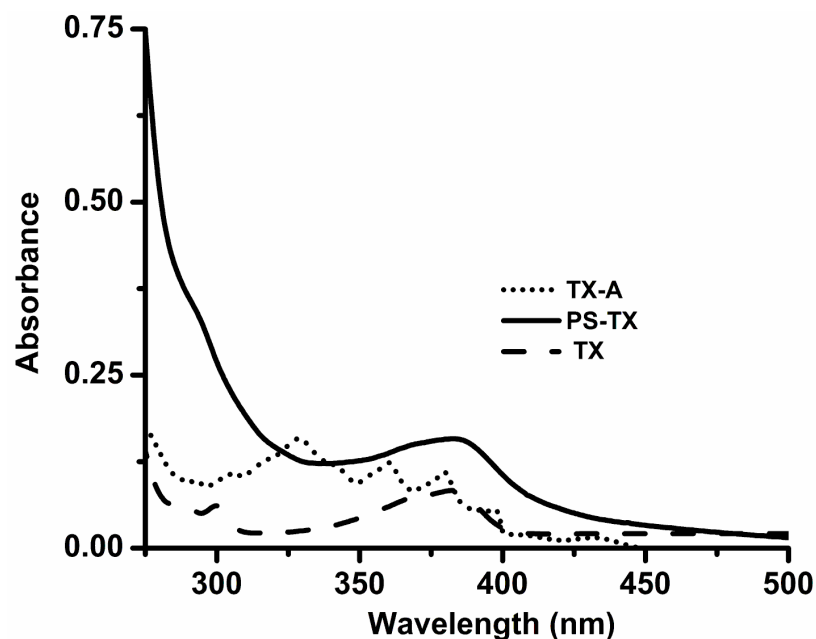


**Figure 4.13:**  $^1\text{H}$  NMR spectrum of TX-A, PS- $\text{N}_3$  and PS-TX (27%) in  $\text{CDCl}_3$  [8].

As can be seen from Figure 4.13, where  $^1\text{H}$  NMR spectra of TX-A and PS- $\text{N}_3$  were recorded, the peaks between 7.4 and 8.5 ppm, characteristic for aromatic protons of

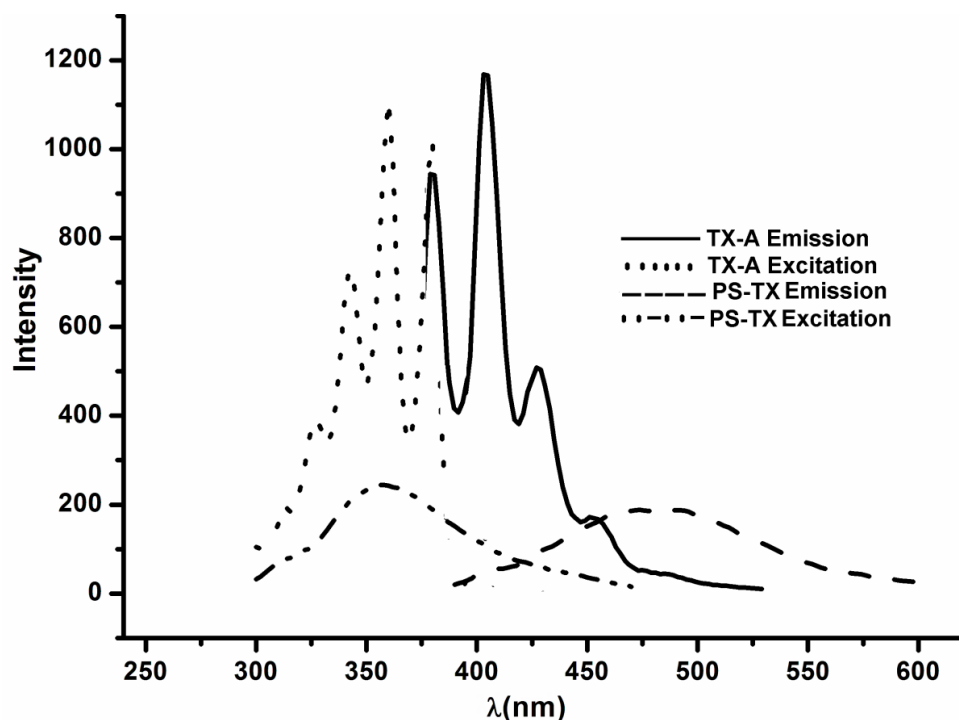
anthracene, disappeared completely. This indicates the loss of the aromaticity of the central phenyl unit of anthracene by Diels-Alder cycloaddition click reaction. Furthermore, the two new signals corresponding to a bridgehead (-CH) proton of the cycloadduct and -CH proton on the fused maleimide ring appeared at 4.74 and 3.20 ppm, respectively. The appearance of the peak belonging to -CH- proton of the triazole ring at 7.46 ppm is a typical indication for the successful completion of the other click reaction, 1,3-dipolar cycloaddition. Based upon a comparison of the integration of the peak intensities at 5.26 ppm and 4.74 ppm, corresponding to the methylene protons linked to triazole ring and adjacent to the cycloadduct, respectively, the obtained ratio of 1:1 clearly indicates the efficiency of the process. The FTIR spectra also confirm quantitative reaction, as the azide stretching band at around  $2094\text{ cm}^{-1}$  disappears completely and a new carbonyl band at  $1709\text{ cm}^{-1}$  appears.

Photophysical characteristics of the obtained PS-TX were investigated by UV and fluorescence spectroscopy (Figures 14 and 15). As can be seen from Figure 14, TX-A displays characteristic five-finger absorbance in 300-400 nm range. On the contrary, the PS-TX macrophotoinitiator shows a different absorption signature with a maximum at 380 nm, which is similar to the absorption spectrum of pure thioxathone indicating that the absorption regime of the precursor has changed as a result of the modification. Indeed, DA reaction between anthracene and deprotected maleimide moieties causes the loss of the aromaticity of central phenyl unit of anthracene. In another words, TX-A group is transformed into thioxanthone group by the so called double click reaction.



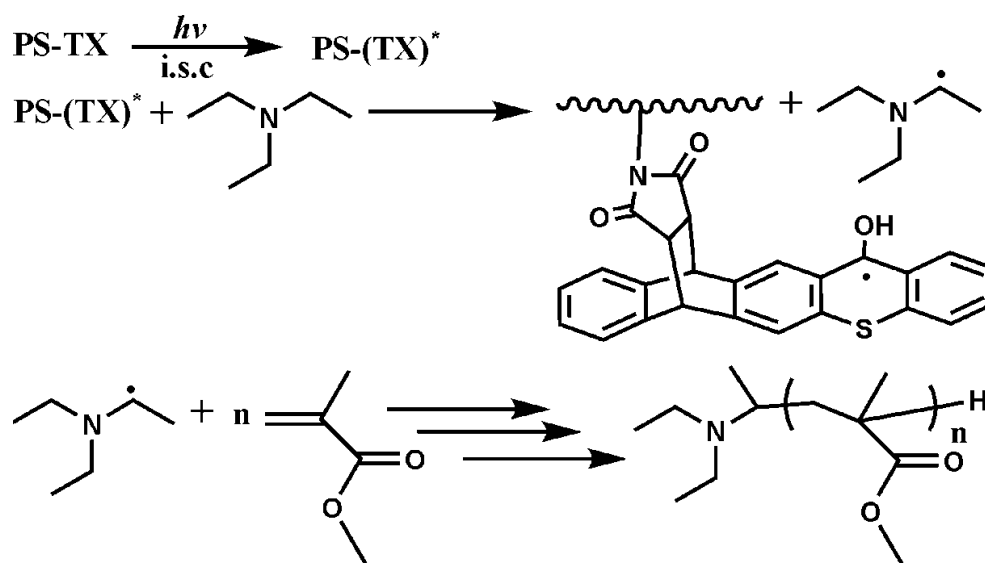
**Figure 4.14:** Absorption spectra of PS-TX (27%), TX-A and TX in  $\text{CH}_2\text{Cl}_2$ . The concentrations are  $1 \times 10^{-5}$  M in terms of thioxanthone moieties [8].

Fluorescence spectra of PS-TX may also provide further evidence for the efficiency of the modification process and information on the nature of the excited states involved. As can be seen from Figure 3, excitation and emission fluorescence spectra in DMF of TX-A and PS-TX obtained by double click reaction are quite different. TX-A exhibits characteristic emission bands of the excited (singlet) of anthracene moiety. In contrast, PS-TX has no significant emission of this kind and the spectrum shows a nearly mirror-image-like relation between absorption and emission again similar to bare TX. Expectedly, the intensities are lower in the case of side-chain thioxanthone bound polymer.



**Figure 4.15:** Emission spectra of TX-A and PS-TX (27%) in DMF;  $\lambda_{exc}=360$  nm. The concentrations are  $2 \times 10^{-5}$  M in terms of thioxanthone moieties [8].

Polymeric systems bearing side-chain TX groups can act as bimolecular photoinitiators when used in conjunction with hydrogen donors analogous to the low molecular weight TXs. PS-TX was used as a photoinitiator for the polymerization of methyl methacrylate (MMA) in the presence of triethyl amine (TEA) as hydrogen donor. The overall process is shown in Figure 4.16.



**Figure 4.16:** Photoinitiated free radical polymerization of methyl methacrylate (MMA) by using PS-TX macrophotoinitiator [8].

Due to steric bulkiness and delocalization, the polymeric ketyl radical is insufficiently reactive to initiate the polymerization of vinyl monomers. Although not entirely elucidated, presumably these radicals undergo bimolecular termination. The results are compiled in Table 4.3. For comparison, photopolymerizations in the absence of either PS-TX itself or TEA are also included. As can be seen, PS-TX is not an efficient photoinitiator in the absence of a co-initiator. The presence of an amine such as TEA is important for effective photoreduction and photopolymerization. In this connection, it should be pointed out that this result also specifies the change of the photophysical properties of TX-A. Previously, it was shown [210] that TX-A generates initiating species without requirement of an additional hydrogen donor. It is also interesting to note the effect of TX content in the macrophotoinitiator. A higher conversion was attained when the TX content was higher indicating that the rate of initiation is proportional to the absorbed light and consequently to the amount of the TX functional side groups.

**Table 4.3:** Photoinitiated polymerization<sup>a</sup> of methyl methacrylate (MMA) with macrophotoinitiator in CH<sub>2</sub>Cl<sub>2</sub> [8].

Macrophotoinitiator <sup>b</sup>	TEA (mol L <sup>-1</sup> )	Conversion (%)	M <sub>n</sub> x10 <sup>-4</sup> (g/mol)	M <sub>w</sub> /M <sub>n</sub>
PS-TX <sup>c</sup>	15x10 <sup>-4</sup>	13.8	21500	1.59
PS-TX <sup>d</sup>	15x10 <sup>-4</sup>	20.0	20600	1.70
PS-TX <sup>d</sup>	-	2.00	75000	2.16
-	15x10 <sup>-4</sup>	0.30	83200	2.10

<sup>a</sup>[MMA]=9.28 mol L<sup>-1</sup>; irradiation time= 2 h.

<sup>b</sup>[PS-TX] = 3.2x10<sup>-4</sup> mol L<sup>-1</sup>.

<sup>c</sup>Obtained from the precursor PS-*co*-PCMS with 13 mol% CMS content.

<sup>d</sup>Obtained from the precursor PS-*co*-PCMS with 27 mol% CMS content.

Among the several solvents tested in our experiments (Table 4.4), dimethylformamide (DMF) seemed to be the most suitable solvent for the photopolymerization initiated by PS-TX. Obviously, the situation is complex and two effects are combined. First, PS-TX dissolves in DMF better than the other solvents. Second, although radical polymerizations are not sensitive to the polarity of the solvent,[202] triplet-state lifetime of photoinitiators involving electron transfer such as TX derivatives may depend on some polarity effects [203].

**Table 4.4:** Effect of solvent on the photoinitiated polymerization <sup>a</sup> of methyl methacrylate (MMA) with PS-TX<sup>b</sup> at room temperature [8].

Solvent	Conversion (%)
DMF	21.5
THF	1.00
CH <sub>2</sub> Cl <sub>2</sub>	13.8
- <sup>c</sup>	19.3

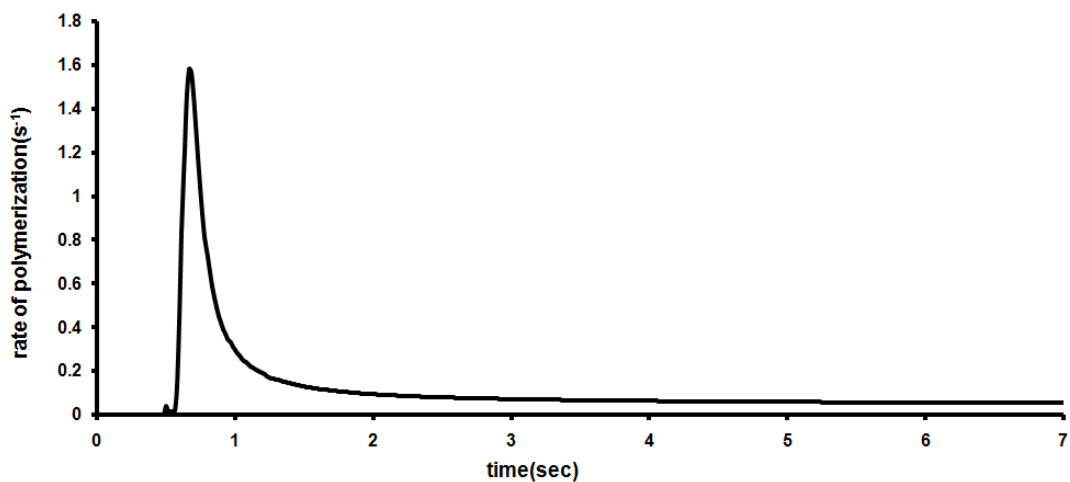
<sup>a</sup>[MMA]=9.28 mol L<sup>-1</sup>; [PS-TX]=3.2x10<sup>-4</sup> mol L<sup>-1</sup>; [TEA]=15x10<sup>-4</sup> mol L<sup>-1</sup>; irradiation time= 2 h.

<sup>b</sup>Obtained from the precursor PS-co-PCMS with 13 mol% CMS.

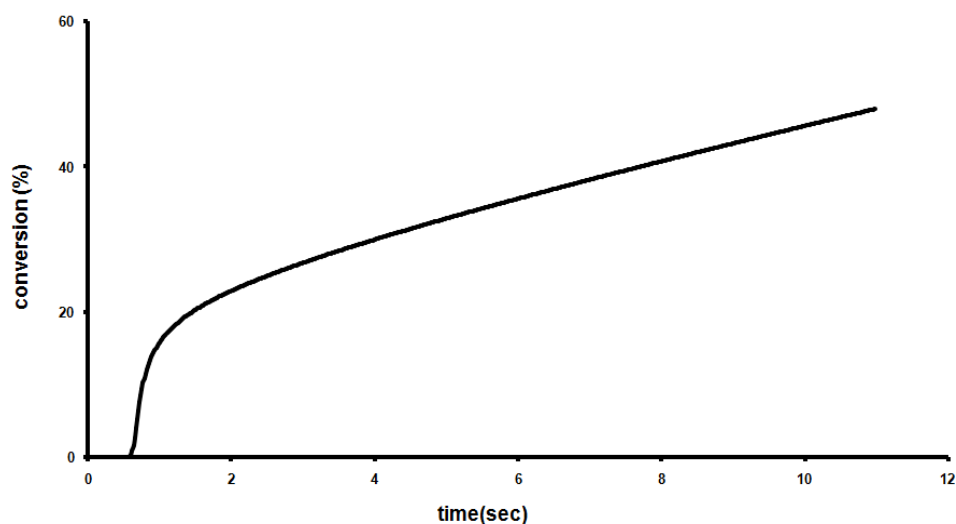
<sup>c</sup>Polymerization was performed in bulk.

We have also tested the polymerizability of styrene (S) monomer with PS-TX. In complete contrast to TX-A, polymerization of S with this macrophotoinitiator in the presence of TEA did not proceed. Although aromatic carbonyl/amine combinations represent an effective photoinitiator system for the polymerization of (meth)acrylates, they appear to be less reactive towards styrene monomers due to the high quenching rate of the monomer and the low reactivity of  $\alpha$ -amino radicals with S [204]. This behavior is in accordance with the spectral findings indicating that PS-TX exhibits photochemical characteristics of typical aromatic carbonyl compounds. The efficiency of the PS-TX in the photocuring of formulations containing multifunctional monomers was also studied. In Figure 4.17, photo DSC exotherm referring to the polymerization of 1,1,1-tris-(hydroxymethyl)-propan-triacrylate (TPTA) containing PS-TX and TEA under polychromatic light is shown. Figure 4.18 displays plot of the conversion versus irradiation time derived from Figure 4. The shape of this “conversion-time” kinetics curve indicates two stages, a rapid first stage followed by a slow stage. At the second stage, gelation and vitrification of the polymerizing trifunctional acrylate most likely render the diffusion of the components more difficult.





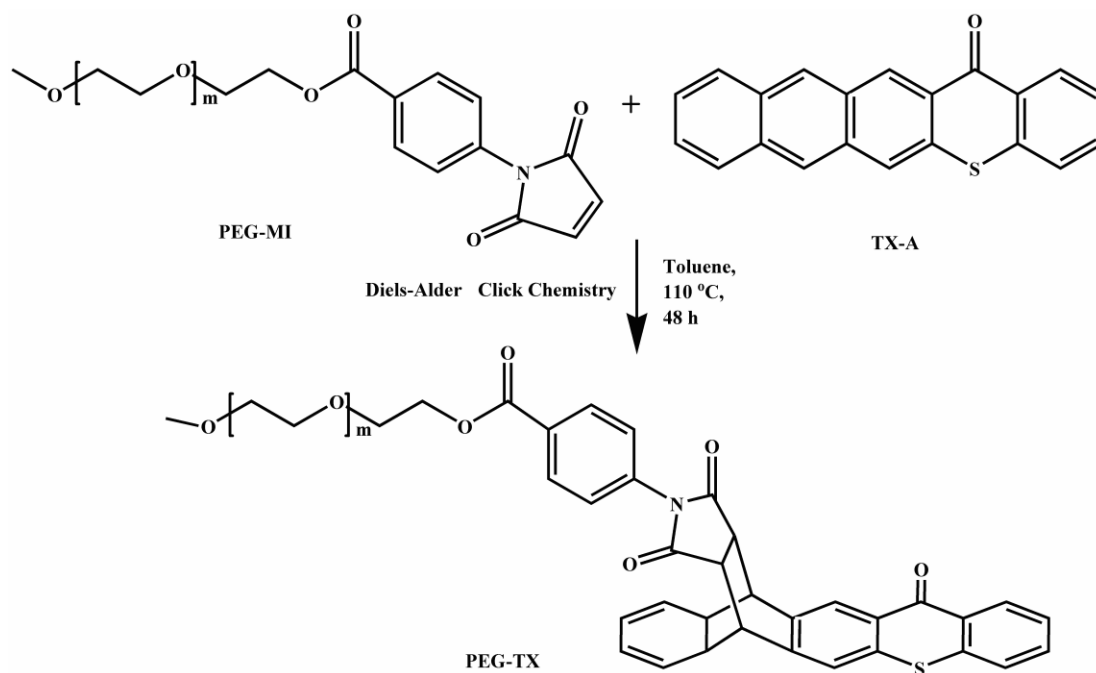
**Figure 4.17:** Photo-DSC profile for polymerization of TPTA in the presence of TEA and PS-TX (27%) macrophotoinitiator, cured at 30°C by Uv light with an intensity of 180 mw/cm<sup>2</sup> [8].



**Figure 4.18:** Conversion vs. time, for polymerization of TPTA in the presence of TEA and PS-TX (27%) macrophotoinitiator, cured at 30°C by Uv light with an intensity of 180 mw/cm<sup>2</sup> [8].

### **4.3 Poly(ethylene glycol)-thioxanthone prepared by Diels-Alder Click Chemistry as one-component polymeric photoinitiator for aqueous free radical polymerization**

Water-soluble PEG-TX macrophotoinitiator was successfully prepared by Diels-Alder click reaction. For this purpose, maleimide end-functionalized PEG (PEG-MI) was reacted with a photoinitiator possessing anthracene (A) and TX, photochromic groups in the structure. The overall process is represented in Figure 4.19.

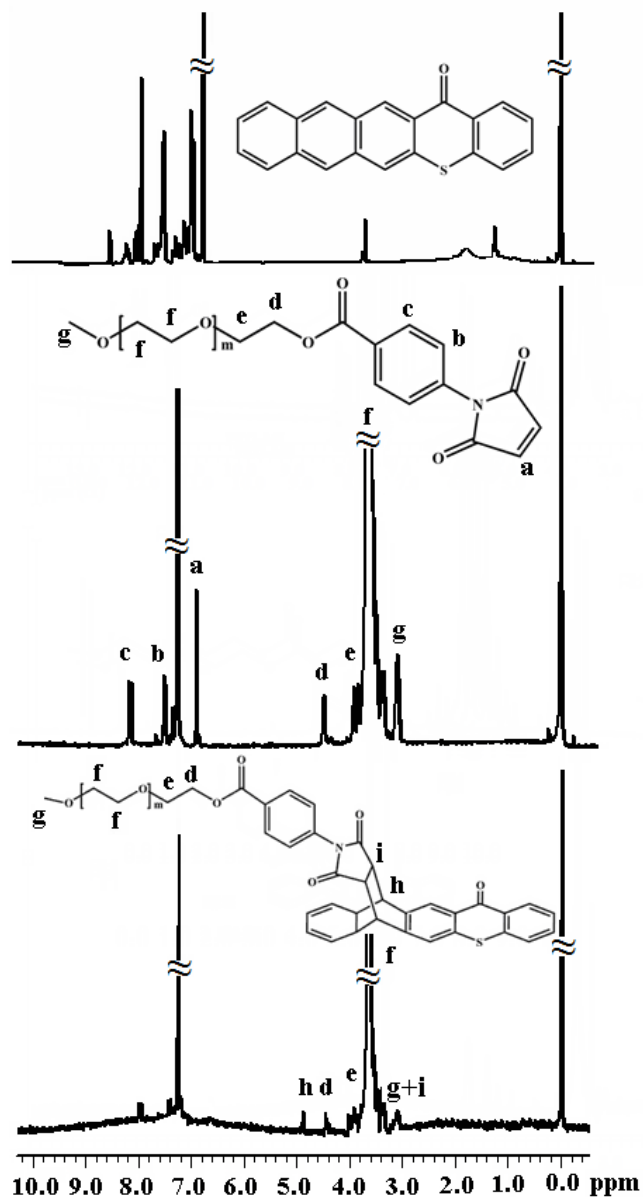


**Figure 4.19:** Synthesis of one-component polymeric photoinitiator by Diels-Alder click chemistry [4].

As a first step, PEG-MI was prepared via an esterification reaction of commercially available Me-PEG ( $M_n=2000$ ) containing monohydroxy end group with 4-maleimido-benzoyl chloride at room temperature.  $^1\text{H}$  NMR spectrum of the resulting product revealed the structure of PEG-MI displaying characteristic peaks such as maleimide  $\text{CH}=\text{CH}$  protons at 6.8 ppm and PEG repeating unit around 3.6 ppm ( $-\text{O}-\text{CH}_2-$ ) (Figure 1). Additionally, integrals of remaining protons were consistent with each other indicating a successful esterification. The FT-IR spectrum also confirms the targeted structure as the new carbonyl stretching band appears at  $1716\text{ cm}^{-1}$ . The other component of DA click reaction, namely thioxanthone-anthracene (TX-A) photoinitiator, 5-thia-pentacene-14-one, was synthesized by a modified procedure [214].

In the final step of the process, PEG-MI and TX-A were reacted in one-pot to yield desired water-soluble PEG-TX macrophotoinitiator. Evidence for the occurrence of the DA click reaction was obtained from  $^1\text{H}$  NMR, UV and fluorescence spectroscopy. As can be seen from Figure 4.20, where  $^1\text{H}$  NMR spectra of TX-A, PEG-MI and PEG-TX were recorded, the peaks between 7.4 and 8.5 ppm, characteristic for aromatic protons of anthracene, disappeared completely. This indicates the loss of the aromaticity of the central phenyl unit of anthracene by DA

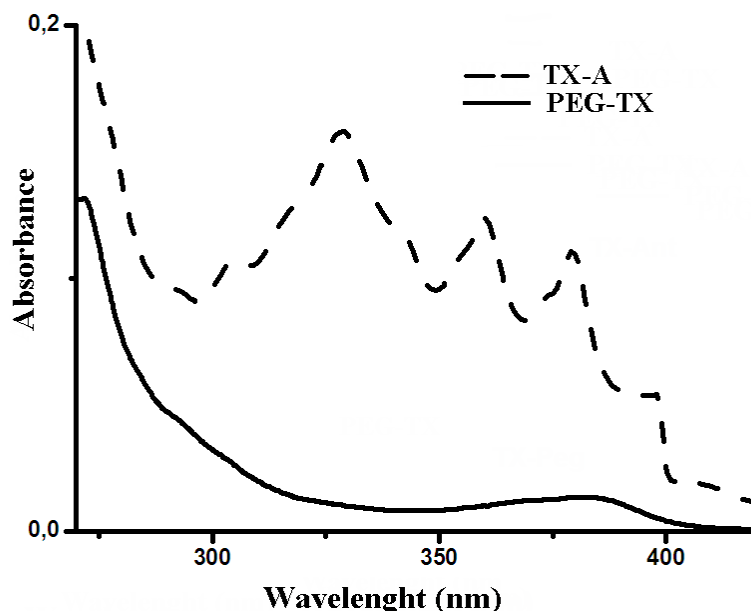
cycloaddition click reaction. Furthermore, a new signal corresponding to bridgehead (-CH) proton of the cyclo adduct appeared at 4.94 ppm.



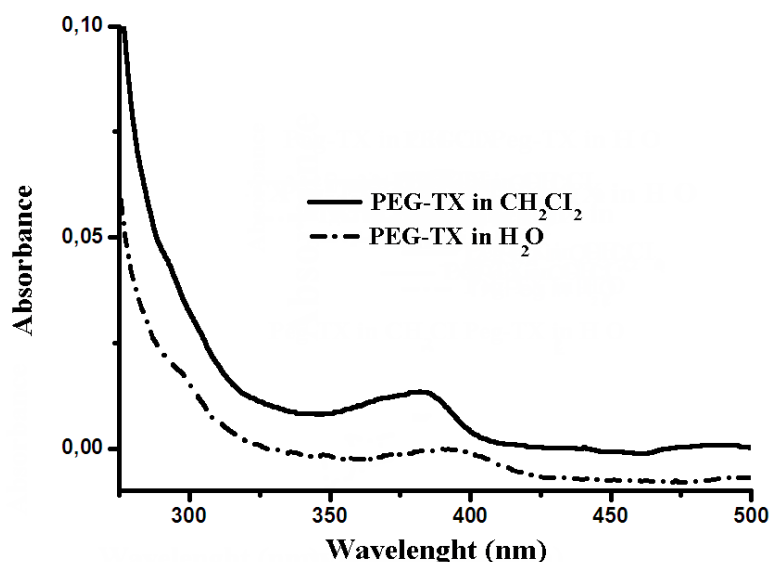
**Figure 4.20:**  $^1\text{H}$  NMR spectra of TX-A, PEG-MI and PEG-TX in  $\text{CDCl}_3$  [4].

Photophysical characteristics of the obtained PEG-TX were investigated by UV and fluorescence spectroscopy (Figures 21 and 22). As can be seen from Figure 2, TX-A displays characteristic five-finger absorbance in the 300–400 nm range. On the contrary, PEG-TX macrophotoinitiator shows a different absorption signature with a maximum at 380 nm, which is similar to the absorption spectrum of pure thioxathone, indicating that the absorption regime of the precursor has changed as a result of the modification. Indeed, DA reaction between anthracene and maleimide

moieties causes the loss of the aromaticity of central phenyl unit of anthracene. In other words, the TX-A group is transformed into thioxanthone group by the click reaction. In water, PEG-TX exhibits typical absorption characteristics of TX with a slight shift of the absorption maxima to higher wavelength probably due to the polarity (Figure 22).



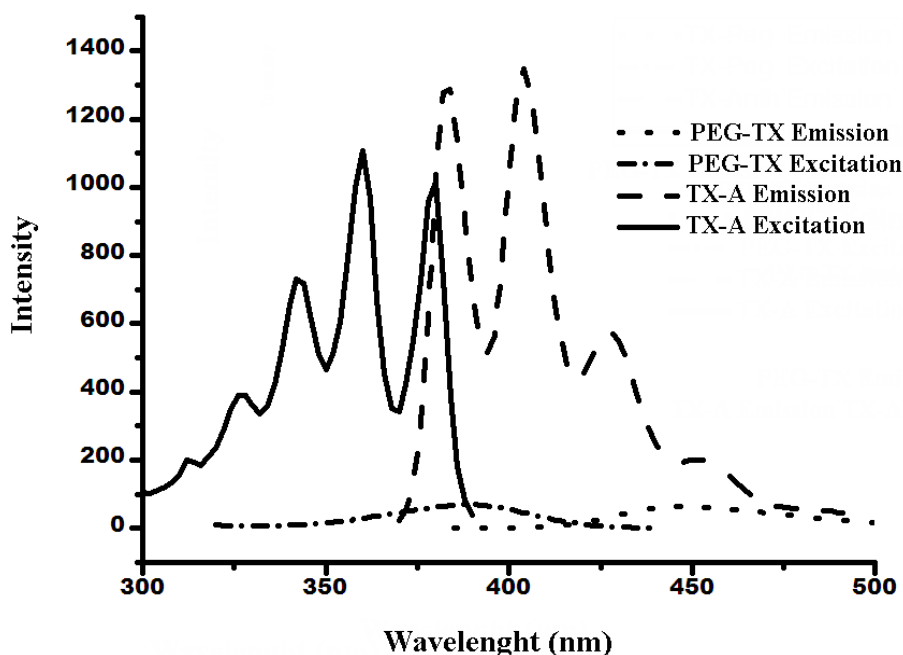
**Figure 4.21:** Absorption spectra of TX-A and PEG-TX in  $\text{CH}_2\text{Cl}_2$ . The concentrations are  $1 \times 10^{-5}$  M [4].



**Figure 4.22:** Absorption spectra of PEG-TX in  $\text{CH}_2\text{Cl}_2$  and water. The concentrations are  $1 \times 10^{-5}$  M [4].

Fluorescence spectrum of PEG-TX also provides further evidence for the efficiency of the modification process and information on the nature of the excited states involved. As can be seen from Figure 23, excitation and emission fluorescence

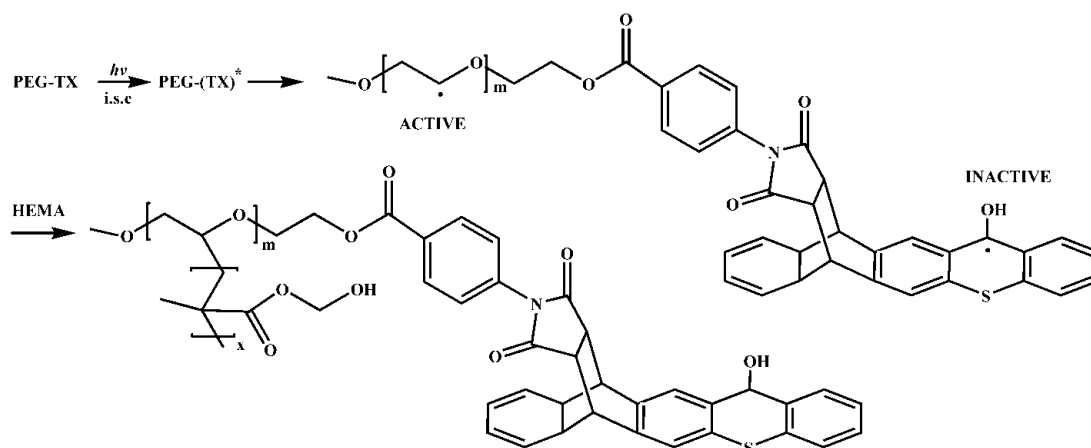
spectra in  $\text{CH}_2\text{Cl}_2$  of TX-A and PEG-TX obtained by DA click reaction are quite different. TX-A exhibits characteristic emission bands of the excited (singlet) of anthracene moiety. In contrast, PEG-TX has no significant emission of this kind and the spectrum shows a nearly mirror-image-like relation between absorption and emission again similar to bare TX. Expectedly, the intensities are lower in the case of thioxanthone end-functionalized polymer.



**Figure 4.23:** Emission spectra of TX-A and PEG-TX in  $\text{CH}_2\text{Cl}_2$ ;  $\lambda_{exc} = 360$  nm. The concentrations are  $2 \times 10^{-5}$  M [4].

The one-component photoinitiating nature of PEG-TX was demonstrated by photopolymerization of hydrophilic vinyl monomers such as acrylic acid (AA), acrylamide (AM), 2-hydroxyethyl acrylate (HEMA) and 1-vinyl-2-pyrrolidone (VP). The overall reaction pathway is depicted in Figure 4.24. It was previously shown [206] that, PEG is a good hydrogen donor for a wide range of photoexcited aromatic carbonyl compounds acting as *Type II* photoinitiators. In the present case, hydrogen abstraction occurs between the photoexcited TX moiety and PEG.

Notably, one of the consequences of the hydrogen abstraction is the formation of graft copolymers, since initiating radicals are generated on the backbone of PEG.



**Figure 4.24:** Photoinitiated free radical polymerization of HEMA by using PEG-TX [4].

This was confirmed by the molecular weight increases and unimodal traces corresponding to the graft copolymers observed in all cases. The results are compiled in Table 4.5. Moreover, the formation of graft copolymers was also evidenced by IR spectra of the resulting polymers. Each spectrum possesses both characteristic main chain ether and carbonyl bands at 1,100 and 1,730  $\text{cm}^{-1}$ , with increased intensity, respectively.

**Table 4.5:** Photoinitiated polymerization<sup>a</sup> of hydrophilic vinyl monomers [4].

Monomer <sup>b</sup>	Conversion <sup>c</sup> (%)	$M_n^d \times 10^3$ (g/mol)	$M_n/M_w^d$
AA	70	232.3	1.83
AM	69	210.0	3.20
HEMA	73	296.0	1.90
VP	72	147.8	1.06

<sup>a</sup>Photoinitiated Polymerization of AA, AM, HEMA and VP with macrophotoinitiator in water.

[PEG-TX] =  $2.5 \times 10^{-8}$  M; irradiation time = 2 h.

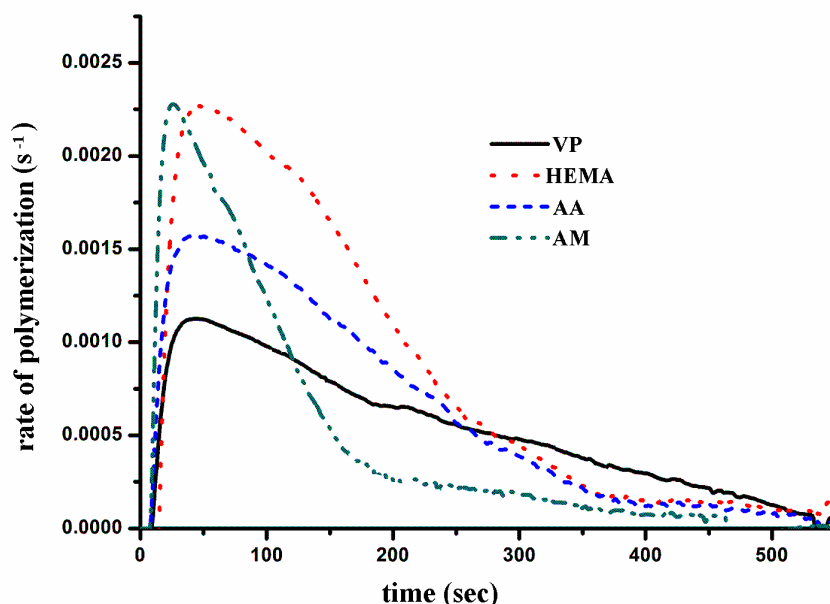
<sup>b</sup>[Monomer] =  $2.76 \times 10^{-6}$  M.

<sup>c</sup>Calculated gravimetrically.

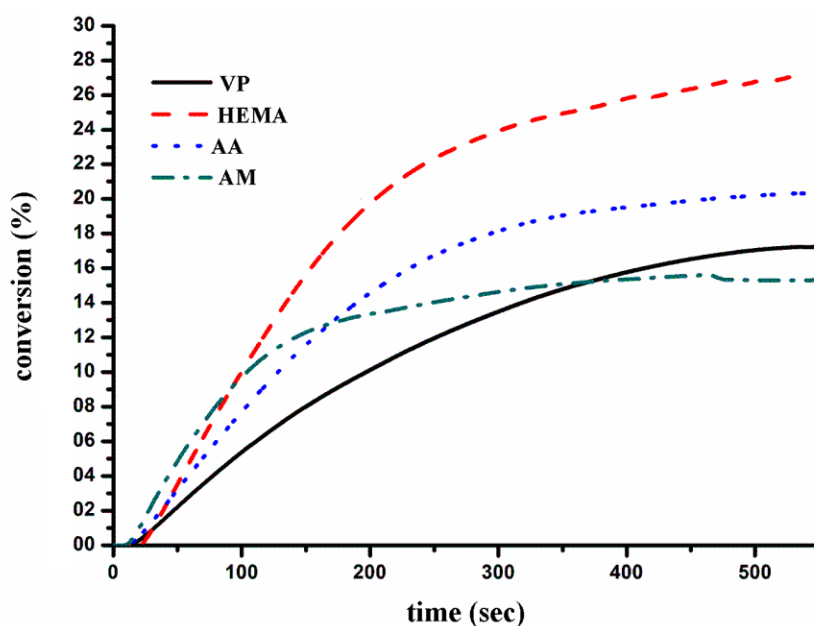
<sup>d</sup>Determined by GPC measurements.

The photo-DSC profiles of the polymerization of water soluble monomers for PEG-TX are shown in Figure 24. Figure 25 displays a plot of the conversion versus irradiation time derived from Figure 24. It is evident from the Figure 5 that monomers more prone to hydrogen bonding exhibit higher rate of polymerization. The observed high reactivity of AM, AA, HEMA can be explained in terms of their

non-covalent dynamical connection favored by hydrogen bonding. This way, monomers behave partly like difunctional species and termination rate constant is dramatically reduced [206]. It is also likely that hydrogen bonding facilitates pre-organization, thereby forcing the double bonds of the monomers in close proximity to each other. As a consequence, the propagation reaction rate constant ( $k_p$ ) is enhanced resulting in higher rate of polymerization [206].



**Figure 4.24:** Photo-DSC profile for photoinitiated polymerization of AM, HEMA, AA and VP in the presence of PEG-TX macrophotoinitiator at 30<sup>0</sup> C. The light intensity: 180 mV/cm<sup>2</sup> [4].



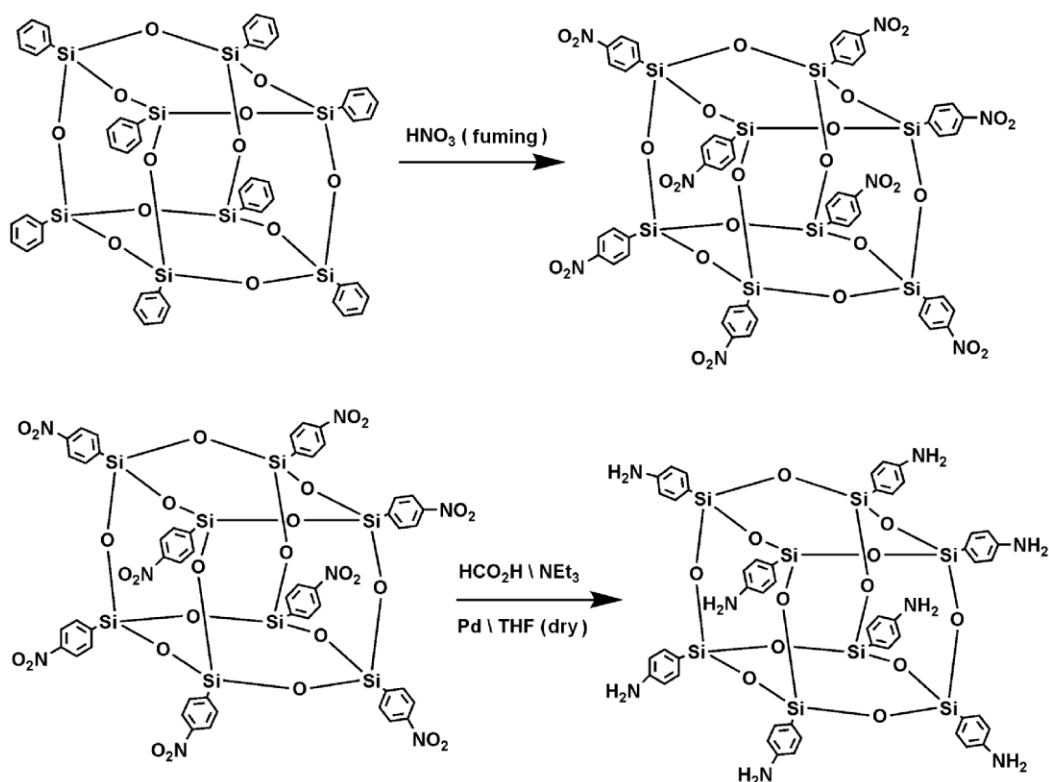
**Figure 4.25:** Conversion versus time for the photoinitiated polymerization of AM, HEMA, AA and VP in the presence of PEG-TX macrophotoinitiator at 30<sup>0</sup>C. The light intensity: 180 mV/cm<sup>2</sup> [4].

#### 4.4 Enhancing electrochromic properties of polypyrrole by silsesquioxane nanocages

We introduce a new approach for improving the electrochromic properties of polypyrrole by attaching polypyrrole chains onto thiophene possessing OPS nanocages which were efficiently synthesized via click chemistry. This process prohibits the dense packing of the rigid chains and gives rise to a nanometer-scale porous structure, and hence greatly facilitates ion extraction and injection. With this approach, not only properties of polypyrrole but also other polymers prepared by the copolymerization of functional POSS with the wide variety of monomers may be tuned easily [9].

We synthesized octa(azidophenyl) silsesquioxane ( $ON_3PS$ ) cube from the corresponding octa(aminophenyl) silsesquioxane ( $ON_3PS$ ) via their diazonium salts and used “click” chemistry as a facile route for the functionalization of octa(phenyl) silsesquioxane (OPS). For this purpose, the octa(nitrophenyl) silsesquioxane ( $ONO_2PS$ ) was synthesized by a modified literature procedure reported by Laine *et al.* [207, 208]. This improved procedure provides  $ONO_2PS$  with one nitro group per phenyl unit.  $ONO_2PS$  is quantitatively transformed to  $ONH_2PS$  by hydrogen-transfer reduction in the presence of formic acid, triethylamine and Pd/C catalyst (Figure 4.26) [207, 208].

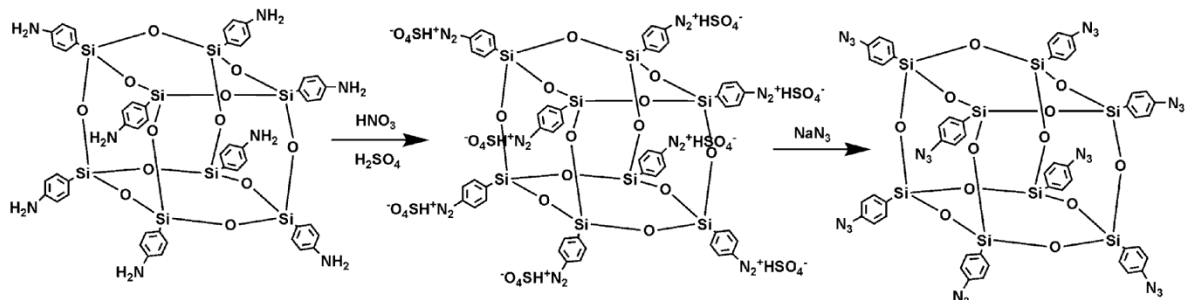




**Figure 4.26:** Synthesis of octa(aminophenyl) silsesquioxane (ON<sub>3</sub>PS) [9].

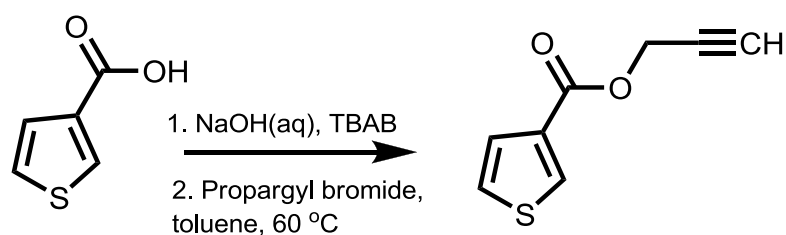
For the synthesis of parent ON<sub>3</sub>PS cube, a simple synthetic strategy was used (Figure 4.27).

The aqueous solution of sodium nitrite in concentrated sulfuric acid (a nitrosium hydrogen sulphate reagent) is used as a very effective diazotizing medium at about 0 °C. The resulting diazonium salt is replaced by azide attached to the aromatic ring by the evolution of molecular nitrogen in quantitative conversion (99–100%).



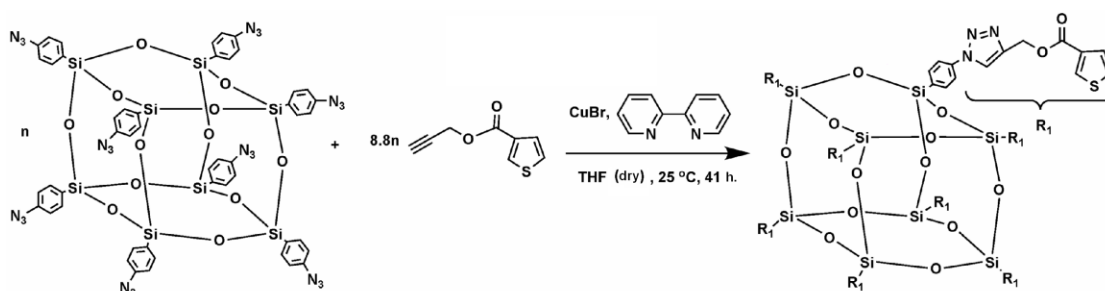
**Figure 4.27:** Synthesis of octa(azidophenyl) silsesquioxane (ON<sub>3</sub>PS) [9].

In this section, propargyl containing thiophene was selected as the electropolymerizable click component which was synthesized via esterification reaction of thiophene-3-carboxylic acid and propargyl bromide (Figure 4.28).



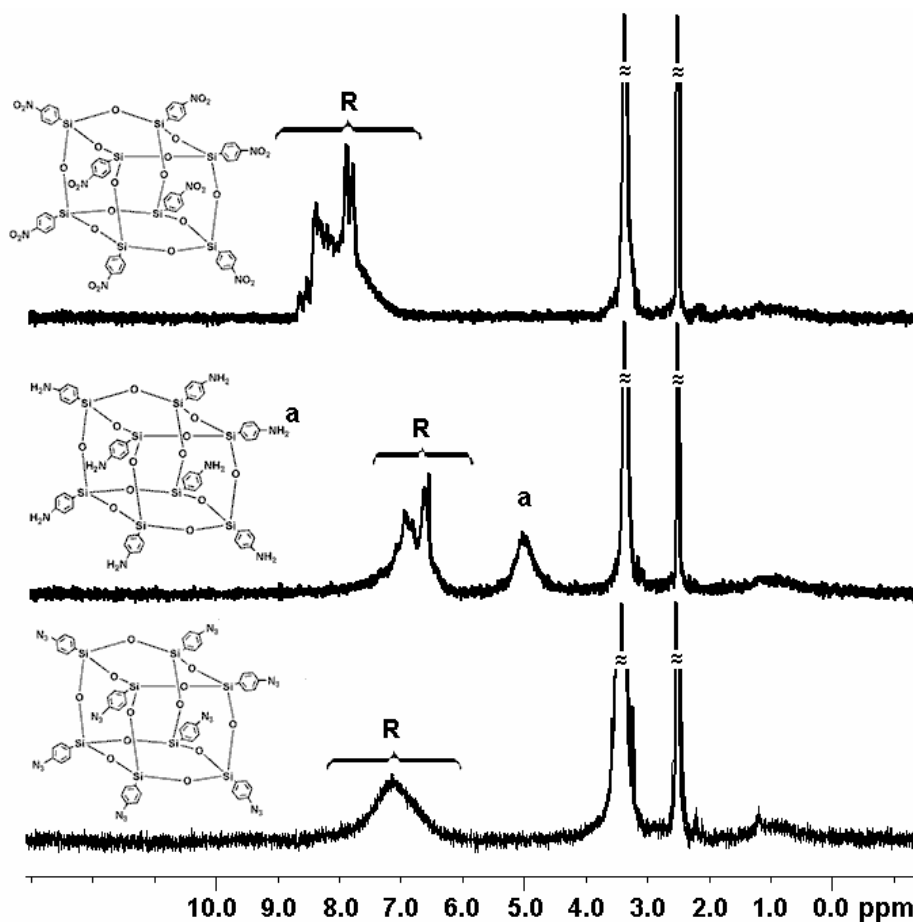
**Figure 4.28:** Synthesis of prop-2-ynyl thiophene-3-carboxylate (*Propargylthiophene*) [9].

Then a standard “click” protocol has been established. The  $ON_3PS$  was dissolved in THF and reacted with propargylthiophene in the presence of a catalytic amount of  $CuBr$ , and bipyridine at room temperature. The reaction afforded the desired product *OThiophenePS* (Figure 4.29). After removing the catalyst, the *OThiophenePS* was precipitated and dried under vacuum.



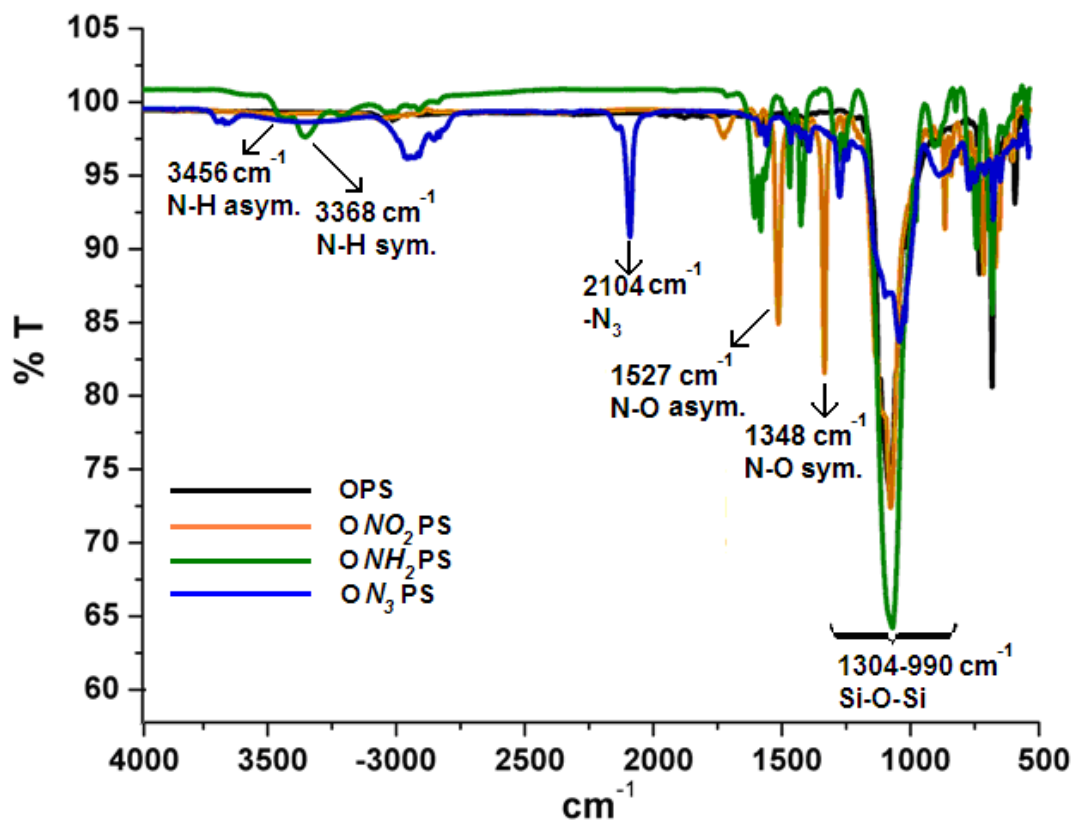
**Figure 4.29:** Synthesis of *OThiophenePS* by Click Chemistry [9].

The structures of the intermediates and final product were confirmed by  $^1H$  NMR spectra ( $d_6$ -DMSO) (Figure 4.30). The aromatic protons of phenyl groups emerge at around 8 ppm, due to the electron withdrawing effect of the  $-NO_2$ . The reduction process led to two changes in the spectra. While N–H protons appeared at 5.50–4.40 as new peaks, the aromatic peaks appear at higher magnetic fields in the range of 7.9–6.1 ppm. The integration ratios of N–H protons to aromatic C–H protons are 1:2, respectively, indicating quantitative reduction of the nitro groups to amino groups. The efficient transformation of  $ONH_2PS$  to  $ON_3PS$  was also evidenced from  $^1H$  NMR spectrum wherein the resonance due to N–H protons disappeared completely.



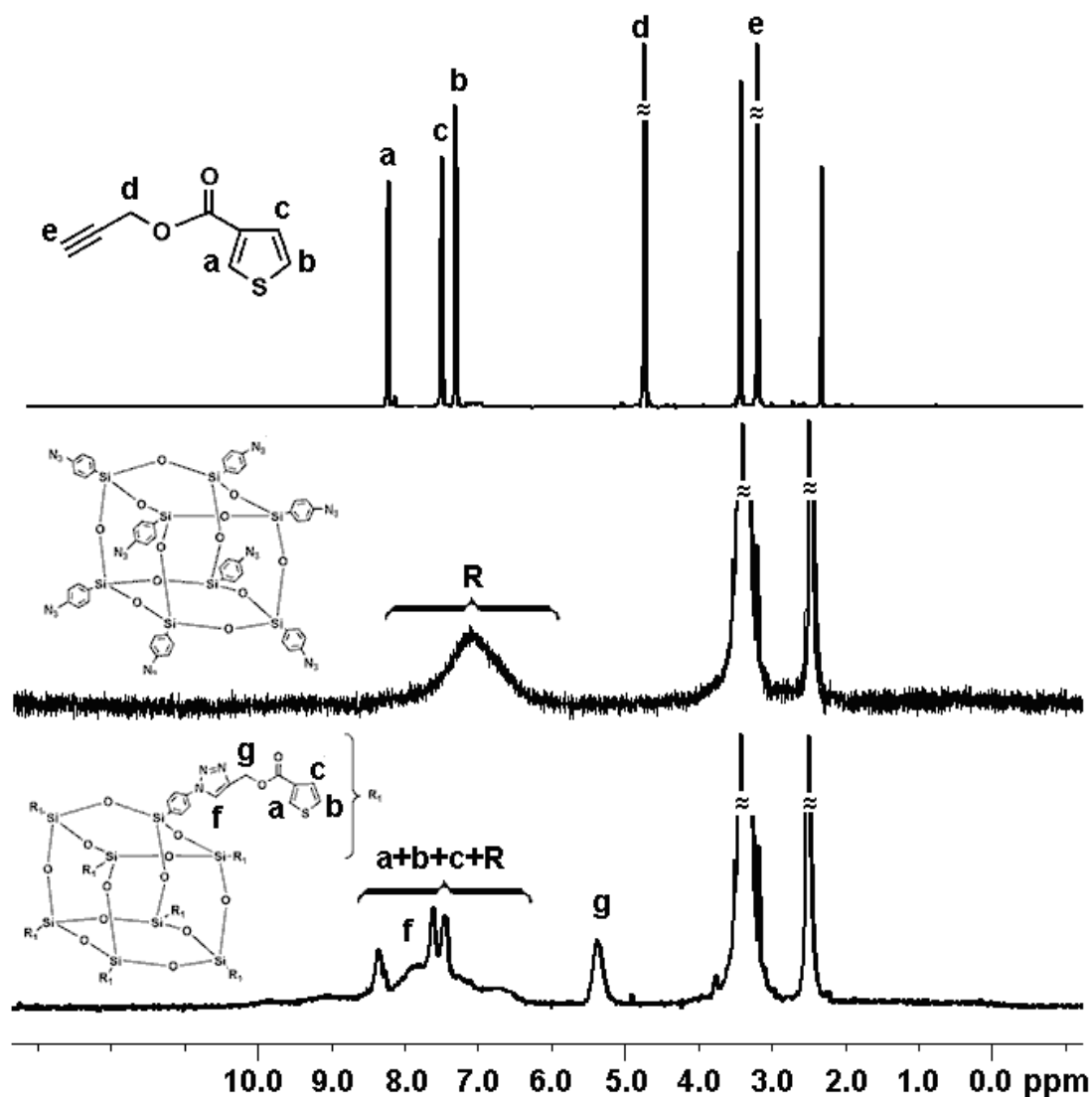
**Figure 4.30:**  $^1\text{H}$  NMR spectra of  $\text{ONO}_2\text{PS}$ ,  $\text{ONH}_2\text{PS}$  and  $\text{ON}_3\text{PS}$  (**R**: Aromatic Protons) [9].

Additionally, FT-IR spectra of the related compounds confirm the NMR data.  $\text{ONO}_2\text{PS}$  exhibits strong symmetric and asymmetric  $\nu\text{N}=\text{O}$  peaks at  $1348$  and  $1527\text{ cm}^{-1}$  (Figure 4.31). These peaks disappear completely after reduction and new broad symmetric and asymmetric  $\nu\text{N}-\text{H}$  peaks appear at  $3368\text{ cm}^{-1}$  and  $3456\text{ cm}^{-1}$ . After the transformation of amine groups to azide groups, a strong and new vibration centered at  $2104\text{ cm}^{-1}$  appeared in the spectrum. Notably, all functionalized OPS, discloses characteristic of  $\nu\text{Si}-\text{O}-\text{Si}$  stretching signals between  $1304-990\text{ cm}^{-1}$  with relatively high intensity.



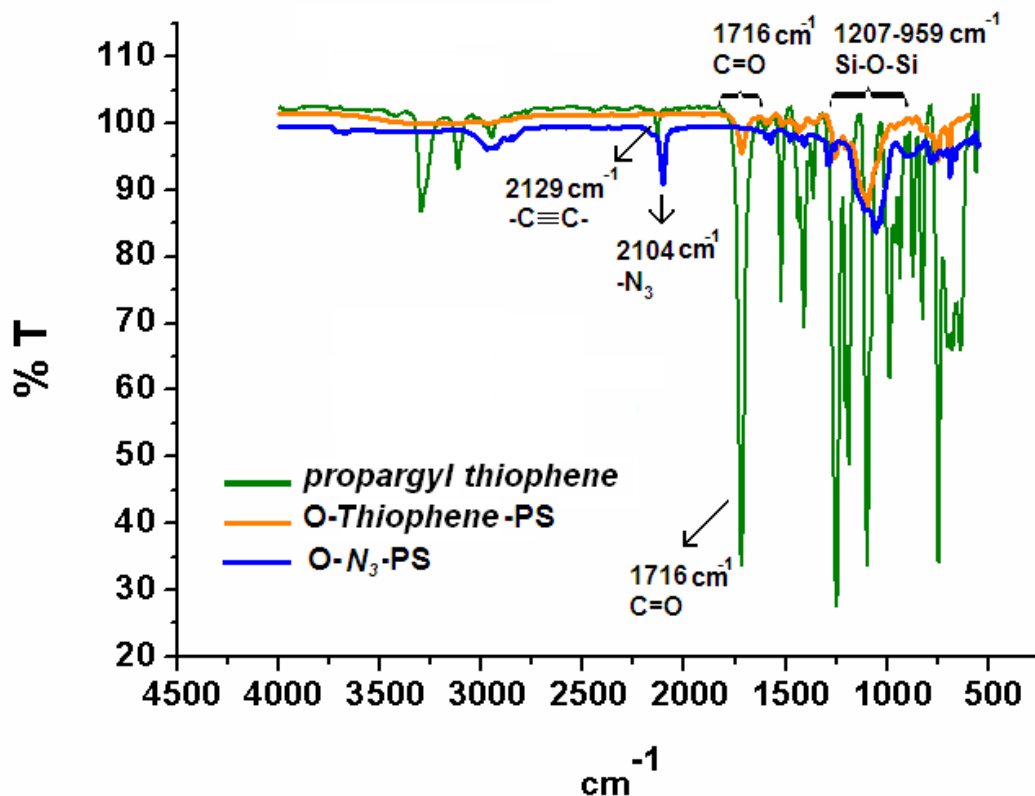
**Figure 4.31:** FT-IR spectra of  $ONO_2PS$ ,  $ONH_2PS$  and  $ON_3PS$  [9].

The successful transformation of azide moieties into triazole was confirmed  $^1H$  NMR. Typically, in the case of *OThiophenePS*, the appearance of the new methylene protons adjacent to the triazole ring at 5.3 ppm (triazole- $CH_2Ph$ ) and new triazole proton at 7.8 ppm were observed (Figure 4.32). Additional peaks corresponding thiophene moiety overlapped with those of aromatic protons of OPS.



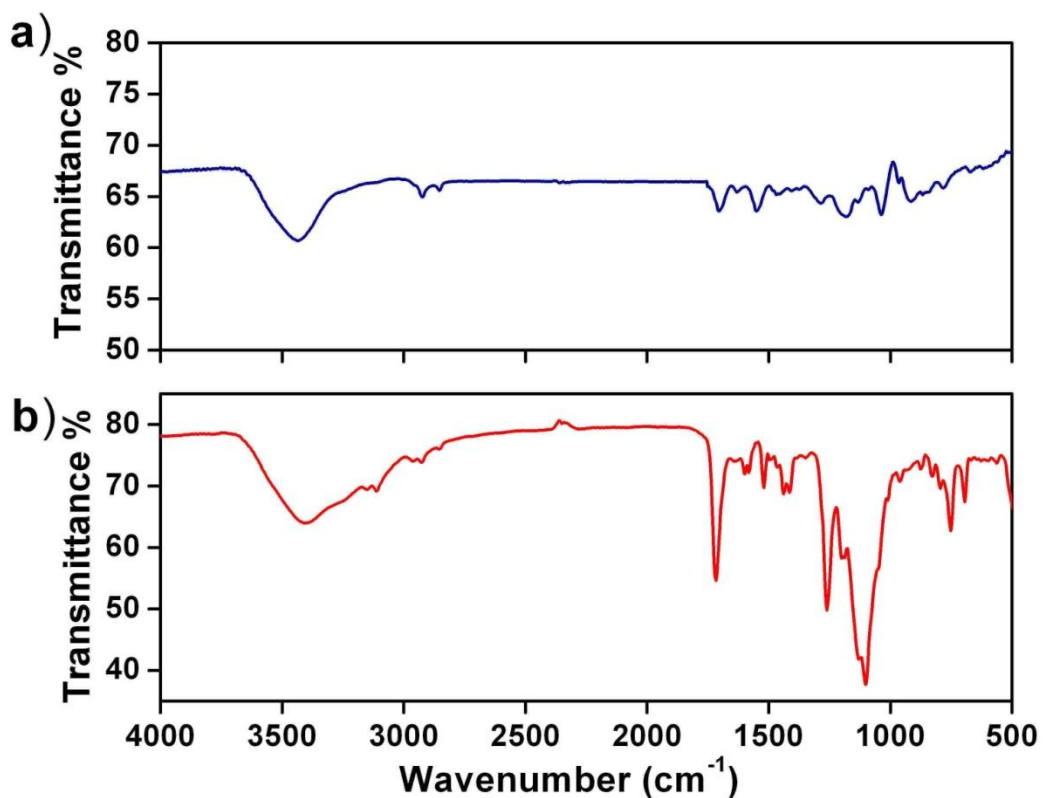
**Figure 4.32:** <sup>1</sup>H NMR spectra of *propargylthiophene*, *ON<sub>3</sub>PS* and *OthiophenePS* (**R**: Aromatic protons) [9].

FT-IR spectrum of the *OThiophenePS* (Fig. 4.33) reveals characteristic of  $\nu$ Si-O-Si stretching signals between  $1304\text{--}990\text{ cm}^{-1}$ . Moreover, the FT-IR spectrum also shows the disappearance of the acetylene peak at  $\sim 3293\text{ cm}^{-1}$  and the azide peak at  $\sim 2104\text{ cm}^{-1}$  while a strong carbonyl band at  $1716\text{ cm}^{-1}$  appears. Thus, click reaction was efficient and almost quantitative as evidenced by spectral methods.



**Figure 4.33:** FT-IR spectra of *propargylthiophene*, *OThiophenePS* and *ON<sub>3</sub>PS* [9].

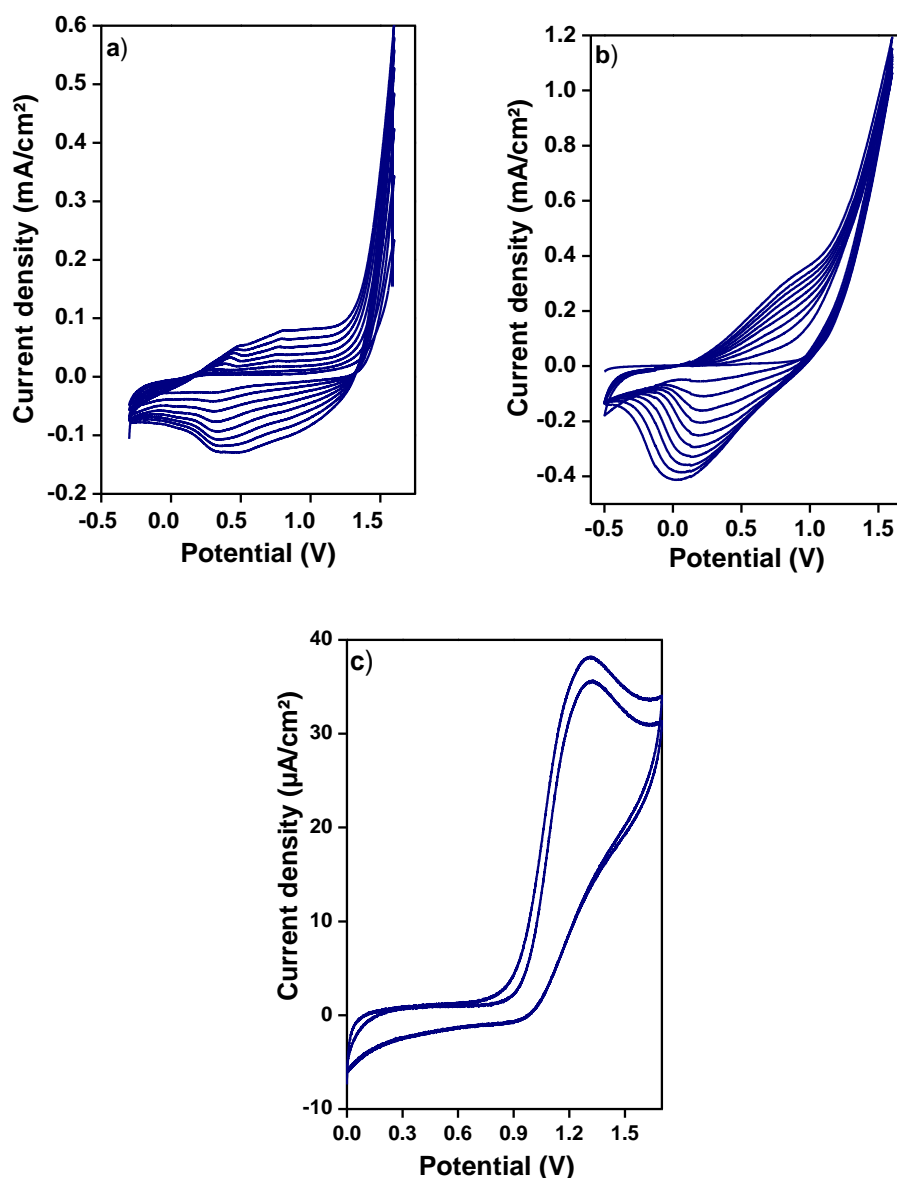
The IR spectral characteristic of the *OThiophenePS* was discussed together with that of the *OPS-PPy*. As can be seen in Figure 5, most of the characteristic peaks of *OThiophenePS* remained unperturbed upon electrochemical polymerization. Because of incorporation *OThiophenePS* into *PPy* chains, peak intensities in the FT-IR spectrum of *OPS-PPy* is decreased.



**Figure 4.34:** FT-IR spectra of a) OPS-PPy b) *OthiophenePS* [9].

#### 4.5 Cyclic voltammetry

Although *OthiophenePS* exhibits an initial electroactivity ( $E_{ox} = 1.35$  V) in TBAFB/DCM, current decreases upon repeated cycling (Fig. 4.35c). When CV behavior of the *OthiophenePS* was investigated in the presence of pyrrole under same experimental conditions (Fig. 4.35a), there was a drastic change in the voltammogram, both the increase in the increments between consecutive cycles and the oxidation potential of the material were different than those of pyrrole (Fig. 4.35b), which in fact could be interpreted as the incorporation of *OthiophenePS* in PPy chains.



**Figure 4.35:** Cyclic voltammograms of a) OPS-PPy b) Py and c) O(*thiophene*)PS [9].

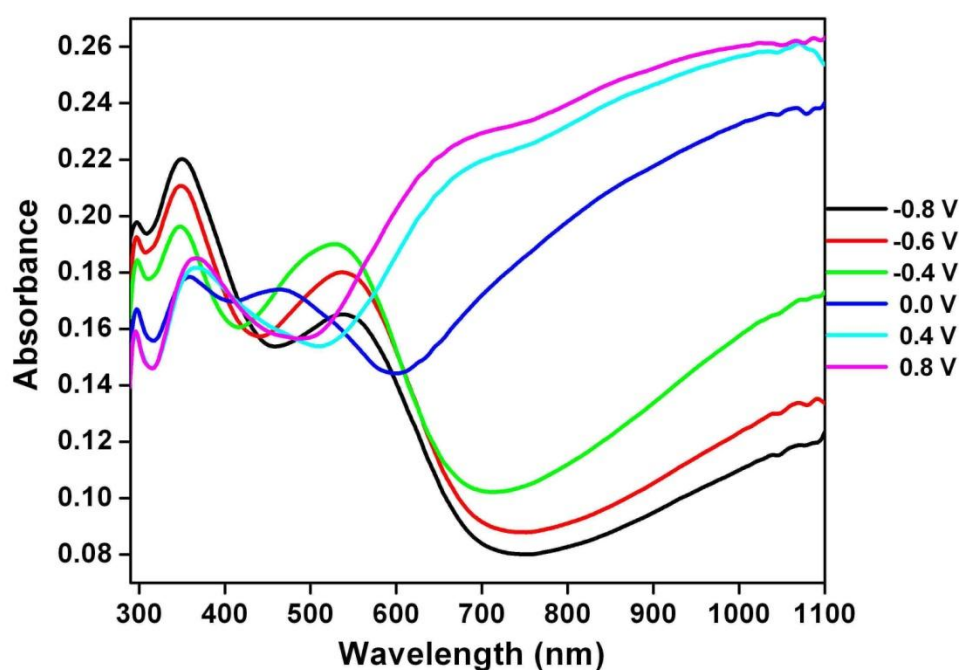
## 4.6 Electrochromic properties of OPS-PPy

### 4.6.1 Spectroelectrochemistry

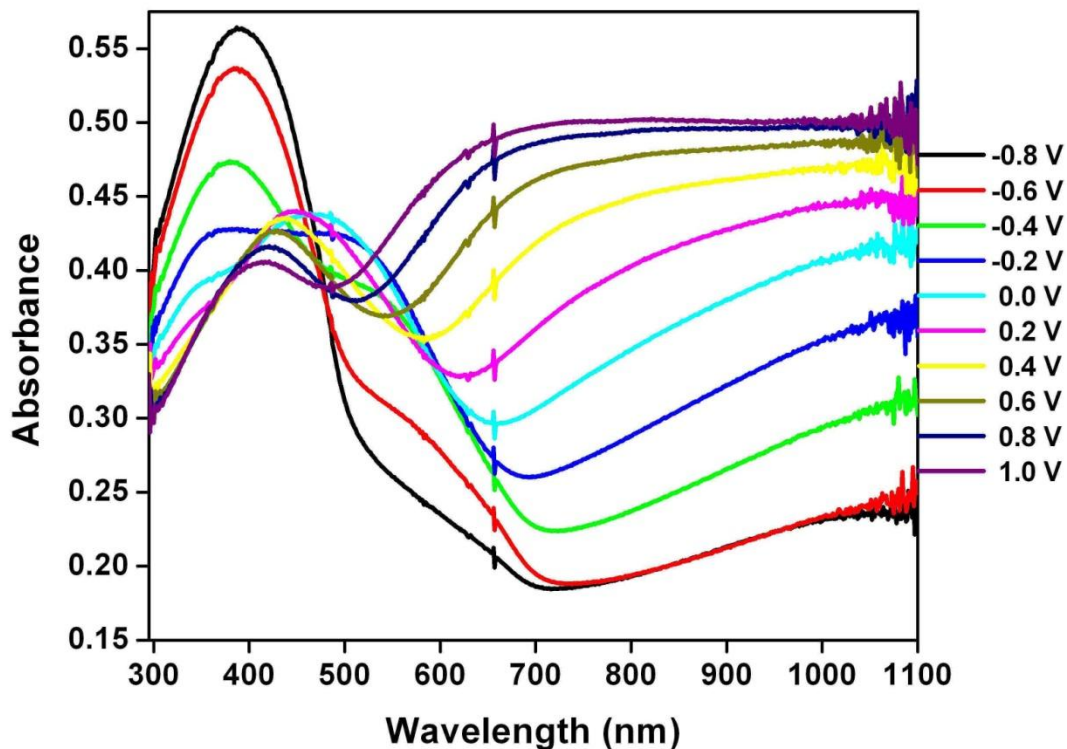
The best way of examining the changes in optical properties of conducting polymers upon voltage change is defined as spectroelectrochemistry. It also gives information about the electronic structure of the polymer such as band gap ( $E_g$ ) and the intergap states that appear upon doping. OPS-PPy film was electrochemically synthesized on ITO electrode. Electrolyte solution was composed of 50 mg O*Thiophene*PS and 10  $\mu$ L Py and TBAFB (0.1 M) / DCM. In order to compare electrochromic properties,



PPy and OPS-PPy were synthesized under the same conditions. Spectroelectrochemical and electrochromic properties of the resultant polymers were studied by applying potentials between -0.8 V and +1.0 V in a monomer free DCM/TBAFB (0.1 M) medium. At the neutral state  $\lambda_{\max}$  due to the  $\pi-\pi^*$  transition of the PPy (Fig. 4.36) and OPS-PPy (Fig. 4.37) were found to be 351 nm and 390 nm respectively. Also band gap of the  $\pi-\pi^*$  transitions were calculated as 2.35 for PPy and 2.25 eV for OPS-PPy. Incorporation of *O*ThiophenePS in the PPy chains gives rise to a nano-scale porous structure, where this unique molecular geometry of OPS-PPy greatly facilitates ion extraction and injection.



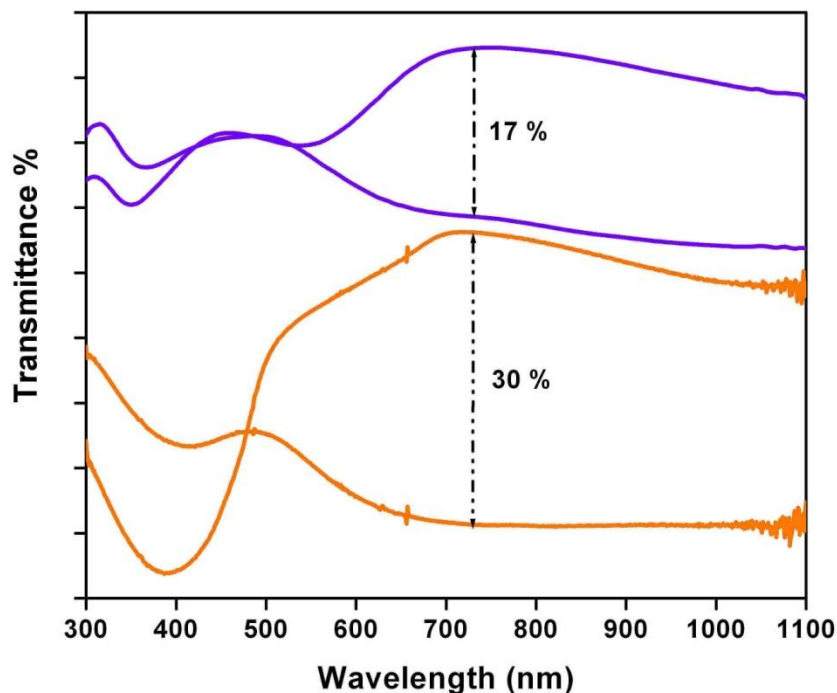
**Figure 4.36:** Spectroelectrochemical properties of the PPy in (0.1M) DCM/TBAFB [9].



**Figure 4.37:** Spectroelectrochemical properties of the OPS-PPy in (0.1M) DCM/TBAFB [9].

#### 4.6.2 Optical contrast

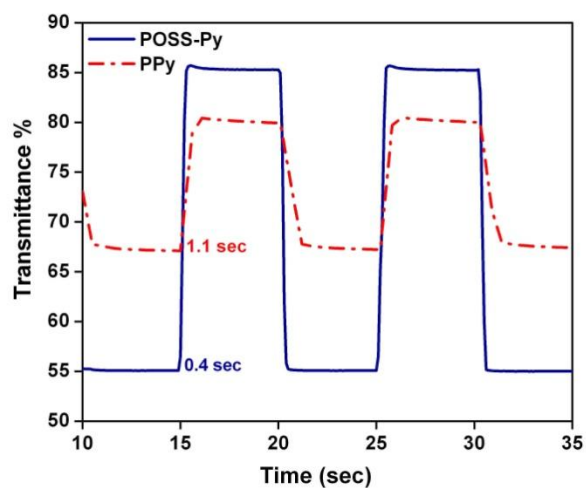
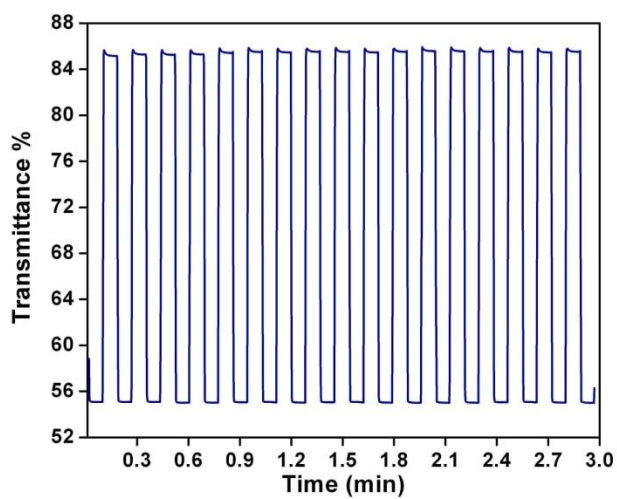
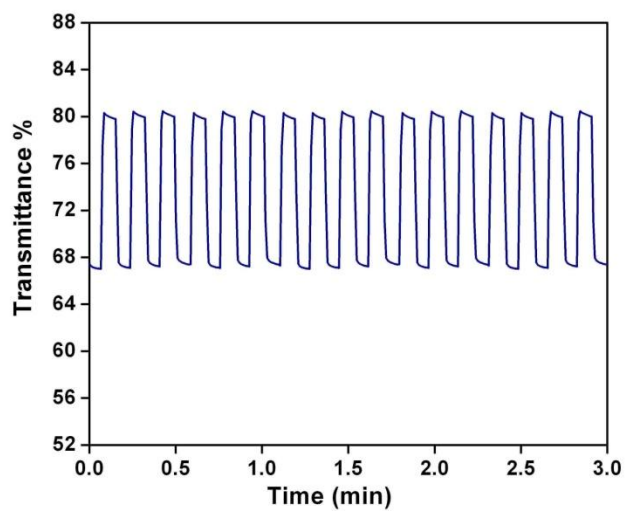
Figure 4.38 shows the transmittance spectra of PPy and OPS-PPy in the two extreme (oxidized and neutral) states. In this study, all the polymer films have approximately the same thickness, as matched by chronocoulometry. By applying voltages between +1 and -1 V, polymers reveal changes between colored and transmissive states. Comparison of the results shows that incorporation *OThiophenePS* in PPy chains causes a noticeable increase in the optical contrast for measured all wavelengths as evidenced by an increase in the transmittance change ( $\Delta\%T$ ) from 17 % to 30 % (730 nm).



**Figure 4.38:** Transmittance spectra of PPy and OPS-PPy in two extreme (oxidized and neutral) states [9].

#### 4.6.3 Switching time

Electrochromic switching studies were carried out to investigate the ability of a polymer to give a short response time, exhibit a striking color change and maintain high stability upon repeated cycles. Spectroelectrochemistry results should be taken into account in order to obtain information on the potentials to be applied for a full switch and wavelength of maximum contrast. A square-wave potential step method coupled with optical spectroscopy known as chronoabsorptometry was applied by stepping the potentials between fully oxidized and reduced states of the polymers for a residence time of 5 s during 3 min. Figure 4.39a and 4.39b demonstrates the transmittance change at 730 nm for PPy and OPS-PPy examined in a repeated switching test. For comparison, we monitored the change in transmittance of a single film with the same thickness. As seen in Figure 4.39 OPS-PPy switches quite rapidly (0.4 sec) when compared to PPy (1.1 sec). This is due to nano-porous structure of OPS-PPy facile ion movement during the switching.



**Figure 4.39:** Electrochromic switching, transmittance change monitored at 730 nm for a) PPy b) OPS-PPy c) OPS-PPy and PPy (Consecutive two cycles) [9].

#### 4.6.4 Colorimetry

The colors of the electrochromic materials were defined accurately by performing colorimetry measurements. CIE system was used as a quantitative scale to define and compare colors. Three attributes of color; hue (a), saturation (b) and luminance (L) were measured and recorded. The OPS-PPy film has distinct electrochromic properties. It shows four different colors in neutral and oxidized states. These colors and corresponding L, a, b values for PPy and OPS-PPy were given in Table 1.

**Table 4.6:** Electrochromic properties of OPS-PPy and PPy [9].

Polymers	Potential	Colors	L	a	b
POSS-PPy	-1.0 V	yellow	85	-5	54
	-0.5 V	red	46	30	-4
	+0.2 V	green-gray	45	-11	21
	+1.0 V	blue	61	-25	9
PPy	-1.0 V	gray	68	-10	29
	+1.0 V	turquoise	58	-26	11



## 5. CONCLUSION

Over the last decade, increasing attention has been devoted to the use of rapid reactions that meet the three main criteria of an ideal synthesis: efficiency, versatility, and selectivity. To date, the most popular reactions that have been adapted to fulfill these criteria are known as “click” reactions. Among these reactions, copper(I)-catalyzed azide-alkyne (CuAAC) and Diels-Alder (DA) cycloaddition reactions and thiol-ene reactions have gained much interest among the chemists not only the synthetic ones but also the polymer chemists.

The study presented in this thesis is aimed at describing the copper (I)-catalyzed azide-alkyne (CuAAC) and Diels-Alder (DA) cycloaddition “click” reactions as a novel route to prepare well-defined graft copolymers, polymeric photoinitiators and reactive precursors for obtaining inorganic–organic conducting composites. The strategy adopted in this study appears to be entirely satisfactory in terms of efficiency and simplicity.

In the first part of the thesis, we have demonstrated a new synthetic approach for the preparation of well-defined graft copolymers on the basis of the DA “click chemistry” between copolymers bearing anthryl pendant groups and maleimide as end-functionalized polymers. The grafting processes were carried out at the reflux temperature of toluene with a quantitative yield and without need for an additional purification step. Moreover,  $^1\text{H}$  NMR, GPC, UV, fluorescence, and DSC measurements of resulting graft copolymers confirmed the high efficiency of DA “click chemistry”. Interestingly, two different  $T_g$  values in the ranges 79-82 and 105-130 °C were detected for PS-g-PMMA, while only one  $T_g$  was observed at 73-79 °C in the case of the corresponding PS-g-PEG. The strategy adopted in this study appears to be entirely satisfactory in terms of efficiency and simplicity.

In the second part of the thesis, we have successfully combined 1,3-dipolar azide-alkyne [3 + 2] and thermoreversible Diels–Alder (DA) [4 + 2] click reactions for the

synthesis of polymers bearing side-chain TX photoactive groups. One of the consequences of the method is that such modification causes a dramatic change in the photochemistry of the precursor TX-A. The obtained polymeric photoinitiators were shown to efficiently initiate the free radical polymerization of mono- and multifunctional monomers via *Type II* mechanism. Generally, the in-situ double click chemistry strategy described here is simple and quantitative and may permit a wide range of derivatives of polymers with various functional groups to be prepared in high yields.

In the third part of the thesis, as a part of our continuing interest in developing photoinitiating systems with improved properties, we have reported synthesis of a novel water-soluble poly(ethylene glycol) (PEG) macrophotoinitiator containing TX end group via Diels–Alder click reaction. The obtained photoinitiator, possessing both light absorbing and hydrogen donating sites as in the same structure, is able to polymerize hydrophilic vinyl monomers without the requirement of an additional coinitiator. This is particularly important for curing applications because formulations containing amine as hydrogen donor at high concentrations cause a decrease in the pendulum hardness of the cured films as a result of the plasticizing effect of amines [210] Moreover, the water solubility of PEG provides the use of initiating system in water-borne formulations. These properties suggest that the polymeric photoinitiator may find use in a variety of practical applications.

Finally, we have presented that “click chemistry” can successfully be utilized to synthesize reactive precursors for obtaining inorganic–organic conducting composites. For this purpose azide functionalized OPS was synthesized and reaction of this intermediate with *propargyl*thiophene resulted in *OThiophene*PS. Electrochemical copolymerization of pyrrole with *OThiophene*PS was performed which resulted in star shaped polypyrrole-attached polyhedral oligomeric silsesquioxane (OPS–PPy) nanocages. The spectroelectrochemical studies showed that the electrochromic properties of PPy such as optical contrast, switching time, color properties were greatly enhanced due to the incorporation of *OThiophene*PS. The significant improvement is due to the loosepacked structure of OPS–PPy brought about by covalent bonding of the PPy chains to the *OThiophene*PS cages. This star shaped novel structure greatly facilitates ion extraction and injection. PPy-attached *OThiophene*PS and its derivatives may find applications in multi-color



electrochromism. With this approach, other polymers prepared by the copolymerization of functional *OThiophene*PS with the wide variety of monomers may be tuned easily. The approach also provides a new platform for the development of high contrast, fast switch time and multicolored electrochromic polymers.



## REFERENCES

- [1] **Kolb, H. C., Finn, M. G., and Sharpless, K. B.**, 2001, Click Chemistry: Diverse Chemical Function from a Few Good Reactions, *Angew. Chem. Int. Ed.* **40**, 2004-2021.
- [2] **Rostovtsev, V. V., Green, G., Fokin, V. V., and Sharpless, K. B.**, 2002, A Stepwise Huisgen Cycloaddition Process: Copper(I)-Catalyzed Regioselective “Ligation” of Azides and Terminal Alkynes, *Angew Chem Int Ed*, **41**, 2596.
- [3] (a) **Lutz, J. F.**, 2007, 1,3-Dipolar Cycloadditions of Azides and Alkynes: A Universal Ligation Tool in Polymer and Materials Science, *Angew. Chem. Int. Ed.*, **46**, 1018; (b) **Binder, W. H., and Sachsenhofer, R.**, 2007, ‘Click’ Chemistry in Polymer and Materials Science, *Macromol. Chem. Rapid. Commun.*, **28**, 15.
- [4] **Akat, H., Gacal, B., Balta, D.K., Arsu, N., and Yağcı, Y.**, 2010, Poly(ethylene glycol)-Thioxanthone Prepared by Diels–Alder Click Chemistry as One-Component Polymeric Photoinitiator for Aqueous Free-Radical Polymerization, *J Polym Sci Part A: Polym Chem*, **48**, 2109-2114.
- [5] **Yagci, Y., and Mishra, M. K.**, 1994, Macromolecular Design: Concept and Practice, *Polymer Frontiers International*, Chapter 6., Eds. Mishra, M. K., New York.
- [6] **Barn, M. A.**, 2009, Synthesis and Characterization of Polystyrene with Side Chain Pyrrole Groups by Combination of NMRP and Click Chemistry, *Ms. Thesis, ITU*.
- [7] **Gacal B., Durmaz, H., Tasdelen, M. A., Hizal G., Tunca, U., Yagci, Y., and Demirel, A. L.**, 2006, Anthracene-Maleimide-Based Diels-Alder “Click Chemistry” as a Novel Route to Graft Copolymers, *Macromolecules*, **39**, 5330-5336.
- [8] **Gacal, B., Akat, H., Balta, D. K., Arsu, N., and Yagci Y.**, 2008, Synthesis and Characterization of Polymeric Thioxanthone Photoinitiators via Double Click Reactions, *Macromolecules*, **41**, 2401-2405.
- [9] **Ak, M., Gacal, B., Kiskan, B., Yagci, Y., and Toppare, L.**, 2008, Enhancing electrochromic properties of polypyrrole by silsesquioxane nanocages, *Polymer*, **49**, 2202–2210.
- [10] **Kolb, H.C., Finn, M.G., and Sharpless, K.B.**, 2001, Click chemistry: Diverse chemical function from a few good reactions, *Angewandte Chemie-International Edition*, **40**, 2004-2021.

- [11] **Durmaz, H.**, 2010, Diels-Alder Click Reaction in Macromolecular Structures, 21-22, *Ph. D. Thesis*, ITU.
- [12] **Wu, Peng, and Fokin, V. V.**, 2007, Catalytic Azide–Alkyne Cycloaddition: Reactivity and Applications, *Aldrichimica Acta*, **40**, 7-17.
- [13] **Clegg, R. S., Reed, S. M., Smith, R. K., Barron, B. L., Rear, J. A. and Hutchison, J. E.**, 1999, The Interplay of Lateral and Tiered Interactions in Stratified Self-Organized Molecular Assemblies, *Langmuir*, **15**, 8876.
- [14] **Lewis, P. A. Smith, R. K. Kelly, K. F. Bumm, L. A., Reed, S. M., Clegg, R. S., Gunderson, J. D., Hutchison, J. E., and Weiss, P. S.**, 2001, The Role of Buried Hydrogen Bonds in Self-Assembled Mixed Composition Thiols on Au{111}, *J. Phys. Chem. B*, **105**, 10630.
- [15] **Smith, R. K., Lewis, P. A., and Weiss, P. S.**, 2004, Patterning Self-Assembled Monolayers, *Prog. Surf. Sci.*, **75**, 1.
- [16] **Smith, R. K., Reed, S. M., Lewis, P. A., Monnell, J. D., Clegg, R. S., Kelly, K. F., Bumm, L. A., Hutchison, J. E., and Weiss, P. S.**, 2001, Phase Separation within a Binary Self-Assembled Monolayer on Au{111} Driven by an Amide-Containing Alkanethiol, *J. Phys. Chem. B*, **105**, 1119-1122.
- [17] **Huisgen, R.**, 1989, Kinetics and reaction mechanisms: selected examples from the experience of forty years, *Pure Appl. Chem.*, **61**, 613.
- [18] **Huisgen, R., Szeimies, G., and Moebius, L.**, 1967, 1,3-Dipolar Cycloadditions. XXXII. Kinetics of the Addition of Organic Azides to Carbon-carbon Multiple Bonds, *Chem. Ber.*, **100**, 2494-2507.
- [19] **Tornøe, C. W., and Meldal, M.**, 2001, Peptides, Proc. Am. Pept.Symp., American Peptide Society and Kluwer Academic Publishers, 263–264, Eds. M. Lebl, R. A. Houghten, San Diego.
- [20] **Tornøe, C. W., Christensen, C., and Meldal, M.**, 2002, Peptidotriazoles on Solid Phase: [1,2,3]-Triazoles by Regiospecific Copper(I)-Catalyzed 1,3-Dipolar Cycloadditions of Terminal Alkynes to Azides, *J. Org. Chem.*, **67**, 3057-3064.
- [21] **Rostovtsev, V. V., Green, L. G., Fokin, V. V., and Sharpless, K. B.**, 2002, A Stepwise Huisgen Cycloaddition Process: Copper(I)-Catalyzed Regioselective Ligation of Azides and Terminal Alkynes, *Angew. Chem. Int. Ed.*, **41**, 2596-2599.
- [22] **Meldal, M.**, 2008, Polymer “Clicking” by CuAAC Reactions, *Macromol. Rapid Commun.*, **29**, 1016–1051
- [23] **Berrisford, D. J., Bolm, C., and Sharpless, K. B.**, 1995, Ligand-Accelerated Catalysis, *Angew. Chem., Int. Ed.*, **34**, 1059-1070.
- [24] **Tome, A. C.**, 2004, Science of Synthesis, **13**, 415–601, *Thieme*, Eds. Storr, R. C., Gilchrist, T. L., New York.
- [25] **Krivopalov, V. P., and Shkurko, O. P.**, 2005, Development of methods for the formation of the triazole ring, *Russ. Chem. Rev.*, **74**, 339-379.

- [26] **Tornøe, C. W., Christensen, C., and Meldal, M.**, 2002, Peptidotriazoles on Solid Phase: [1,2,3]-Triazoles by Regiospecific Copper(I)-Catalyzed 1,3-Dipolar Cycloadditions of Terminal Alkynes to Azides, *J. Org. Chem.*, **67**, 3057-3064.
- [27] **Bock, V. D., Heimsha, H., and van Morsteeen, S. H.**, 2006, Cu(I)-Catalyzed Alkyne-Azide "Click" Cycloadditions from a Mechanistic and Synthetic Perspective, *Eur. J. Org. Chem.*, **51**.
- [28] **Himo, F., Lovell, T., Hilgraf, R., Rostovtsev, V. V., Noodleman, L., Sharpless, K. B., and Fokin, V. V.**, 2005, Copper(I)-Catalyzed Synthesis of Azoles. DFT Study Predicts Unprecedented Reactivity and Intermediates, *J. Am. Chem. Soc.*, **127**, 210-216.
- [29] **Himo, F., Demko, Z. P., Noodleman, L., and Sharpless, K. B.**, 2002, Mechanisms of Tetrazole Formation by Addition of Azide to Nitriles, *J. Am. Chem. Soc.*, **124**, 12210-12216.
- [30] **Binder, W. H., and Sachsenhofer, R.**, 2007, 'Click' Chemistry in Polymer and Materials Science, *Macromol. Rapid Commun.*, **28**, 15-54.
- [31] **Himo, F., Lovell, T., Hilgraf, R., Rostovtsev, V. V., Noodleman, L., Sharpless, K. B., and Fokin, V. V.**, 2005, Copper(I)-Catalyzed Synthesis of Azoles. DFT Study Predicts Unprecedented Reactivity and Intermediates, *J. Am. Chem. Soc.* **127**, 210-216.
- [32] **Rostovtsev, V. V., Green, L. G., Fokin, V. V., and Sharpless, K. B.**, 2002, A Stepwise Huisgen Cycloaddition Process: Copper(I)-Catalyzed Regioselective Ligation of Azides and Terminal Alkynes, *Angew. Chem., Int. Ed.*, **41**, 2596-2599.
- [33] **Rodionov, V. O., Fokin, V. V., and Finn, M. G.**, 2005, Mechanism of the Ligand-Free Cu(I)-Catalyzed Azide-Alkyne Cycloaddition Reaction, *Angew. Chem., Int. Ed.*, **44**, 2210-2215.
- [34] **Mykhalichko, B. M., Temkin, O. N., and Mys'kiv, M. G.**, 2000, Polynuclear complexes of copper(I) halides: coordination chemistry and catalytic transformations of alkynes, *Russ. Chem.Rev.*, **69**, 957-984.
- [35] **Ahlquist, M., and Fokin, V. V.**, 2007, Enhanced Reactivity of Dinuclear Copper(I) Acetylides in Dipolar Cycloadditions, *Organometallics*, **26**, 4389-4391.
- [36] **Meldal, M., and Tornøe, C.W.**, 2008, Cu-Catalyzed Azide-Alkyne Cycloaddition, *Chem. Rev.*, **108**, 2952-3015.
- [37] **Bock, V. D.; Hiemstra, H., and Van Maarseveen, J. H.**, 2006, CuI-catalyzed alkyne-azide "click" cycloadditions from a mechanistic and synthetic perspective, *Eur. J. Org. Chem.*, **51-68**.
- [38] **Baut, N. L.; Di'az, D. D., Punna, S., Finn, M. G., and Brown, H. R.**, 2007, Study of high glass transition temperature thermosets made from the copper(I)-catalyzed azide-alkyne cycloaddition reaction, *Polymer*, **48**, 239.
- [39] **Hassane, F. S., Frisch, B., and Schuber, F.**, 2006, Targeted Liposomes: Convenient Coupling of Ligands to Preformed Vesicles Using "Click Chemistry", *Bioconjugate Chem.*, **17**, 849-854.

- [40] **Lee, B. Y., Park, S. R., Jeon, H. B., and Kim, K. S.**, 2006, A new solvent system for efficient synthesis of 1,2,3-triazoles, *Tetrahedron Lett.*, **47**, 5105.
- [41] **Golas, P. L., Tsarevsky, N. V., Sumerlin, B. S., and Matyjaszewski, K.**, 2006, "Catalyst Performance in "Click" Coupling Reactions of Polymers Prepared by ATRP: Ligand and Metal Effects", *Macromolecules*, **39**, 6451.
- [42] **Wu, Y. M., Deng, J., Fang, X., and Chen, Q. Y.**, 2004, Regioselective synthesis of fluoroalkylated 1,2,3-triazole by Huisgen cycloaddition, *J. Fluorine Chem.*, **125**, 1415.
- [43] **Petchprayoon, C., Suwanborirux, K., Miller, R., Sakata, T., and Marriott, G.**, 2005, Synthesis and Characterization of the 7-(4-Aminomethyl-1H-1,2,3-triazol-1-yl) Analogue of Kabiramide C, *J. Nat. Prod.*, **68**, 157-161.
- [44] **Link, A. J., Vink, M. K. S., and Tirrell, D. A.**, 2004, Presentation and Detection of Azide Functionality in Bacterial Cell Surface Proteins, *J. Am. Chem. Soc.*, **126**, 10598-10602.
- [45] **M. Sawa, T. L. Hsu, T. Itoh, M. Sugiyama, S. R. Hanson, P. K. Vogt, C. H., and Wong, P.**, 2006, Glycoproteomic probes for fluorescent imaging of fucosylated glycans in vivo. *Natl. Acad. Sci.*, **103**, 12371-12376.
- [46] **Beatty, K. E., Xie, F., Wang, Q., and Tirrell, D. A.**, 2005, Selective Dye-Labeling of Newly Synthesized Proteins in Bacterial Cells, *J. Am. Chem. Soc.*, **127**, 14150-14151.
- [47] **Tornøe, C. W., and Meldal, M.**, 2001, Peptides, Proc. Am. Pept.Symp., American Peptide Society and Kluwer Academic Publishers, 263-264, Eds. M. Lebl, R. A. Houghten, San Diego.
- [48] **Yoo, E. J., Ahlquist, M., Kim, S. H., Bae, I., Fokin, V. V., Sharpless, K. B., and Chang, S.**, 2007, Copper-Catalyzed Synthesis of N-Sulfonyl-1,2,3-Triazoles: Controlling Selectivity, *Angew. Chem. Int. Ed.*, **46**, 1730-1733.
- [49] **Bertrand, P., and Gesso, J. P.**, 2007, Click Chemistry with *O*-Dimethylpropargylcarbamate for Preparation of pH-Sensitive Functional Groups. A Case Study., *J. Org. Chem.*, **72**, 3596-3599.
- [50] **Zhang, Z., and Fan, E.**, 2006, Solid phase synthesis of peptidotriazoles with multiple cycles of triazole formation, *Tetrahedron Lett.*, **47**, 665-669.
- [51] **Girard, C., Onen, E., Aufort, M., Beauvière, S., Samson, E., and Herscovici, J.**, 2006, Reusable Polymer-Supported Catalyst for the [3+2] Huisgen Cycloaddition in Automation Protocols, *Org. Lett.*, **8**, 1689-1692.
- [52] **Rostovtsev, V. V., Green, L. G., Fokin, V. V., and Sharpless, K. B.**, 2002, A stepwise Huisgen cycloaddition process: copper(I)-catalyzed regioselective "ligation" of azides and terminal alkynes, *Angew. Chem. Int. Ed.*, **41**, 2596-2599.

- [53] **Rostovtsev, V. V., Green, L.G., Fokin, V.V., Sharpless K.B.**, 2002, A Stepwise Huisgen Cycloaddition Process: Copper(I)-Catalyzed Regioselective “Ligation” of Azides and Terminal Alkynes, *Angew. Chem. Int. Ed.*, **41**, 14.
- [55] **Sreedhar, B., and Reddy, P. S.**, 2007, *Synthetic Commun.*, **37**, 3259-3262.
- [56] **Zhu, L., Lynch, V. M., and Anslyn, E. V.**, 2004, FRET induced by an ‘allosteric’ cycloaddition reaction regulated with exogenous inhibitor and effectors, *Tetrahedron*, **60**, 7267-7275.
- [67] **Guezguez, R., Bougrin, K., El Akri, K., and Benhida, R.**, 2006, A Highly Efficient Microwave-Assisted Solvent-Free Synthesis of  $\alpha$ - and  $\beta$ -2'-Deoxy-1,2,3-Triazolyl-Nucleosides, *Tetrahedron Lett.*, **47**, 4807 *Tetrahedron Lett.*, **47**, 4807-4811.
- [58] **Lewis, W. G., Magallon, F. G., Fokin, V. V., and Finn, M. G.**, 2004, Discovery and Characterization of Catalysts for Azide–Alkyne Cycloaddition by Fluorescence Quenching, *J. Am. Chem. Soc.*, **126**, 9152-9153.
- [59] **Wang, Q., Chan, T. R., Hilgraf, R., Fokin, V. V., Sharpless, K. B., and Finn, M. G.**, 2003, Bioconjugation by Copper(I)-Catalyzed Azide–Alkyne [3 + 2] Cycloaddition, *J. Am. Chem. Soc.*, **125**, 3192.
- [60] **Rodionov, V. O., Presolski, S. I., Gardinier, S., Lim, Y. H., and Finn, M. G.**, 2007, Benzimidazole and Related Ligands for Cu-Catalyzed Azide–Alkyne Cycloaddition, *J. Am. Chem. Soc.*, **129**, 12696-12704.
- [61] **Tornøe, C. W. Christensen, C. Meldal, M.**, 2002, Peptidotriazoles on Solid Phase: [1,2,3]-Triazoles by Regiospecific Copper(I)-Catalyzed 1,3-Dipolar Cycloadditions of Terminal Alkynes to Azides, *J. Org. Chem.*, **67**, 3057-3064.
- [62] **Humenik, M., Huang, Y., Wang, Y., and Sprinzl, M.**, 2007, C-Terminal Incorporation of Bio-Orthogonal Azide Groups into a Protein and Preparation of Protein–Oligodeoxynucleotide Conjugates by CuI-Catalyzed Cycloaddition, *ChemBioChem* **8**, 1103.
- [63] **Gupta, S. S., Kuzelka, J., Singh, P., Lewis, W. G., Manchester, M., and Finn, M. G.**, 2005, Accelerated Bioorthogonal Conjugation: A Practical Method for the Ligation of Diverse Functional Molecules to a Polyvalent Virus Scaffold, *Bioconjugate Chem.*, **16**, 1572-1579.
- [64] **Kacprzak, K.**, 2005, Efficient one-pot synthesis of 1,2,3-triazoles from benzyl and alkyl halides, *Synlett*, 943-946.
- [65] **Yoo, E. J., Ahlquist, M., Kim, S. H. Bae, I., Fokin, V. V., Sharpless, K. B., and Chang, S.**, 2007, Copper-Catalyzed Synthesis of N-Sulfonyl-1,2,3-Triazoles: Controlling Selectivity, *Angew. Chem., Int. Ed.*, **46**, 1730-1733.
- [66] **Wu, Y. M., Deng, J., Fang, X., and Chen, Q. Y.**, 2004, Regioselective synthesis of fluoroalkylated [1,2,3]-triazoles by Huisgen cycloaddition, *J. Fluorine Chem.*, **125**, 1415-1423.

- [67] **Feldman, A. K., Colasson, B., Sharpless, K. B., and Fokin, V. V.**, 2005, The Allylic Azide Rearrangement: Achieving Selectivity, *J. Am. Chem. Soc.*, **127**, 1344-13445.
- [68] **Qin, A., Jim, C. K. W., Lu, W., Lam, J. W. Y., Haussler, M., Dong, Y., Sung, H. H. Y., Williams, I. D., Wong, G. K. L., and Tang, B. Z.**, 2007, Click Polymerization: Facile Synthesis of Functional Poly(aroyltriazoles) by Metal-Free, Regioselective 1,3-Dipolar Polycycloaddition, *Macromolecules*, **40**, 2308-2317.
- [69] **Molander, G. A., and Ham, J.**, 2006, Synthesis of Functionalized Organotrifluoroborates via the 1,3-Dipolar Cycloaddition of Azides, *Org. Lett.*, **8**, 2767-2770.
- [70] **Sumerlin, B. S., Tsarevsky, N. V., Louche, G., Lee, R. Y., and Matyjaszewski, K.**, 2005, Highly Efficient "Click" Functionalization of Poly(3-azidopropyl methacrylate) Prepared by ATRP, *Macromolecules*, **38**, 7540-7545.
- [71] **Ryu, E. H., and Zhao, Y.**, 2005, Efficient Synthesis of Water-Soluble Calixarenes Using Click Chemistry, *Org. Lett.*, **7**, 1035-1037.
- [72] **Rodionov, V. O., Fokin, V. V., and Finn, M. G.**, 2005, Mechanism of the Ligand-Free Cu-Catalyzed Azide-Alkyne Cycloaddition Reaction, *Angew. Chem., Int. Ed.*, **44**, 2210-2215.
- [73] **Bock, V. D., Hiemstra, H., and Van Maarseveen, J. H.**, 2006, Cu(I)-Catalyzed Alkyne-Azide "Click" Cycloadditions from a Mechanistic and Synthetic Perspective, *Eur. J. Org. Chem.*, **51**.
- [74] **Ryu, E. H., and Zhao, Y.**, 2005, Efficient Synthesis of Water-Soluble Calixarenes Using Click Chemistry, *Org. Lett.*, **7**, 1035-1037.
- [75] **Diels, O., and Alder, K.**, 1928, Synthesen in der hydroaromatischen Reihe, *Liebigs Ann. Chem.*, **460**, 98-122.
- [76] **Sauer, J., and Sustmann, R.**, 1980, Mechanistic aspect of Diels-Alder reactions : A Critical Survey, *Angew. Chem. Int. Ed.*, **19**, 779-807.
- [77] **Nicolaou, K. C., Snyder, S. A., Montagnon, T., and Vassilikogiannakis, G.**, 2002, The Diels-Alder Reaction in Total Synthesis, *Angew. Chem. Int. Ed.*, **41**, 1668-1698.
- [78] **Tietze L. F., and Kettischau, G.**, 1997, Hetero Diels-Alder Reactions in Organic Chemistry, *Top. Curr. Chem.*, **189**, 1-120.
- [79] **Ripoll, J. L., Rouessac A., and Rouessac, F.**, 1978, Applications recentes de la reaction de retro-diels-alder en synthese organique, *Tetrahedron*, **34**, 19-40.
- [80] **Fringuelli, F., and Taticchi, A.**, 2002, *The Diels-Alder Reaction: Selected Practical Methods*, Eds. Fringuelli, F, Taticchi, A., John Wiley & Sons Ltd
- [81] **Sauer J.**, 1967, Diels-Alder Reactions, *Angew. Chem. Int. Ed. Engl.*, **6**, 16.
- [82] **Fringuelli F., Minuti L., Pizzo F., and Taticchi A.**, 1993, Reactivity and Selectivity in Lewis Acid-Catalyzed Diels-Alder Reactions of 2-Cyclohexenones, *Acta Chem. Scand.*, **47**, 255-263.



- [83] **Bodwell G. J., and Pi, Z.**, 1997, Electron deficient dienes I. Normal and inverse electron demand Diels-Alder reaction of the same carbon skeleton, *Tetrahedron Lett.*, **38**, 309-312.
- [84] a) **Fringuelli F., and Taticchi A.**, 1990, *Dienes in the Diels-Alder Reaction*, Wiley, New York; b) **Paquette L. A.**, 1991, *Comprehensive Organic Synthesis*, **5**, Pergamon Press, Oxford, 1991.
- [85] a) **Loncharich R. J., Brown F. K., and Houk K. N.**, 1989, *J. Org. Chem.*, **54**, 1129; b) **Sauer J. and Sustmann R.**, 1980, *Angew. Chem. Int. Ed. Engl.*, **19**, 779.
- [86] **Ginsburg D.**, 1983, Tetrahedron report number 149 : The role of secondary orbital interactions in control of organic reactions *Tetrahedron*, **39**, 2095-2135.
- [87] **Fleming I.**, 1976, *Frontier Orbitals and Organic Chemical Reactions*, Wiley, New York.
- [88] **Woodward R. B. and Baer H.**, 1944, Studies on Diene-addition Reactions. II.1 The Reaction of 6,6-Pentamethylenefulvene with Maleic Anhydride, *J. Am. Chem. Soc.*, **66**, 645.
- [89] **Herndon W. C. and Hall L. H.**, 1967, *Tetrahedron*, **27**, 3095.
- [90] **Houk K. N. and Strozier R. W.**, 1973, On Lewis Acid Catalysis of Diels-Alder Reactions, *J. Am. Chem. Soc.*, **95**, 4094.
- [91] **Yates P. and Eaton P.**, 1960, Acceleration of the Diels-Alder Reaction by Aluminum Chloride, *J. Am. Chem. Soc.*, **82**, 4436.
- [92] **Carruthers W.**, 1990, *Cycloaddition Reactions in Organic Synthesis*, Pergamon Press, Oxford, 1990.
- [93] **Fringuelli, F. and Taticchi, A.**, 2002. *The Diels Alder reaction : selected practical methods*. Chichester, New York, Wiley.
- [94] **Birney, D.M. and Houk, K.N.**, 1990, Transition Structures of the Lewis Acid-Catalyzed Diels-Alder Reaction of Butadiene with Acrolein - the Origins of Selectivity, *Journal of the American Chemical Society*, **112**, 4127-4133.
- [95] **Houk, K.N. and Strozier, R.W.**, 1973, Lewis acid catalysis of Diels-Alder reactions, *Journal of the American Chemical Society*, **95**, 4094-4096.
- [96] **Cativiela, C., Garcia, J.I., Mayoral, J.A., and Salvatella, L.**, 1996, Modelling of solvent effects on the Diels-Alder reaction, *Chemical Society Reviews*, **25**, 209-218.
- [97] **Furlani, T.R. and Gao, J.L.**, 1996, Hydrophobic and hydrogen-bonding effects on the rate of Diels-Alder reactions in aqueous solution, *Journal of Organic Chemistry*, **61**, 5492-5497.
- [98] **Kong, S. and Evanseck, J.D.**, 2000, Density functional theory study of aqueous-phase rate acceleration and endo/exo selectivity of the butadiene and acrolein Diels-Alder reaction, *Journal of the American Chemical Society*, **122**, 10418-10427.

- [99] **Meijer, A., Otto, S., and Engberts, J.B.F.N.**, 1998, Effects of the hydrophobicity of the reactants on Diels-Alder reactions in water, *Journal of Organic Chemistry*, **63**, 8989-8994
- [100] **Ichihara, A.**, 1987, Retro-Diels-Alder Strategy in Natural Product Synthesis, *Synthesis*, **3**, 207.
- [101] **Bunnage, M. E. and Nicolau K. C.**, 1997, The Oxide Anion Accelerated Retro-Diels-Alder Reaction *Chem. Eur. J.*, **3**, 187-192.
- [102] **Rajan Babu T. V., Eaton D. F. and Fukunaga T.**, 1983, Chemistry of bridged aromatics. A study of the substituent effect on the course of bond cleavage of 9,10-dihydro-9,10-ethanoanthracenes and an oxyanion-assisted retro-Diels-Alder reaction, *J. Org. Chem.* **48**, 652-657.
- [103] **Dondoni, A.**, 2008, The Emergence of Thiol-Ene Coupling as a Click Process for Materials and Bioorganic Chemistry, *Angewandte Chemie-International Edition*, **47**, 8995-8997.
- [104] **Hoyle, C.E. and Bowman, C.N.**, 2010, Thiol-Ene Click Chemistry, *Angewandte Chemie-International Edition*, **49**, 1540-1573.
- [105] **Morgan, C.R., Magnotta, F., and Ketley, A.D.**, 1977, Thiol-ene photocurable polymers, *Journal of Polymer Science Part a-Polymer Chemistry*, **15**, 627-645.
- [106] **Griesbau, K.**, 1970, Problems and possibilities of free-radical addition of thiols to unsaturated compounds, *Angewandte Chemie-International Edition*, **9**, 273-287.
- [107] **Mather, B.D., Viswanathan, K., Miller, K.M., and Long, T.E.**, 2006, Michael addition reactions in macromolecular design for emerging technologies, *Progress in Polymer Science*, **31**, 487-531.
- [108] **Singh, R.**, 1994, A Sensitive Assay for Maleimide Groups, *Bioconjugate Chemistry*, **5**, 348-351.
- [109] **Mantovani, G., Lecolley, F., Tao, L., Haddleton, D.M., Clerx, J., Cornelissen, J.J.L.M., and Velonia, K.**, 2005, Design and synthesis of N-maleimido-functionalized hydrophilic polymers via copper-mediated living radical polymerization: A suitable alternative to PEGylation chemistry, *Journal of the American Chemical Society*, **127**, 2966-2973.
- [110] **Tolstyka, Z.P., Kopping, J.T., and Maynard, H.A.**, 2008, Straightforward synthesis of cysteine-reactive telechelic polystyrene, *Macromolecules*, **41**, 599-606.
- [111] **Stanford, M.J. and Dove, A.P.**, 2009, One-Pot Synthesis of alpha,omega-Chain End Functional, Stereoregular, Star-Shaped Poly(lactide), *Macromolecules*, **42**, 141-147.
- [112] **Pounder, R.J., Stanford, M.J., Brooks, P., Richards, S.P., and Dove, A.P.**, 2008, Metal free thiol-maleimide 'Click' reaction as a mild functionalisation strategy for degradable polymers, *Chemical Communications*, 5158-5160.

- [113] **Aydođan, B.**, 2010, *Long Wavelength Acting Photoinitiating Systems for Cationic Polymerization*, PhD. Thesis, ITU.
- [114] **Fouassier, J.-P.**, 1995: Photoinitiation, Photopolymerization, and Photocuring: Fundamentals and Applications, Hanser/Gardner, Munich.
- [115] **Davidson, R. S.**, 1998: Exploring the Science, Technology and Applications of U.V and E.B. Curing, SITA Technology Ltd., London.
- [116] **Roffey, C. G.**, 1997: Photogeneration of Reactive Species for Uv Curing, Wiley, Chichester.
- [117] **Kloosterboer, J. G.**, 1988: Network Formation by Chain Crosslinking Photopolymerization and Its Applications in Electronics, *Advances in Polymer Science*, **84**, 1-61.
- [118] **Bunning, T. J., Natarajan, L. V., Tondiglia, V. P. and Sutherland, R. L.**, 2000: Holographic Polymer-Dispersed Liquid Crystals (H-PdLcs), *Annual Review of Materials Science*, **30**, 83-115.
- [119] **Anseth, K. S., Newman, S. M. and Bowman, C. N.**, 1995: Polymeric Dental Composites: Properties and Reaction Behavior of Multimethacrylate Dental Restorations, in *Biopolymers Ii*, Vol. **122**, pp. 177-217,
- [120] **Sun, H. B. and Kawata, S.**, 2004: Two-Photon Photopolymerization and 3d Lithographic Microfabrication, in *Nmr - 3d Analysis - Photopolymerization*, Vol. **170**, pp. 169-273,
- [121] **Fisher, J. P., Dean, D., Engel, P. S. and Mikos, A. G.**, 2001: Photoinitiated Polymerization of Biomaterials, *Annual Review of Materials Research*, **31**, 171-181.
- [122] **Yagci, Y., Jockusch, J. and Turro, N. J.**, 2010: Photoinitiated Polymerization: Advances, Challenges, and Opportunities, *Macromolecules*, **43**, 6245-6260.
- [123] **Kahveci, M. U., Yilmaz, A. G. and Yagci, Y.**, 2010: Photoinitiated Cationic Polymerization: Reactivity and Mechanistic Aspects, in *Photochemistry and Photophysics of Polymer Materials*, Allen, N. S., Ed. pp. 421-478, John Wiley & Sons, Inc., New Jersey.
- [124] **Davidson, R. S.**, 1993: The Chemistry of Photoinitiators - Some Recent Developments, *Journal of Photochemistry and Photobiology a-Chemistry*, **73**, 81-96.
- [125] **Gruber, H. F.**, 1992: Photoinitiators for Free-Radical Polymerization, *Progress in Polymer Science*, **17**, 953-1044.
- [126] **Hageman, H. J.**, 1985: Photoinitiators for Free-Radical Polymerization, *Progress in Organic Coatings*, **13**, 123-150.
- [127] **Monroe, B. M. and Weed, G. C.**, 1993: Photoinitiators for Free-Radical-Initiated Photoimaging Systems, *Chemical Reviews*, **93**, 435-448.
- [128] **Davidson, R. S.**, 1983: in *Advances in Physical Chemistry*, Bethel, D. and Gold, V., Eds., p. 1, Academic Press, London.

- [129] **Ledwith, A., Bosley, J. A. and Purbrick, M. D.**, 1978: Exciplex Interactions in Photoinitiation of Polymerization by Fluorenone-Amine Systems, *Journal of the Oil & Colour Chemists Association*, **61**, 95-104.
- [130] **Ledwith, A. and Purbrick, M. D.**, 1973: Initiation of Free-Radical Polymerization by Photoinduced Electron-Transfer Processes, *Polymer*, **14**, 521-522.
- [131] **Jauk, S. and Liska, R.**, 2008: Photoinitiators with Functional Groups 9: New Derivatives of Covalently Linked Benzophenone-Amine Based Photoinitiators, *Journal of Macromolecular Science Part a-Pure and Applied Chemistry*, **45**, 804-810.
- [132] **Catalina, F., Tercero, J. M., Peinado, C., Sastre, R., Mateo, J. L. and Allen, N. S.**, 1989: Photochemistry and Photopolymerization Study on 2-Acetoxy and Methyl-2-Acetoxy Derivatives of Thioxanthone as Photoinitiators, *Journal of Photochemistry and Photobiology a-Chemistry*, **50**, 249-258.
- [133] **Peinado, C., Catalina, F., Corrales, T., Sastre, R., Amatguerri, F. and Allen, N. S.**, 1992: Synthesis of Novel 2-(3'-Dialkylaminopropoxy)-Thioxanthone Derivatives - Photochemistry and Evaluation as Photoinitiators of Butyl Acrylate Polymerization, *European Polymer Journal*, **28**, 1315-1320.
- [134] **Balta, D. K., Temel, G., Aydin, M. and Arsu, N.**, Thioxanthone Based Water-Soluble Photoinitiators for Acrylamide Photopolymerization, *European Polymer Journal*, **46**, 1374-1379.
- [135] **Temel, G. and Arsu, N.**, 2007: 2-Methylol-Thioxanthone as a Free Radical Polymerization Initiator, *Journal of Photochemistry and Photobiology a-Chemistry*, **191**, 149-152.
- [136] **Karasu, F., Arsu, N., Jockusch, S. and Turro, N. J.**, 2009: Mechanistic Studies of Photoinitiated Free Radical Polymerization Using a Bifunctional Thioxanthone Acetic Acid Derivative as Photoinitiator, *Macromolecules*, **42**, 7318-7323.
- [137] **Balta, D. K., Karasu, F., Aydin, M. and Arsu, N.**, 2007: The Effect of the Amine Structure on Photoinitiated Free Radical Polymerization of Methyl Methacrylate Using Bisketocoumarin Dye, *Progress in Organic Coatings*, **59**, 274-277.
- [138] **Polykarpov, A. Y., Hassoon, S. and Neckers, D. C.**, 1996: Tetramethylammonium Tetraorganylborates as Coinitiators with 5,7-Diiodo-3-Butoxy-6-Fluorone in Visible Light Polymerization of Acrylates, *Macromolecules*, **29**, 8274-8276.
- [139] **Shi, J. M., Zhang, X. P. and Neckers, D. C.**, 1992: Xanthenes - Fluorone Derivatives .1, *Journal of Organic Chemistry*, **57**, 4418-4421.
- [140] **Shi, J. M., Zhang, X. P. and Neckers, D. C.**, 1993: Xanthenes - Fluorone Derivatives .2, *Tetrahedron Letters*, **34**, 6013-6016.
- [141] **Tanabe, T., Torresfilho, A. and Neckers, D. C.**, 1995: Visible-Light Photopolymerization - Synthesis of New Fluorone Dyes and

Photopolymerization of Acrylic-Monomers Using Them, *Journal of Polymer Science Part a-Polymer Chemistry*, **33**, 1691-1703.

- [142] **Valdesaguilera, O., Pathak, C. P., Shi, J., Watson, D. and Neckers, D. C.**, 1992: Photopolymerization Studies Using Visible-Light Photoinitiators, *Macromolecules*, **25**, 541-547.
- [143] **Aydin, M., Arsu, N. and Yagci, Y.**, 2003: One-Component Bimolecular Photoinitiating Systems, 2 - Thioxanthone Acetic Acid Derivatives as Photoinitiators for Free Radical Polymerization, *Macromolecular Rapid Communications*, **24**, 718-723.
- [144] **Cokbaglan, L., Arsu, N., Yagci, Y., Jockusch, S. and Turro, N. J.**, 2003: 2-Mereapthioxanthone as a Novel Photoinitiator for Free Radical Polymerization, *Macromolecules*, **36**, 2649-2653.
- [145] **Aydin, M., Arsu, N., Yagci, Y., Jockusch, S. and Turro, N. J.**, 2005: Mechanistic Study of Photoinitiated Free Radical Polymerization Using Thioxanthone Thioacetic Acid as One-Component Type Ii Photoinitiator, *Macromolecules*, **38**, 4133-4138.
- [146] **Temel, G., Arsu, N. and Yagci, Y.**, 2006: Polymeric Side Chain Thioxanthone Photoinitiator for Free Radical Polymerization, *Polymer Bulletin*, **57**, 51-56.
- [147] **Temel, G., Aydogan, B., Arsu, N. and Yagci, Y.**, 2009: Synthesis and Characterization of One-Component Polymeric Photoinitiator by Simultaneous Double Click Reactions and Its Use in Photoinduced Free Radical Polymerization, *Macromolecules*, **42**, 6098-6106.
- [148] **Temel, G. and Arsu, N.**, 2009: One-Pot Synthesis of Water-Soluble Polymeric Photoinitiator Via Thioxanthonation and Sulfonation Process, *Journal of Photochemistry and Photobiology a-Chemistry*, **202**, 63-66.
- [149] **Corrales, T., Catalina, F., Peinado, C. and Allen, N. S.**, 2003: Free Radical Macrophotoinitiators: An Overview on Recent Advances, *Journal of Photochemistry and Photobiology a-Chemistry*, **159**, 103-114.
- [150] **Corrales, T., Catalina, F., Peinado, C., Allen, N. S., Rufs, A. M., Bueno, C. and Encinas, M. V.**, 2002: Photochemical Study and Photoinitiation Activity of Macroinitiators Based on Thioxanthone, *Polymer*, **43**, 4591-4597.
- [151] **Wang, H. Y., Wei, J., Jiang, X. S. and Yin, J.**, 2007: Highly Efficient Sulfur-Containing Polymeric Photoinitiators Bearing Side-Chain Benzophenone and Coinitiator Amine for Photopolymerization, *Journal of Photochemistry and Photobiology a-Chemistry*, **186**, 106-114.
- [152] **Wei, J., Wang, H. Y., Jiang, X. S. and Yin, J.**, 2006: Effect on Photopolymerization of the Structure of Amine Coinitiators Contained in Novel Polymeric Benzophenone Photoinitiators, *Macromolecular Chemistry and Physics*, **207**, 1752-1763.
- [153] **Wei, J., Wang, H. Y., Jiang, X. S. and Yin, J.**, 2007: Study of Novel Pu-Type Polymeric Photoinitiators Comprising of Side-Chain

Benzophenone and Coinitiator Amine: Effect of Macromolecular Structure on Photopolymerization, *Macromolecular Chemistry and Physics*, **208**, 287-294.

- [154] **Wang, Y. L., Jiang, X. S. and Yin, J.**, 2009: Novel Polymeric Photoinitiators Comprising of Side-Chain Benzophenone and Coinitiator Amine: Photochemical and Photopolymerization Behaviors, *European Polymer Journal*, **45**, 437-447.
- [155] **Davidson, R. S., Dias, A. A. and Illsley, D.**, 1995: A New Series of Type-Ii (Benzophenone) Polymeric Photoinitiators, *Journal of Photochemistry and Photobiology a-Chemistry*, **89**, 75-87.
- [156] **Jiang, X. S., Luo, X. W. and Yin, J.**, 2005: Polymeric Photoinitiators Containing in-Chain Benzophenone and Coinitiators Amine: Effect of the Structure of Coinitiator Amine on Photopolymerization, *Journal of Photochemistry and Photobiology a-Chemistry*, **174**, 165-170.
- [157] **Carlini, C., Ciardelli, F., Donati, D. and Gurzoni, F.**, 1983: Polymers Containing Side-Chain Benzophenone Chromophores - a New Class of Highly Efficient Polymerization Photoinitiators, *Polymer*, **24**, 599-606.
- [158] **Catalina, F., Peinado, C., Mateo, J. L., Bosch, P. and Allen, N. S.**, 1992: Polymeric Photoinitiators Based on Thioxanthone - Photochemistry and Free-Radical Photoinitiation Study by Photodilatometry of the Polymerization of Methyl-Methacrylate, *European Polymer Journal*, **28**, 1533-1537.
- [159] **Gacal, B., Akat, H., Balta, D. K., Arsu, N. and Yagci, Y.**, 2008: Synthesis and Characterization of Polymeric Thioxanthone Photoinitiators Via Double Click Reactions, *Macromolecules*, **41**, 2401-2405.
- [160] **Jiang, X. S. and Yin, J.**, 2004: Copolymeric Photoinitiators Containing in-Chain Thioxanthone and Coinitiator Amine for Photopolymerization, *Journal of Applied Polymer Science*, **94**, 2395-2400.
- [161] **Balta, D. K., Arsu, N., Yagci, Y., Jockusch, S. and Turro, N. J.**, 2007: Thioxanthone-Anthracene: A New Photoinitiator for Free Radical Polymerization in the Presence of Oxygen, *Macromolecules*, **40**, 4138-4141.
- [162] **Yilmaz, G., Aydogan, B., Temel, G., Arsu, N., Moszner, N. and Yagci, Y.**, Thioxanthone-Fluorenes as Visible Light Photoinitiators for Free Radical Polymerization, *Macromolecules*, **43**, 4520-4526.
- [163] **Turro, N. J.**, 1978: Modern Molecular Photochemistry, University Press, Menlo Park, CA.
- [164] **Rehm, D. and Weller, A.**, 1970: Kinetics of Fluorescence Quenching by Electron and H-Atom Transfer, *Israel Journal of Chemistry*, **8**, 259-271.
- [165] **Bendyk, M., Jedrzejewska, B., Paczkowski, J. and Linden, L. A.**, 2002: Hexaarylbisimidazoles and Ketocyanine Dyes as Effective Electron Transfer Photoinitiating Systems, *Polimery*, **47**, 654-656.

- [166] **Jakubiak, J. and Rabek, J. F.**, 1999: Photoinitiators for Visible Light Polymerization, *Polimery*, **44**, 447-461.
- [167] **Kawamura, K., Aotani, Y. and Tomioka, H.**, 2003: Photoinduced Intramolecular Electron Transfer between Carbazole and Bis(Trichloromethyl)-S-Triazine Generating Radicals, *Journal of Physical Chemistry B*, **107**, 4579-4586.
- [168] **Padon, K. S. and Scranton, A. B.**, 2000: A Mechanistic Investigation of a Three-Component Radical Photoinitiator System Comprising Methylene Blue, N-Methyldiethanolamine, and Diphenyliodonium Chloride, *Journal of Polymer Science Part a-Polymer Chemistry*, **38**, 2057-2066.
- [169] **Koleske, J. V.**, 2002, *Radiation Curing of Coatings*, Astm International, West Conshohocken, Pa.
- [170] **Roffey, C. G.**, 1989, *Photopolymerization of Surface Coatings*, Wiley, New York.
- [171] **Bellobono, I. R. and Zeni, M.**, 1986, Kinetic-Study of Photoinduced Polymerization of Diallyl Oxydiethylene Dicarboxate [Diethylene Glycol Bis(Allylcarbonate)], *Makromolekulare Chemie-Rapid Communications*, **7**, 733-738.
- [172] **Garcia, C., Fimia, A. and Pascual, I.**, 2001, Holographic Behavior of a Photopolymer at High Thicknesses and High Monomer Concentrations: Mechanism of Photopolymerization, *Applied Physics B-Lasers and Optics*, **72**, 311-316.
- [173] **Villegas, L., Encinas, M. V., Rufs, A. M., Bueno, C., Bertolotti, S. and Previtali, C. M.**, 2001, Aqueous Photopolymerization with Visible-Light Photoinitiators: Acrylamide Polymerization Photoinitiated with a Phenoxazine Dye/Amine System, *Journal of Polymer Science Part a-Polymer Chemistry*, **39**, 4074-4082.
- [174] **Yao, H. W., Huang, M. J., Chen, Z. Y., Hou, L. S. and Gan, F. X.**, 2002, Optimization of Two-Monomer-Based Photopolymer Used for Holographic Recording, *Materials Letters*, **56**, 3-8.
- [175] **White, L. A., Hoyle, C. E., Jonsson, S. and Mathias, L. J.**, 2002: Bulk Free-Radical Photopolymerizations of 1-Vinyl-2-Pyrrolidinone and Its Derivatives, *Journal of Polymer Science Part a-Polymer Chemistry*, **40**, 694-706.
- [176] **Jacobine, A. F., Glaser, D. M., Grabek, P. J., Mancini, D., Masterson, M., Nakos, S. T., Rakas, M. A. and Woods, J. G.**, 1992: Photocrosslinked Norbornene Thiol Copolymers - Synthesis, Mechanical-Properties, and Cure Studies, *Journal of Applied Polymer Science*, **45**, 471-485.
- [177] **H. Shirakawa, E. J. Louis, A. G. MacDiarmid, C. K. Chiang, A. J. Heeger, J.**, 1977. Synthesis of Electrically Conducting Organic Polymers - Halogen derivatives of Polyacetylene, *Chem. Soc. Chem. Commun.*, 578 - 580.

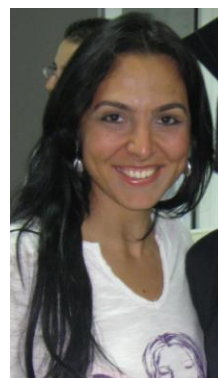
- [178] **Shirakawa, H., Louis, E. J., Macdiarmid, A. G., Chiang, C. K. and Heeger, A. J.**, 1977: Synthesis of Electrically Conducting Organic Polymers - Halogen Derivatives of Polyacetylene, (Ch)X, *Journal of the Chemical Society-Chemical Communications*, 578-580.
- [179] **Chiang, C. K., Fincher, C. R., Park, Y. W., Heeger, A. J., Shirakawa, H., Louis, E. J., Gau, S. C. and Macdiarmid, A. G.**, 1977: Electrical-Conductivity in Doped Polyacetylene, *Physical Review Letters*, **39**, 1098-1101.
- [180] **Chiang, C. K., Park, Y. W., Heeger, A. J., Shirakawa, H., Louis, E. J. and Macdiarmid, A. G.**, 1978: Conducting Polymers - Halogen Doped Polyacetylene, *Journal of Chemical Physics*, **69**, 5098-5104.
- [181] **Shirakawa, H., Louis, E.J., MacDiarmid, A.G., Chiang, C.K. and Heeger, A.J.**, 1977, Synthesis of electrically conducting organic polymers - halogen derivatives of polyacetylene, (CH)X, *J. Chem. Soc., Chem. Commun.*, **16**, 578-580.
- [182] **Yilmaz, F.**, 2004, Electroactive Intermediates for the Synthesis of Conducting Block and Graft Copolymers. PhD. Thesis.
- [183] **Skotheim, T. A., Elsenbaumer, R. L. and Reynolds, J. R.**, 1998: Handbook of Conducting Polymers, Marcel Dekker, New York.
- [184] **Heinze, J.**, 1990. In *Topics in Current Chemistry*, Springer-Verlag, Berlin, **152**, 2.
- [185] **Diaz, A.**, 1981: Electrochemical Preparation and Characterization of Conducting Polymers, *Chemica Scripta*, **17**, 145-148.
- [186] **Zotti, G., Schiavon, G., Berlin, A. and Pagani, G.**, 1993. Thiophene oligomers as polythiophene models. 1. Anodic coupling of thiophene oligomers to dimers: a kinetic investigation, *Chem. Mater.*, **5 (4)**, 430-436.,
- [187] **Okada, T., Ogata, T. and Ueda, M.**, 1996. Synthesis and characterization of regiocontrolled poly(2,5-di-*n*-butoxy-1,4-phenylene) by oxovanadium-catalyzed oxidative coupling polymerization, *Macromolecules*, **29 (24)**, 7645-7650.
- [188] **Yoshino, K., Hayashi, R. and Sugimoto, R.**, 1984. Preparation and properties of conducting heterocyclic polymer-films by chemical method, *Jpn. J. Appl. Phys.*, **23 (2)**, 899-900.
- [189] **Toshima, N. and Hara, S.**, 1995. Direct synthesis of conducting polymers from simple monomers, *Prog. Polym. Sci.*, **20 (1)**, 155-183.
- [190] **Kovacic, P. and Jones, M.B.**, 1987. Dehydro coupling of aromatic nuclei by catalyst-oxidant systems: poly(p-phenylene), *Chem. Rev.*, **87 (2)**, 357-379,



- [191] **Butler, G.B., Olson, K.G. and Tu, C-L.**, 1984. Monomer orientation control by donor-acceptor complex participation in alternating copolymerization, *Macromolecules*, **17** (9), 1884-1887.
- [192] **Andrews, L.J. and Keefer, R.M.**, 1964. In "Molecular Complexes in Organic Chemistry"; Holden-Day, Inc.: San Francisco,.
- [193] **Olson, K.G. and Butler, G.B.**, 1984. Stereochemical evidence for participation of a Donor-acceptor complex in alternating copolymerization. 1. Model compound synthesis, *Macromolecules*, **17**, 480-2486.
- [194] **Gandini, A. and Belgacem, M.N.**, 1997, Furans in polymer chemistry, *Prog. Polym. Sci.*, **22**, 1203-1379.
- [195] **Moore, J.S., Stupp, S.I.**, 1990, Metallo-Supramolecular Graft Copolymers: A Novel Approach Toward Polymer-Analogous Reactions, *Macromolecules*, **23**, 65-70.
- [196] **Mantovani, G., Lecolley, F., Tao, L., Haddleton, D. M., Clerx, J., Cornellisen, J. J. L. M., and Velonia, K.**, 2005, Design and Synthesis of N-Maleimido-Functionalized Hydrophilic Polymers via Copper-Mediated Living Radical Polymerization: A Suitable Alternative to PEGylation Chemistry, *J. Am. Chem. Soc.*, **127**, 2966-2973.
- [197] **Kim, S.G., Choi, J., Tamaki, R., and Laine, R.M.**, 2005, Synthesis of amino-containing oligophenylsilsesquioxanes, *Polymer*, **46**, 4514-4524.
- [198] **Barral K., Moorhouse A. D., and Moses J. E.**, 2007, Efficient Conversion of Aromatic Amines into Azides: A One-Pot Synthesis of Triazole Linkages *Org. Lett.*, **9** (9), pp 1809–1811
- [199] **Schubert, U. S., Hofmeier, H.** 2002, Metallo-Supramolecular Graft Copolymers: A Novel Approach Toward Polymer-Analogous Reactions, *Macromol. Rapid Commun.* **23**, 561-566.
- [200] **Ghoy, J. F., Hofmeier, H., Alexeev, A., Schubert, U. S.** 2003, Aqueous Micelles from Supramolecular Graft Copolymers, *Macromol.Chem. Phys.* **204**, 1524-1530.
- [201] **Balta, D. K., Arsu, N., Yagci, Y., Jockusch, S., Turro, N. J.** 2007, Thioxanthone-anthracene: A new photoinitiator for free radical polymerization in the presence of oxygen, *Macromolecules* **40**, 4138–4141.
- [202] **Binder, W. H., Kluger, C.** 2004, Combining Ring-Opening Metathesis Polymerization (ROMP) with Sharpless-Type "Click" Reactions: An Easy Method for the Preparation of Side Chain Functionalized Poly(oxynorbornenes), *Macromolecules* **37**, 9321–9330.
- [203] **Pouliquen, L., Coqueret, X., Morlet-Savary, F., Fouassier, J.-P.** 1995, Functionalized Polysiloxanes with Thioxanthone Side Groups: A Study of Their Reactivity as Radical Polymerization Macroinitiators, *Macromolecules* **28**, 8028–8030.

- [204] **Pappas, S. P.** 1987, Photoinitiated Radical Polymerization, *J. Radiat. Curing*, **14**, 6–8.
- [205] **Brandrup, J., Immergut, E. H.** 1975, In *Polymer Handbook*; Wiley-Interscience: New York.
- [206] **Tasdelen, M. A.; Moszner, N.; Yagci, Y.** 2009, The use of poly(ethylene oxide) as hydrogen donor in type II photoinitiated free radical polymerization, *Polym Bull* **63**,173–183.
- [207] **Jansen, J. F. G. A., Dias, A. A., Dorschu, M., Coussens, B.** 2003, Fast Monomers: Factors Affecting the Inherent Reactivity of Acrylate Monomers in Photoinitiated Acrylate Polymerization, *Macromolecules* **36**, 3861–3873.
- [208] **Kim S. G., Choi J., Tamaki R., Laine R. M.** 2005, Synthesis of amino-containing oligophenylsilsesquioxanes, *Polymer*, **46**, 4514-4524.
- [209] **Tamaki R, Tanaka Y, Asuncion M.Z, Choi J., Laine R. M.** 2001, Octa(aminophenyl) silsesquioxane as a Nanoconstruction Site, *J Am Chem Soc*, **123**,12416.
- [210] **Paul, S.** 1986, In *Surface Coating: Science and Technology*, Wiley-Interscience, New York,.

## CURRICULUM VITAE



**Candidate's full name:** Burçin Gacal

**Place and date of birth:** İstanbul, 11.06.1980

**Permanent Address:** Department of Chemistry, 34469 Istanbul Technical  
University Maslak 34469, Istanbul, Turkey

**Universities and Colleges attended:** B.Sc. in Chemistry, Istanbul Technical  
University. M.Sc. in Polymer Science and Technology, Istanbul Technical  
University.

### Publications:

- **Gacal B.**, Durmaz H., Tasdelen M. A., Hizal G., Tunca U., Yagci Y., and Demirel A. L. 2006: Anthracene-Maleimide-Based Diels-Alder “Click Chemistry” as a Novel Route to Graft Copolymers *Macromolecules* 2006, 39, 5330-5336.
- Kiskan B., **Gacal B.**, Tasdelen M. A., Colak D., and Yagci Y. 2006: Design and Synthesis of Thermally Curable Polymers with Benzoxazine Functionalities *Macromol. Symp.* 2006, 245–246, 27–33.
- **Gacal, B.** Cianga, L. Agag, T. Takeichi T. and Yagci, Y. 2007: Synthesis and Characterization of Maleimide (Co)polymers with Pendant Benzoxazine Groups by Photoinduced Radical Polymerization and Their Thermal Curing *Journal of Polymer Science: Part A: Polymer Chemistry*, Vol. 45, 2774–2786 (2007).
- Ergin M., Kiskan B., **Gacal B.**, and Yagci Y. 2007: Thermally Curable Polystyrene via Click Chemistry *Macromolecules* 2007, 40, 4724-4727.
- **Gacal B.**, Akat H., D. K. Balta, Arsu, N. and Yagci Y. 2008: Synthesis and Characterization of Polymeric Thioxanthone Photoinitiators via Double Click Reactions *Macromolecules* 2008, 41, 2401-2405.

- **Gacal B.**, Kiskan B., and Yagci Y. 2008: “Click” Chemistry as a Novel Route for the Introduction of Functional Groups to Octaphenylsilsesquioxane *Polymer Preprints* 2008, 49(1),145
- Ak M., **Gacal B.**, Kiskan B., Yagci Y., and Toppare L.2008: Enhancing Electrochromic Properties of Polypyrrole by Silsesquioxane Nanocages *Polymer* 49 (2008) 2202–2210
- **B. Gacal**, H. Akat, B. Kiskan, M. Ergin, D. Balta, N. Arsu and Y. Yagci Thermally and Photochemically Active Polymers by Click Chemistry *Polymer Preprints* 2008, 49(1),228
- Gacal B. N., Koz B., **Gacal B.**, Kiskan B., Erdogan M. and Yagci Y. 2009: Pyrene Functional Poly(vinyl alcohol) by “Click” Chemistry *Journal of Polymer Science: Part A: Polymer Chemistry*, Vol. 47, 1317–1326 (2009).
- D. Odaci, B. N. **Gacal**, B. Gacal, S. Timur, and Y. Yagci 2009: Fluorescence Sensing of Glucose Using Glucose Oxidase Modified by PVA-Pyrene Prepared via “Click” Chemistry *Biomacromolecules* 2009, 10, 2928–2934.
- Medine E. I., Odaci D., Gacal B. N., **Gacal B.**, Sakarya S.,Unak P., Timur S., and Yagci Y., 2010: A New Approach for in vitro Imaging of Breast Cancer Cells by Anti-Metadherin Targeted PVA-Pyrene *Macromolecular Bioscience*, 2010, 10, 657–663
- Akat H., **Gacal B.**, Balta D. K., Arsu N. and Yagci Y. 2010: Poly(ethylene glycol)-Thioxanthone Prepared by Diels–Alder Click Chemistry as One-Component Polymeric Photoinitiator for Aqueous Free-Radical Polymerization *Journal of Polymer Science: Part A: Polymer Chemistry*, Vol. 48, 2109–2114 (2010).
- Ervithayasuporn V., Wang X., **Gacal B.**, Gacal B. N., Yagci Y., and Kawakami Y., 2011: Formation Of Trimethylsilylated Open-Cage Oligomeric Azidophenylsilsesquioxanes *Journal of Organometallic Chemistry*, 696 (2011) 2193-2198.

#### Chapters:

- Aydogan B., **Gacal B.**, Yildirim A., Yonet N., Yuksel Y. and Yagci Y., 2006: Wavelength Tunability in Photoinitiated Cationic Polymerization, Photochemistry and UV Curing: New Trends, Ed. J. P. Fouassier, Research Signpost., Trivandrum, Ch. 17, pp. 187-201.